A CLINICAL, GENETIC AND BIOCHEMICAL STUDY OF HEREDITARY SPASTIC PARAPLEGIA

Thesis submitted to the University of London

for the degree of

Doctor of Philosophy

by

Philip Wilkinson

2007

Department of Clinical Neurosciences

Royal Free and University College Medical School

University of London

ProQuest LLC
789 East Eisenhower Parkway
P.O. Box 1346
Ann Arbor, MI 48106-1346

ABSTRACT

The hereditary spastic paraplegias (HSPs) represent a clinically and genetically heterogeneous group of neurological disorders. The phenotype is classified as pure or uncomplicated when the spastic paraparesis occurs in isolation and complicated when there are significant additional neurological or other clinical features. Inheritance may be autosomal dominant, autosomal recessive or X-linked.

Twenty families from the UK were identified with autosomal recessive HSP. Clinical analysis of affected individuals demonstrated a variety of different phenotypes with a slight preponderance of complicated cases. Genetic linkage analysis in the largest of these families identified linkage to the previously described SPG5A locus with a maximum LOD score of 4.84. Marker saturation analysis subsequently refined the locus to a 23.6cM region on chromosome 8q. In 6 of the remaining families linkage to the SPG7 locus could not be excluded. An affected individual from each of these families and 29 sporadic HSP cases were subsequently screened for SPG7 gene mutations using a combination of SSCP and sequencing. Three sporadic patients were found to have compound heterozygous SPG7 mutations, five of which were novel and one that had been described previously. Muscle biopsies in two of the patients with SPG7 mutations failed to demonstrate histological evidence of oxidative phophorylation defects but did reveal mitochondrial respiratory chain complex I-III defects in muscle and complex I deficiency in cultured myoblasts.

A similar combination of SSCP and sequencing was used to screen a group of 12 families with early onset autosomal dominant HSP for SPG3A gene mutations. Only the previously reported R239C mutation was identified in one family suggesting that SPG3A mutations are relatively uncommon in this population.

Genome wide linkage analysis in a consanguineous Bedouin family from Kuwait with a complicated HSP phenotype including cognitive impairment, dysarthria and distal amyotrophy identified linkage to a 22.8cM interval on chromosome 12 with a maximum LOD score of 5.1. No coding sequence mutations were identied in the KIF5A gene, associated with pure autosomal dominant HSP, located within this region. This interval has therefore been proposed as a novel locus for complicated autosomal recessive HSP (SPG26).

ACKNOWLEDGEMENTS

Throughout the course of this work I have been assisted by so many people it would not be possible to acknowledge them all. I would however like to give particular thanks to the following individuals and organisations:

All the patients and their families who participated in this work without whom it would not have been possible.

The FSP support group UK for their encouragement throughout the course of this research.

All the clinicians who provided clinical information and DNA samples on patients used in this study.

Dr L Ginsberg, Dr R Orrell, Dr J Workman, Dr R King and Professor A Shapira for performing, preparing and reporting the muscle biopsies.

Dr A Crosby, Dr H Patel, and Dr M Simpson for their instruction and supervision of the molecular genetic aspects of this work.

Dr J Bradley, Dr C Turner, Dr M Placzek, Dr A Misbahuddin, Dr L Bradley, Dr C Proukakis and Dr J Taanman for their help with the molecular biology, cell culture and mitochondrial respiratory chain assay techniques.

I am particularly grateful to my supervisor Dr T Warner for his support and encouragement with all aspects of this work from beginning to end.

Finally I would like to thank my wife, Caroline for her unquestioning support and belief in me throughout this period in our lives.

This work was supported by a research training fellowship from Action Medical Research UK.

CONTENTS

LIST OF FIGURES

LIST OF TABLES

LIST OF ABBREVIATIONS

AAA – Adenosine triphosphatases associated with various cellular activities

AD – Autosomal dominant

ALD – Adrenoleukodystrophy

AMN – Adrenomyeloneuropathy

APS – Ammonium persulphate

AR – Autosomal recessive

ATP – Adenosine triphosphate

ATPase – Adenosine triphosphatase

BSA – Bovine serum albumin

BSCL – Berardinelli-Seip congenital lipodystrophy

cM - Centimorgan

COX – Cytochrome oxidase

COQ1 – Coenzyme Q1

ddNTP - Dideoxynucleotide

DNA – Deoxyribonucleic acid

dNTP – Deoxynucleotide

DTNB – 5,5-dithio bis-2-nitrobenzoid acid

EDTA – Ethylenediaminetetraacetic acid

EEG – Electroencephalogram

EMG – Electromyography

FISH – Fluorescence in situ hybridisation

HCl – Hydrochloric acid

HIV – Human immunodeficiency virus

HSP – Hereditary spastic paraplegia

HTLV-1 – Human T-cell lymphotropic virus type 1

HMN – Hereditary motor neuronopathy

$KHCO_3$ – Potassium hydrogen carbonate

KCN – Potassium cyanide

$MgCl_2$ – Magnesium chloride

LD – Learnig difficulties

LOD – Logarithm of odds

MLD – Metachromatic leukodystrophy

MRI – Magnetic resonance imaging

NAD – Nicotinamide adenine dinucleotide

NADH – Reduced nicotinamide adenine dinucleotide

NaCl – Sodium chloride

NaOH – Sodium hydroxide

NOR – Nucleolus organiser region

OAA – Oxaloacetate

PAGE – Polyacrylamide gel electrophoresis

PCR – Polymerase chain reaction

PIC – Polymorphism information content

PMD – Pelizaeus-Merzbacher disease

SDS – Sodium dodecyl sulphate

SSCP – Single strand conformation polymorphism

Taq – Thermus aquaticus

TCC – Thin corpus callosum

TEMED – Tetramethylethylenediamine

Tris – Trishydroxymethylaminomethane

VDRL - Venereal disease research laboratory test

VLCFA – Very long chain fatty acids

Chapter 1

GENERAL INTRODUCTION

1.1 Definition

The term hereditary spastic paraplegia (HSP) is used to define a clinically and genetically heterogeneous group of inherited neurological disorders in which the predominant clinical feature is progressive spasticity and weakness of the lower limbs. The phenotype is further classified as "pure" or "uncomplicated" when symptoms and signs are confined to those of a progressive spastic paraparesis (with possible posterior column or bladder involvement) and "complicated" when major additional neurological or other clinical features are present (Harding, 1981). Inheritance may occur in an autosomal dominant, autosomal recessive or X-linked pattern for both pure and complicated forms of HSP.

1.2 Historical aspects

The first recorded description of HSP was published by Seeligmüller in 1876 in which he described four children from the same family affected by progressive spasticity and weakness of the lower limbs (Seeligmüller, 1876). Although often attributed with the earliest report of HSP, reflected in the fact that for many years the clinical syndrome came to bear his name, it was actually four years later that Von Strümpell (figure 1.1) reported the occurrence of a progressive spastic parapresis affecting two brothers (Strümpell, 1880). In his article Von Strümpell also referred to the father as being "a little lame", the first suggestion of autosomal dominant inheritance of HSP and demonstrating what would subsequently be recognised as a relatively common phenomenon of variable disease expression even within the same family. Subsequently Von Strümpell and the French physician Lorrain would add further cases to the literature in the late 19th century (Strümpell, 1893; Lorrain, 1898).

In the early part of the 20th century the condition became widely recognised with numerous cases described throughout the medical literature across different communities. Reports began to appear of families in which additional neurological or other clinical features were inherited in association with the spastic paraparesis, although there was much debate as to whether these represented separate disease entities. It was not until the pioneering works of Harding in the 1980's that formal criterion for the classification of HSP cases was proposed. She suggested the division into pure (uncomplicated) HSP in which the features were confined to those of a spastic paraparesis and complicated HSP where additional neurological or other

clinical features were present (Harding, 1981). She also recognised different patterns in disease phenotype and progression according to the age of onset and proposed a further division into type I (onset before 35 years) and type II (onset after 35 years) disease (Harding, 1984). It is only in recent years that this system of classification has been superseded through a greater understanding of the genetic mechanisms underlying HSP where it has become apparent that both pure and complicated HSP with either early or late onset may occur due to abnormalities in the same gene (Fink 2003).

Figure 1.1 Ernst Adolph Gustav Gottfried von Strümpell (1853-1925) [from http://clendening.kumc.edu/dc/pc/strumpell.jpg]

1.3 Epidemiology

HSP has been reported worldwide although the prevalence may vary between different communities. A number of epidemiological surveys carried out over the years have recorded population prevalence ranging from 0.1 to 9.6 per 100,000 (Silva et al., 1997). These are summarised in table 1.1. Some of these variations may be explained by differences in methodology between studies. Increased disease prevalence has been reported in surveys where secondary cases were identified by examination of all at risk relatives. The high proportion of asymptomatic individuals and those not seeking medical attention mean that in reports based solely on examination of hospital records the condition is likely to be under diagnosed.

Overall autosomal dominant inheritance is observed in approximately 80% of HSP cases with the majority of families demonstrating a pure phenotype (Reid, 1999). In the Republic of Ireland the prevalence of pure autosomal dominant HSP has recently been estimated to be 1.27/100,000 (McMonagle et al., 2002). Autosomal recessive HSP is observed less frequently outside areas where consanguineous marriages are commonplace (Sridharan et al., 1985), although may account for a significant proportion of apparently sporadic cases. Complicated phenotypes predominate in autosomal recessive HSP families with a number of distinct clinical syndromes observed in isolated communities such as the Old Order Amish in the USA (Cross and McKusick, 1967a; Cross and McKusick, 1967b).

Table 1.1 Epidemiological studies of HSP

Author (Survey year)	**Country (Region)**	**Population**	**Total number of patients**	**Prevalence/100,000**
Skre (1968)	Norway (Western)	725,000	31	4.3
Werdelin (1961-1975)	Denmark (Zealand)	1,179,000	22	1.9
Lucci (1980)	Italy (Reggio-Emilia)	412,324	4	1.0
Brignolio (1982)	Italy (Turin)	2,327,996	31	1.3
Sridharan (1984)	Libya (Benghazi)	519,000	11	2.1
Polo (1986)	Spain (Cantabria)	510,000	49	9.6
Hirayama (1987)	Japan	123,000,000	109	0.1
Filla (1989)	Italy (Molise)	335,211	9	2.7
Leone (1991)	Italy (Valle d'Aosta)	115,270	5	4.3
Silva (1994)	Portugal (Viana do Castelo)	250,061	5	2.0
McMonagle* (2002)	Republic of Ireland	5,436,000	69	1.27

* Pure autosomal dominant HSP only

1.4 Neuropathology

Autopsy findings in patients with HSP are rarely reported. Early studies were typically of patients with longstanding uncomplicated HSP phenotypes and focussed on changes within the spinal cord. The common pathological features, shown in figure 1.2, are axonal degeneration of the longest motor and sensory fibres of the central nervous system i.e. the corticospinal tracts, the fasciculus gracilis and the spinocerebellar tracts (Behan and Maia, 1974). Degeneration is maximal in the terminal portion of these axons (Deluca et al., 2004). In addition, there may be mild loss of anterior horn cells. Recently, additional cortical pathology including neuronal loss with tau-immunoreactive neurofibrillary tangles and balloon cells has been described in a patient carrying a SPG4 mutation with associated dementia although the significance of these changes remains uncertain (White et al., 2000).

Figure 1.2 Transverse section through the cervical spinal cord, stained for myelin with Luxol fast blue, in a patient with pure HSP demonstrating loss of myelinated axons in the corticospinal tracts and gracile fasciculi (from Harding AE. The hereditary ataxias and related disorders; Churchill Livingstone 1984)

1.5 Clinical features

The predominant clinical characteristic in HSP is of a progressive spastic paraparesis. However, disease variability both between and within families is a striking feature. The disease may present at any time from early childhood, with delayed motor milestones, to late in adult life. The onset of spasticity is often insidious, demonstrating variable rates of disease progression, but without distinct exacerbations or remissions. The spectrum of resulting disability ranges from entirely asymptomatic (10-20% of cases) to wheelchairbound, or in the most extreme cases bedridden individuals (Reid, 1999). Although disease severity increases with time, considerable variation is present.

The commonest presenting symptoms are of stiffness in the legs leading to difficulty walking or running with frequent stumbling or falls, premature wear on the shoes or the observation by others of an abnormal gait (Dürr et al., 1994). Urgency and frequency of micturition are also frequently reported although urinary symptoms tend to present later in the course of the disease (Neerup Jensen et al., 1998). Urinary incontinence may eventually become a problem although this is often exacerbated by problems with mobility.

The findings on neurological examination in patients with uncomplicated HSP phenotypes are typical of a spastic paraparesis with increased tone, a pyramidal pattern of muscle weakness, hyperreflexia and extensor plantar responses. However, unlike in acquired neurological diseases, spasticity is often out of proportion to the degree of weakness and may be the most disabling feature (Harding 1981). Pes cavus and other foot deformities are commonly reported, particularly in early onset cases (Coutinho et al., 1999). Abnormalities of posterior column function are a frequent finding with varying degrees of diminished vibration sense and proprioception (Figlewicz and Bird, 1999). Minor upper limb incoordination has also been described in some patients although it is unclear if this is due to sensory or cerebellar ataxia. Mild muscle wasting may also occur in longstanding uncomplicated cases although this most often reflects disuse atrophy in immobile patients. Subtle cognitive defects are however increasingly being recognised in patients with pure HSP phenotypes (Byrne et al., 2000; Tallaksen et al., 2003).

1.6 Complicated HSP phenotypes

Complicated HSP phenotypes, in which lower limb spasticity and weakness are accompanied by further neurological or other clinical features account for a significant proportion of cases (McDermott et al., 2002). Unlike pure forms of HSP they are most commonly inherited in an autosomal recessive fashion. The majority of X-linked cases, although rare overall, also present with complicated phenotypes.

A system for classification of complicated HSP phenotypes was first proposed by Harding and has since been regularly updated (table 1.2). A number of distinct clinical syndromes have been described. However, this system remains far from comprehensive, as many families do not fall into such clear categories. A number of syndromes have also been included, not generally recognised as forms of HSP, in which spasticity is a minor or variable feature.

Variability in clinical features has long been recognised both between and even within HSP pedigrees. It is now well established that mutations in the same gene may result in different clinical phenotypes. With advances in the understanding of the genetic basis of other neurological disorders it has become apparent that some families previously described as complicated HSP phenotypes may represent atypical presentations of other diseases such as Friedreich's ataxia or Alzheimer's disease (Gates et al., 1998; Crook et al., 1998). Eventually, a genetic system of classification of HSP will supersede clinically based ones, although until further advances in the molecular genetics of rare forms of HSP are made clinical classifications remain a useful tool for grouping families for research purposes and genetic counselling.

Table 1.2 Complicated HSP phenotypes

TYPE	CLINICAL FEATURES	INHERITANCE/GENE
CRASH syndrome	Agenesis of the corpus callosum, mental retardation, adducted thumbs, spastic paraparesis and hydrocephalus	X-linked – L1CAM
MASA syndrome	Mental retardation, aphasia, spasticity and adducted thumbs	X-linked – L1CAM
Silver syndrome	With distal amyotrophy	AD – SPG17
Kjellin syndrome	With mental retardation, amyotrophy and macular dystrophy	AR – SPG15
Troyer syndrome	With dysarthria, amyotrophy and skeletal abnormalities found in Old Order Amish population	AR – SPG20 (Spartin)
Mast syndrome	With dementia, cerebellar signs and extra-pyramidal features found in Old Order Amish population	AR – SPG21 (Maspardin)
Sjogren-Larsson syndrome	With icthyosis and mental retardation	AR – Fatty aldehyde dehydrogenase
Charlevoix-Saguenay syndrome	Spastic ataxia, neuropathy, dysarthria and myelinated nerve fibres on fundoscopy most commonly in Quebec	AR - Sacsin
With hyperekplexia	Single family with GLRA1 mutation in which hyperekplexia and spastic paraparesis cosegregate	AD – GLRA1
With dementia	Variable degrees of cognitive decline	AD/AR (including presenilin 1, spastin)
With cataracts and gastroesophogeal reflux	Plus distal amyotrophy	AD - SPG9
With cerebellar signs	Dysarthria, nystagmus, ataxia	AD/AR
With neuropathy	Motor and sensory neuropathies described	AD/AR
With optic atrophy	Decreased visual acuity	AD/AR
With disordered skin pigmentation	Hypo and hyper pigmented skin lesions described	AD/AR (including SPG24)
With thin corpus callosum	Associated with cognitive decline, most commonly in Japanese	AR (including SPG11)
With epilepsy	Absence, myoclonic, partial or generalised seizures	AD/AR
With extra-pyramidal features	Choreoathetosis, dystonia and rigidity all described	AD/AR
With syndactyly	Syndactyly in upper limbs	AD

1.7 Neurophysiology

Neurophysiological studies in HSP have shown variable results although some generalisations can be made. Most studies have found nerve conduction studies to be normal in pure forms of HSP, although subclinical sensory neuropathy may be detected (McLeod et al., 1977). Complicated HSP phenotypes can be associated with both axonal and demyelinating neuropathies (Cavanagh et al., 1979).

Cortical evoked potentials typically show reduced corticospinal tract conduction velocity and amplitude of the evoked potential in the lower limbs (Pelosi et al., 1991). In contrast, these may be normal or only mildly reduced in the upper limbs (Cruz Martinez and Tejada 1999). Similarly, somatosensory evoked potentials usually demonstrate conduction delay in dorsal column fibres from the lower limbs, which is less apparent when nerves in the upper limbs are stimulated (Bruyn et al., 1994).

Visual evoked responses and brainstem evoked potentials have been less extensively studied in HSP. A delayed or reduced P100 and various abnormalities of the brainstem auditory evoked responses have, however, been reported in a small number of patients (Rossini PM and Cracco JB, 1987). This raises the possibility of more widespread fibre loss in central conduction pathways.

1.8 Management

At present there are no treatments to alter the progress of the disease. Physiotherapy remains the most important method for managing spasticity. In some circumstances oral anti-spasticity drugs such as baclofen or tizanidine may be used to reduce muscle tone although risk increasing lower limb weakness and adversely affecting functional capacity. Their use may also be limited by side effects such as somnolence. In rare circumstances where oral baclofen is felt to be of benefit but poorly tolerated due to sedative effects intrathecal baclofen delivered via a pump has proved successful (Meythaler et al., 1992). Selective use of botulinum toxin injection may also be considered in the treatment of spasticity (Dunne et al., 1995). Bilateral foot drop stimulators have also been used to improve gait and reduce the risk of falls (Lyons et al., 2002). A number of other surgical appliances and mobility aids may be

tried to improve daily function and prevent complications. Surgical procedures such as tendon transfers or tenotomies may be considered when less invasive interventions have failed.

Bladder dysfunction is a common problem occurring in up to a third of all cases (Cartlidge and Bone 1973). The main cause is detrusor instability, which may be helped by medications such as oxybutynin (Neerup Jensen et al., 1998). Genetic counselling is available for patients who are planning a family and HSP support groups in the UK and abroad can provide advice and support to patients and their families. Genetic testing for mutations in the SPG4 gene has recently become available in the UK.

1.9 Molecular genetics

In recent years molecular genetic research has lead to significant advances in the understanding of the pathophysiology underlying the various forms of HSP. At the time of completion of this study (September 2003), 23 HSP loci had been mapped and pathogenic mutations identified in 11 different genes (table 3). These developments have helped establish a number of common, overlapping molecular mechanisms associated with abnormal development or degeneration of the corticospinal pathways in HSP and other neurodegenerative disorders (Crosby, 2003; Reid, 2003).

Table 1.3 Genetic classification of HSP

SPG locus	Chromosomal location	Inheritance	Gene product	Phenotype
SPG1	Xq28	X-linked	L1CAM	Complicated
SPG2	Xq22	X-linked	PLP/DM20	Pure and complicated
SPG3	14q11-q21	AD	Atlastin	Pure
SPG4	2p22-p21	AD	Spastin	Pure and complicated
SPG5	8q11.1-q21.2	AR	-	Pure
SPG6	15q11.1	AD	NIPA1	Pure
SPG7	16q24.3	AR	Paraplegin	Pure and complicated
SPG8	8q24	AD	-	Pure
SPG9	10q23.3-q24.2	AD	-	Complicated
SPG10	12q13	AD	KIF5A	Pure
SPG11	15q13-q15	AR	-	Pure and complicated
SPG12	19q13	AD	-	Pure
SPG13	2q24-q34	AD	HSP60	Pure
SPG14	3q27-q28	AR	-	Complicated
SPG15	14q22-q24	AR	-	Complicated
SPG16	Xq11.2	X-linked	-	Pure and Complicated
SPG17	11q12-q14	AD	BSCL2	Complicated
SPG18	Reserved	-	-	-
SPG19	9q33-q34	AD	-	Pure
SPG20	13q12.3	AR	Spartin	Complicated
SPG21	15q22.3	AR	Maspardin	Complicated
SPG22	Reserved	-	-	-
SPG23	1q24-q32	AR	-	Complicated
SPG24	13q14	AR	-	Pure
SPG25	6q23-q24.1	AR	-	Complicated

AD – autosomal dominant, AR – autosomal recessive

1.9.1 X-linked HSP

X-linked forms of HSP demonstrate both clinical and genetic heterogeneity. Mutations in two genes (L1CAM and PLP) have been identified in association with X-linked HSP, with at least two further genetic loci postulated. While an X-linked mode of inheritance cannot be definitively excluded in families lacking male-to-male transmission, overall they appear to be relatively rare. The phenotypes associated with X-linked HSP are predominantly complicated with a number of distinct clinical syndromes described.

1.9.1.1 SPG1 (L1CAM)

Mutations in the gene that encodes the neural cell adhesion molecule L1 (L1CAM) were the first to be described in patients with complicated X-linked forms of HSP (Jouet et al., 1994). L1CAM mutations may result in a broad range of clinical presentations including varying degrees of hydrocephalus, mental retardation, lower limb spasticity and flexion-adduction abnormalities of the thumbs (Jouet et al., 1995; Fransen et al., 1996). In addition to enlargement of the cerebral ventricles there may also be abnormal development of the corpus callosum and corticospinal tracts. The term CRASH syndrome (Corpus callosum hypoplasia, Retardation, Adducted thumbs, Spastic paraparesis and Hydrocephalus) has been adopted for L1CAM mutations with variations of this constellation of features (Fransen et al., 1995).

L1 is a transmembrane glycoprotein that is part of the superfamily of immunoglobulin-related cell adhesion molecules (Schachner, 1991). It is composed of six immunoglobulin-like domains and five fibronectin type-III repeats in the extracellular region, a single transmembrane domain and a short cytoplasmic tail (Schachner 1991). L1 therefore acts not only as an adhesion molecule but also functions as a receptor and plays a critical role in growth and guidance of axons in the developing nervous system (Burden-Gulley et al., 1997; Joosten and Gribnau, 1998). Over 90 different L1 mutations have now been described. These studies have revealed a striking correlation between the type of mutation in the L1CAM gene and the severity of the disease. Mutations that produce truncations in the extracellular domain of the L1 protein are more likely to produce severe hydrocephalus, grave mental retardation or early death compared with point mutations in the extracellular domain or mutations affecting only the cytoplasmic domain of the protein. Point mutations in the extracellular domain

generally produce more severe neurologic problems than mutations in just the cytoplasmic domain which tend to result in hydrocephalus alone (Jouet et al., 1995).

1.9.1.2 SPG2 (PLP)

Linkage analysis in additional pure and complicated X-linked HSP pedigrees identified a further disease locus (SPG2) at Xq21-22 (Bonneau et al., 1992). Pelizaeus-Merzbacher disease (PMD), an infantile-onset progressive leukodystrophy characterised by neonatal hypotonia, nystagmus, psychomotor retardation, spasticity, dystonia and ataxia, had previously been mapped to this region (Boulloche and Aicardi, 1986). PMD is caused by mutations in or duplications of the proteolipid protein (PLP) gene, whose protein product and its splice variant DM20 are major protein components of myelin in the CNS (Gencic et al., 1989). The PLP gene was therefore considered a potential candidate as the second X-linked HSP gene.

Subsequently, mutations in SPG2 families were identified in PLP, confirming both pure and complicated forms of X-linked HSP were allelic with PMD (Saugier-Veber et al., 1994). The mechanisms underlying genotype-phenotype correlations between these different presentations associated with PLP mutations remains incompletely understood. An association between the trafficking capability of mutant PLP and the severity of the disease has been postulated (Yool et al., 2000). Disruptions of PLP mediated axonal-glial interactions are thought to underlie axonal degeneration identified in both patients and animal models (Griffiths et al., 1998). An increased dose of PLP due to gene duplication or mutations resulting in structurally altered translated PLP are thought to engulf the secretory pathway and compromise oligodendrocyte function leading to the PMD phenotype (Ellis et al., 1994). Conversely, mutations allowing PLP and DM20 to traverse the secretory pathway and reach the cell surface generally result in milder phenotypes (Cailloux et al., 2000). However, there may be phenotypic variation even within families indicating additional genetic and possibly environmental factors act as disease modifiers.

1.9.1.3 Further genetic heterogeneity in X-linked HSP

At least two further loci for X-linked HSP have been proposed. In 1997 Steinmüller and colleagues studied a 4-generation family with severe X-linked spastic paraplegia in which affected males were quadriplegic with motor aphasia, reduced vision, mild mental retardation, and dysfunction of the bowel and bladder (Steinmüller et al., 1997). Disease onset occurred during the first 3 months of life. All females of the family were normal. By linkage and haplotype analysis they assigned the disease locus to Xq11.2-q23. This region contains the PLP gene although no mutations were identified and the existence of a third X-linked HSP locus was proposed.

Subsequently, Tamagaki and colleagues described a Japanese family with a pure form of spastic paraplegia in 2 brothers and a maternal uncle, associated with a variant X chromosome that showed a faintly stained gap at Xq11.2 (Tamagaki et al., 2000). The mother of the brothers also had the variant X chromosome but was clinically unaffected. The gaps were Ag-NOR staining positive, C-banding negative, rDNA FISH analysis positive, and alpha-satellite FISH analysis negative. This gap, therefore, represented an insertion of the nucleolus organiser region (NOR) derived from the short arm of an acrocentric chromosome. The variant X chromosome of the mother was randomly inactivated. It was therefore proposed that the NOR insertion in the affected members of the family disrupted a hitherto unknown gene for a pure form of spastic paraplegia, situated at Xq11.2, and caused the disorder. This region has been assigned the SPG16 locus and overlaps that mapped by Steinmuller. The diseases observed in the two families may therefore represent allelic disorders.

Claes and colleagues have described a further pedigree with a complicated X-linked HSP phenotype in which four males in two generations were affected by severe mental retardation, slowly progressive spastic paraplegia, facial hypotonia, and maxillary hypoplasia (Claes et al., 2000). Linkage to the known X-linked HSP loci was excluded and although the size of the pedigree was too small to generate statistically significant LOD scores, multipoint linkage analysis indicated two possible candidate regions at Xp21.1-Xq21.3 and Xq23-Xq27.

Additional evidence for a further HSP locus on the X-chromosome comes from Starling and colleagues who also mapped a family with a pure HSP phenotype to an approximately 4cM region overlapping the PLP gene in which a mutation was excluded (Starling et al., 2002).

Spasticity may also be a feature in a number of other well-defined X-linked disorders not classified amongst the HSPs.

1.9.2 SPG3A (Atlastin)

SPG3A was the first autosoaml dominant HSP locus to be mapped in 1993. Hazan and colleagues performed linkage analysis in 3 large pure autosomal dominant HSP pedigrees and identified tight linkage to chromosome 14q in one family (Hazan et al., 1993). The remaining two families were excluded from this region confirming that autosomal dominant HSP was genetically heterogeneous. In 1995 Gispert and colleagues also identified linkage to 14q in one of three German autosomal dominant HSP pedigrees permitting the reduction of the disease locus to approximately 7cM (Gispert et al., 1995). Finally Rainier and colleagues further refined the SPG3A locus to a 2.7cM region at chromosome 14q11-q21 in a large early onset pure autosomal dominant HSP family before disease-specific mutations were identified in the SPG3A gene (Rainier et al., 2001).

From within the refined SPG3A interval Zhao and colleagues sequenced 13 candidate genes in 3 SPG3A linked pedigrees (Zhao et al., 2001). All three were found to possess pathogenic mutations in a gene encoding a novel protein with significant homology to the dynamin family of GTPases, which they named atlastin. The mutations were all situated within the N-terminal region, resulting in the alteration of amino acids in the conserved GTPase domain. Sequencing of the SPG3A gene in a further 10 early onset autosomal dominant HSP kindred, in which linkage analysis had not been performed, identified a further two families in whom all affected individuals possessed the same R239C mutation found in one of the original linked pedigrees. Although these families were not apparently related a distant founder effect could not be excluded.

Dynamins, the proteins most closely associated with atlastin, are known to play a role in a wide variety of vesicle trafficking events (McNiven et al., 2000). In addition, this group of proteins has been implicated in the maintenance and distribution of mitochondria (Pitts et al., 1999) and have been shown to associate with cytoskeletal elements such as actin and microtubules (Ochoa et al., 2000). The precise mechanism by which atlastin mutations result in HSP remains unclear. Recent studies have confirmed that the atlastin protein is localised

predominantly in adult brain, particularly pyramidal neurons in the cerebral cortex and in the hippocampus (Zhu et al., 2003). In cultured cortical neurons, atlastin co-localised most prominently with markers of the Golgi apparatus and membrane fractionation and protease protection assays confirmed that atlastin is an integral membrane protein with two transmembrane domains (Zhu et al., 2003). This would suggest that atlastin is predominantly involved in Golgi membrane dynamics or vesicle trafficking and that disruption of this process in the adult central nervous system underlies the neurodegenerative process.

1.9.3 SPG4 (Spastin)

The SPG4 locus on chromosome 2p was first identified in 1994 (Hazan et al., 1994; Hentati et al., 1994b). Linkage studies in further autosomal dominant HSP families suggested that this was by far the commonest cause of HSP, accounting for between 40-50% of all autosomal dominant cases (Hazan et al., 1999). After obtaining sequence data of the entire SPG4 locus Hazan and colleagues identified a potential candidate gene encoding a novel AAA protein, subsequently named spastin (Hazan et al., 1999). Sequencing of this gene in 7 SPG4 linked families confirmed the presence of missense, nonsense and splice site mutations in affected individuals.

SPG4 mutation screening in autosomal dominant HSP patients from around the world has now identified over 100 different mutations, the majority being unique to each family (Lindsey et al., 2000; Sauter et al., 2002; Meijer et al., 2002). The phenotype is typically of a pure form of HSP but with variable age of onset and disease severity (Dürr et al., 1996; Santorelli et al., 2000a). No clear correlation has been observed between genotype and phenotype (Yip et al., 2003). Subtle cognitive impairment has, however, increasingly been recognised in association with disease progression (Byrne et al., 2000; Tallaksen et al., 2003).

Spastin is expressed ubiquitously in adult and foetal tissues (Hazan et al., 1999). Both nuclear and cytoplasmic subcellular localisations have been postulated (Errico et al., 2002; Charvin et al., 2003;). Two isoforms exist with alternative splicing of exon 4 (Svenson et al., 2001). The isoform lacking exon 4 predominates in adult spinal cord tissue and as no mutations have yet been identified in exon 4 suggesting that this is the pathologically relevant form (Proukakis et al., 2002).

Recent studies have confirmed that spastin interacts with microtubules in an ATP dependent manner (Errico et al., 2002). The microtubule-binding region lies within the N-terminal region of the protein. Studies using cells expressing mutant forms of spastin have shown disruption to microtubule dynamics (McDermott et al., 2003). The impairment of the microtubule skeleton in long axons and in particular the disruption of intracellular transport have therefore been proposed as a potential mechanism underlying the neurodegeneration in this form of HSP (Reid, 2003).

1.9.4 SPG5A

In 1994 Hentati and colleagues established linkage to a 32.8cM locus (SPG5A) at the pericentromeric region of chromosome 8 in four of five Tunisian autosomal recessive HSP families (Hentati et al., 1994). The clinical picture in all affected individuals was of early disease onset (ranging from 1-20 years) with bladder dysfunction and mild posterior column sensory impairment. An additional Tunisian family with a clinically indistinguishable phenotype was excluded from linkage to this locus, providing the first evidence for genetic heterogeneity in autosomal recessive HSP. Subsequently, linkage to the SPG5A locus was identified in one further Algerian family from a total of 23 Algerian and Portuguese pedigrees (Coutinho et al., 1999). It was therefore postulated that SPG5A linked autosomal recessive HSP was likely to be rare and may be restricted to the North African population.

1.9.5 SPG6 (NIPA1)

Fink and colleagues mapped the third autosomal dominant HSP locus (SPG6) to the centromeric region of chromosome 15q in 1995 (Fink et al., 1995a). The SPG6 critical interval was subsequently further refined to a 6.1cM region between D15S128 and the centromere (Rainier et al., 2000). This part of the chromosome is commonly involved in deletions in patients with Prader-Willi syndrome or Angelman syndrome, conditions characterised by genetic imprinting (Nicholls and Knepper, 2001). Analysis of a large autosomal dominant HSP family linked to SPG6 did not demonstrate any evidence of imprinting (Fink et al., 1995b). Ranier and colleagues therefore sequenced the non-imprinted genes within the SPG6 critical region and identified a missense mutation in exon 1 of the NIPA1 gene (159 C to G). This sequence change was not identified in control samples but the

same mutation was found in an additional unrelated autosomal dominant HSP family, providing further evidence of the pathogenic nature of the mutation (Rainier et al., 2003).

The precise function of the NIPA1 protein remains unclear, although predictions based on the amino acid sequence and hydrophobicity analysis suggest it is an integral membrane protein acting as either a receptor or transporter (Rainier et al., 2003). The fact that patients with Prader-Willi syndrome or Angelman syndrome do not develop features of a spastic paraparesis would seem to indicate that mutations in NIPA1 exert a pathogenic effect through a gain of function or dominant negative mechanism.

1.9.6 SPG7 (Paraplegin)

SPG7 was the first autosomal recessive HSP gene to be characterised. Following linkage to 16q24.3 in a large consanguineous Italian family with a variable complicated phenotype (De Michele et al., 1998), Casari and colleagues discovered a 9.5kb deletion corresponding to the last five exons of the SPG7 gene (Casari et al., 1998). SPG7 consists of 17 exons spanning approximately 52 kb. The protein product, named paraplegin, is composed of 795 amino acids and localises to mitochondria. It was originally found to share its closest amino acid sequence homology with the yeast mitochondrial metalloproteases Afg3, Rca1 and Yme1 (Casari et al., 1998; Settasatian et al., 1999). These proteins are members of the AAA protein superfamily (ATPase associated with diverse cellular activities) which are found widely in both prokaryotic and eukaryotic cells and play an important role in a variety of cellular activities including cell division, transcription, organelle biogenesis, vesicle transport and enzyme assembly (Patel and Latterich, 1998). More specifically, yeast mitochondrial ATPases are known to possess both proteolytic and chaperone-like activities at the inner mitochondrial membrane where they are involved in the assembly and degradation of proteins in the respiratory chain complex (Pearce, 1999).

SPG7 mutations have been identified in patients with both pure and complicated HSP phenotypes (Casari et al., 1998). Muscle biopsy analysis from severely affected individuals revealed characteristic changes of mitochondrial oxidative phosphorylation defects including ragged-red fibres, cytochrome oxidase negative (COX) and succinate dehydrogenase (SDH) positive fibres. Electron microscopy confirmed an accumulation of abnormal mitochondria

containing paracrystalline inclusions in a "parking lot" pattern. However, in two less severely affected individuals only a few scattered COX negative fibres were seen.

1.9.7 SPG8

Hedera and colleagues identified tight linkage to chromosome 8q23-24 in a large autosomal dominant HSP kindred in 1999 (Hedera et al., 1999a). Clinical analysis showed an uncomplicated phenotype indistinguishable from other pure forms of HSP (Hedera et al., 1999b). Reid and colleagues then subsequently mapped a further family to 8q24 and refined the SPG8 locus from 6.2 cM to a 3.4-cM region between markers D8S1804 and D8S1179 (Reid et al., 1999). Affected individuals from this family also had an uncomplicated phenotype but with an older age of onset and increased disability when compared to non-SPG8 linked families. Linkage to SPG8 has also been established in a Brazilian autosomal dominant HSP kindred in whom the authors studied muscle from affected individuals for the beta 1 syntrophin protein, the gene for which is located within the refined SPG8 locus (Rocco et al., 2000). Immunohistochemical and Western Blot studies showed that the distribution, expression, and apparent molecular weight of the beta 1 syntrophin protein were comparable to those of normal control individuals. Abnormalities of the beta 1 syntrophin gene were therefore felt unlikely to be implicated in this form of autosomal dominant HSP.

1.9.8 SPG9

Seri and colleagues first reported a rare form of autosomal dominant HSP in an Italian family associated with bilateral cataracts, persistent vomiting secondary to gastroesophageal reflux and distal amyotrophy (Seri et al., 1999). Linkage analysis mapped the locus for this syndrome to chromosome 10q23.3-q24.2 (SPG9). Subsequently a further British family with the same phenotype was also linked to the SPG9 locus although further refinement of the critical interval was not possible (Lo Nigro et al., 2000). Muscle biopsy was, however, performed in an affected individual in which no evidence of mitochondrial dysfunction was found.

1.9.9 SPG10 (KIF5A)

After exclusion of linkage to the known autosomal dominant HSP loci Reid and colleagues mapped a further large pure autosomal dominant HSP family to a 9.2cM region on chromosome 12q13, SPG10 (Reid et al., 1999). Additional detailed mapping in this family then refined the SPG10 locus to a 6.95cM region between markers D12S270 and D12S335 (Reid et al., 2001). Sequencing of the sodium channel gene SCN8A excluded this as a candidate from within this region. Reid and colleagues then sequenced a further 30 candidate genes from within the SPG10 critical interval and identified a missense mutation (A767G) in the motor domain of the neuronal kinesin heavy chain gene KIF5A (Reid et al., 2002). The mutation was not identified in over 200 control subjects supporting a pathogenic role in this form of HSP.

The microtubule-associated proteins of the kinesin and dynein families act as molecular motors that transport intracellular material along microtubules, kinesins in the anterograde direction and dyneins in the retrograde direction (Goldstein and Yang, 2000). The missense mutation in KIF5A has been predicted to disrupt stimulation of the motor ATPase by microtubule binding (Reid et al., 2002). This has provided some of the strongest evidence to date implicating defective axonal transport in the pathogenesis of HSP.

1.9.10 SPG11

A complicated form of autosomal recessive HSP with thin corpus callosum (TCC) was first described in Japan (Iwabuchi et al., 1994). In 1999 a recessive HSP locus (SPG11) was mapped to chromosome 15q13-15 in Italian and North American families with and without TCC (Martinez Murillo et al., 1999). Subsequently linkage analysis showed tight linkage to the chromosome 15q13-15 locus in 10 of 13 Japanese families with HSP complicated by TCC and mental impairment (Shibasaki et al., 2000).

Progressive cognitive impairment is a characteristic feature of HSP with TCC (Ueda et al., 1998). Other families have been reported with cataracts, peripheral neuropathy and ataxia (Nakamura et al., 1995; Okuda et al., 2002). Although most families described have been too small for meaningful linkage analysis on an individual basis the majority are consistent with

linkage to 15q13-15. However, linkage to SPG11 has been excluded in several families with TCC, confirming the genetic heterogeneity of this form of HSP.

1.9.11 SPG12

In 2000 Reid's group in Cambridge mapped their third autosomal dominant HSP locus to a 16.1-cM region on chromosome 19q, SPG12 in a large family with an uncomplicated phenotype (Reid et al., 2000). Ashley-Koch and colleagues then identified an additional autosomal dominant HSP kindred linked to SPG12 and refined the critical region to a 5 cM region between markers D19S868 and D19S220 (Ashley-Koch et al., 2001). Most recently, Orlacchio and colleagues described a third SPG12 linked family allowing a further refinement of the critical interval to a 3.3 cM region between D19S416 and D19S220 and excluded a homologue of the proteasome 26S subunit ATPase as a candidate from within the refined locus (Orlacchio et al., 2002).

1.9.12 SPG13 (Hsp60)

SPG13 was initially mapped to chromosome 2q24-34 in a French family with a pure form of autosomal dominant HSP (Fontaine et al., 2000). The genes encoding the human mitochondrial chaperonin Hsp60 and its co-chaperonin Hsp10 were also localised to this region and therefore considered as potential candidates in this family. Sequencing of these genes revealed a missense mutation, G292A, in the Hsp60 gene, co-segregating with the disease, resulting in the substitution of a valine residue at position 72 in the Hsp60 protein with isoleucine, V72I (Hansen et al., 2002). The mutation was not identified in 800 control chromosomes supporting a pathogenic role. To further support this a complementation assay demonstrated that wild-type Hsp60 but not Hsp 60 with the V72I mutation, in combination with Hsp10 was able to support the growth of E. coli whose own chaperonin genes had been deleted.

1.9.13 SPG14

Using homozygosity mapping in a consanguineous family with a complicated form of autosomal recessive HSP, Vazza and colleagues identified a 4.5cM region on chromosome 3q27-28 (SPG14) that co-segregated with the disease (Vazza et al., 2000). The phenotype in the three affected individuals included a spastic paraparesis with cognitive impairment including memory difficulties, visual agnosia, perseveration and confabulation. MRI of the brain and EEG were normal in their index case but EMG studies showed evidence of a distal motor neuropathy. To date this is the only family linked to the SPG14 locus.

1.9.14 SPG15

In 1959 Kjellin first described a family with autosomal recessive HSP complicated by central retinal degeneration with macular pigmentation, cognitive impairment and amyotrophy (Kjellin, 1959). In 1997 Webb and colleagues described 2 further Irish families with a complicated form of autosomal recessive HSP almost identical to that described by Kjellin in whom they also noted dysarthria with progressive cognitive decline from the second decade (Webb et al., 1997). Genetic linkage analysis in these families generated a combined LOD score of 4.2 at zero recombination for a marker on chromosome 14 (D14S77). Subsequent haplotype analysis then defined an interval of approximately 19cM on chromosome 14q (SPG15) associated with the disease (Hughes et al., 2001).

1.9.15 SPG17 (BSCL2)

Silver syndrome, first described in 1966, is a rare form of autosomal dominant HSP complicated by distal amyotrophy (Silver, 1966). The small muscle weakness and wasting is usually most prominent in the hands (figure 1.3) but may also affect the feet. However, families may show evidence of incomplete penetrance with a wide variability in clinical expression. EMG studies in patients with Silver syndrome have shown evidence of both a motor neuronopthy and peripheral motor neuropathy (Windpassinger et al., 2003).

Following exclusion of linkage to any of the known autosomal dominant HSP loci, Patel and colleagues mapped a Silver syndrome locus (SPG17) to a 13cM region on chromosome 11q12-14 in a single large English family (Patel et al., 2001a; Patel et al., 2001b). However, a

further family with the same clinical phenotype was excluded from this locus demonstrating genetic heterogeneity of the syndrome. Further linkage studies by Windpassinger and colleagues in four Austrian families with Silver syndrome refined the candidate gene interval to 5.9cM between markers D11S1765 and D11S987 before they eventually identified hereozygous mutations in the Berardinelli-Seip congenital lipodystrophy (BSCL2) gene in families with SPG17 linked Silver syndrome (Windpassinger et al., 2003; Windpassinger et al., 2004). Mutations were also identified in patients with a phenotype in which distal amyotrophy and weakness were the only features designated as hereditary motor neuronopathy type V (HMNV). These mutations were restricted to the N-glycosylation motif.

Null mutations in BSCL2, which encodes the protein seipin, were previously shown to be associated with autosomal recessive Berardinelli-Seip congenital lipodystrophy. Seipin is a transmembrane protein that is localized to the endoplasmic reticulum. The precise function of seipin remains unknown although its homology to midasin, an AAA (ATPases associated with various cellular activities) domain-containing nuclear protein that is involved in RNA transport, might explain how mutant forms of seipin can cause such clinically distinct syndromes (Windpassinger et al., 2004).

Figure 1.3 Distal amyotrophy of the small hand muscles in Silver syndrome (SPG17)

1.9.16 SPG19

Valente and colleagues reported a large Italian family with a late onset, relatively mild form of autosomal dominant HSP. Linkage analysis and haplotype reconstruction established a further locus (SPG19) on chromosome 9q33-q34 (Valente et al., 2002). To date this is the only family linked to this locus.

1.9.17 SPG20 (Spartin) and SPG21 (Maspardin)

Troyer syndrome and Mast syndrome are complicated forms of autosomal recessive HSP originally described in the Old Order Amish population. The cardinal features of Troyer syndrome are of a progressive spastic paraparesis associated with pseudobulbar palsy, distal amyotrophy, mild developmental delay and short stature (Cross and McKusick, 1967a). While there have been a few reports of similar cases outside the Old Order Amish community these have not manifested all the characteristic features of the Troyer syndrome and have been labelled Troyer-like syndromes.

In 2002 Patel and colleagues mapped the Troyer syndrome locus to a 731kb region on chromosome 13q12.3, SPG20 (Patel et al., 2002). Sequencing of all coding exons and adjacent splice signals within this region detected a single base deletion (1110delA) in exon 4 of a gene encoding a novel protein named spartin. The precise role of spartin remains unclear but the identification of a conserved functional domain, also present in spastin and molecules involved in endosomal trafficking (MIT domain) suggest a possible role in microtubule dynamics and cellular trafficking (Ciccarelli et al., 2003).

The Mast syndrome is characterised by a later onset spastic paraparesis associated with progressive cognitive decline (Cross and McKusick, 1967b). Cerebellar and extrapyramidal features may also occur in advanced cases. Homozygosity mapping in 14 affected patients together with haplotype analysis defined the Mast syndrome locus to a 156kb interval at chromosome 15q22.31, SPG 21 (Simpson et al., 2003). Sequencing of the three overlapping transcripts from within this region identified a single base insertion (601insA) in 33kDa acid-cluster protein gene (ACP33). This frameshift mutation results in the truncation of the protein product maspardin. Maspardin localises to endosomal and trans-Golgi transport vesicles and is predicted to play a role in protein transport and sorting.

Since the characterisation of these two genes responsible for Troyer syndrome and Mast syndrome there have yet to be any confirmed cases outside the Old Order Amish population.

1.9.18 SPG23

Autosomal recessive HSP complicated by skin hypopigmentation has been described in two consanguineous Arab families (Lison et al., 1981; Mukamel et al., 1985). Blumen and colleagues performed a genome wide screen in one of these kindred in which four individuals were affected by spastic paraparesis, skin hypopigmentation, microcephaly and cognitive impairment (Blumen et al., 2003). They mapped the gene locus to a 25cM region on chromosome 1q24-q32 (SPG23) with a peak LOD score of 3.05.

1.9.19 SPG24

Hodgkinson and colleagues recently reported a consanguineous family from northern Saudi Arabia in which children were affected by either a spastic paraparesis, sensorineural deafness or both (Hodgkinson et al., 2002). The two conditions segregated independently. Using homozygosity mapping the paraparesis mapped to a 1.8Mb region of chromosome 13q14 (SPG24).

1.9.20 SPG25

Zortea and colleagues reported a consanguineous Italian family in which 4 of 8 siblings were affected with adult-onset (range 30 to 46 years) pyramidal symptoms in the lower limbs (Zortea et al., 2002). In all 4 affected individuals, the paraparesis was accompanied or preceded by spinal pain radiating to the upper or lower limbs, with MRI showing evidence of spinal disc herniation in the cervical or thoracic spine. Surgery resulted in a partial improvement in all of them, although a compressive myelopathy was not felt to be the cause of the spastic paraparesis. A genome wide search with subsequent multipoint analysis yielded a maximum LOD score of 3.28 between markers D6S1699 and D6S314 on chromosome 6q23.3-q24.1. This is the first example of disc herniation associated with a neurological

syndrome linked to a human chromosomal region and has been classified as a locus for autosomal recessive HSP (SPG25).

1.10 Common molecular themes

The identification of some of the genes responsible for different forms of HSP has highlighted a number of common molecular mechanisms underlying the pathogenesis of the disease. Abnrormal development of the corticospinal tracts, mitochondrial dysfunction and defective intracellular transport have all been shown to play a role in the pathogeneisis of various forms of HSP (figure 1.4). These theories are discussed further in section 8.9

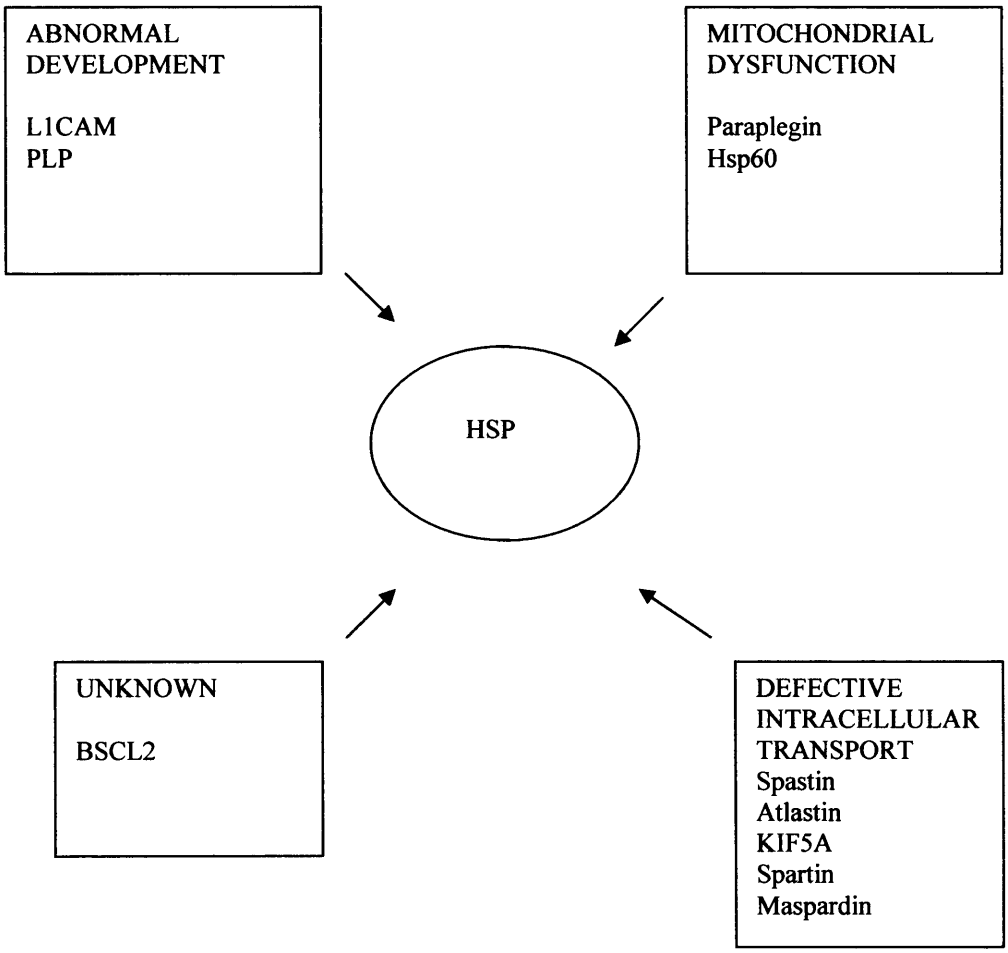

Figure 1.4 Pathological mechanisms associate with HSP genes (adapted from Wilkinson PA and Swash M. Hereditary spastic paraplegia and primary lateral sclerosis. In: Gilman S ed. Neurobiology of disease. Elsevier 2007)

1.11 Aims of the study

The aim of this project was to study the clinical, biochemical and molecular genetic features of patients with autosomal recessive hereditary spastic paraplegia, predominantly in the UK population. This included:

1) Detailed clinical assessment of patients to establish the nature and frequency of different phenotypes present in the UK population.
2) Linkage analysis using markers around previously identified loci to identify the relevance of these in UK pedigrees and refine these loci further to allow the screening of potential candidate genes.
3) SPG7 gene mutation screening of patients in whom linkage analysis had not excluded the chromosome 16 locus.
4) Genome wide linkage analysis in autosomal recessive pedigrees not linked to any of the known loci in an attempt to identify new loci for autosomal recessive HSP.
5) Analysis of muscle biopsies in a selected number of patients for histology and mitochondrial respiratory chain function to assess the role of oxidative phosphorylation defects in the pathogenesis of the disease.

In addition, during the course of the study the SPG3A gene was identified, therefore patients with early onset pure autosomal dominant HSP were identified from an existing database for screening for mutations in this gene. DNA from a Kuwaiti family with a complicated form of autosomal recessive HSP also became available and this family was included for genome wide linkage analysis.

Chapter 2

MATERIALS AND METHODS

2.1 Overview of general principles

2.1.1 Polymorphic genetic markers

The location of a disease-causing gene within the genome can be determined using the techniques of linkage mapping. This methodology is used in locating the gene by detecting the cosegregation of the disease phenotype with a previously positioned genetic marker of known location. Polymorphic markers are specific DNA sequences that have more than one form in the population. Many types of polymorphic marker exist, but the most commonly used in linkage analysis are the short tandem repeat polymorphisms, also known as microsatellite markers. Microsatellite DNA consists of multiple copies of motifs that can occur in perfect tandem, as interrupted repeats, or together with another repeat type (Weber, 1990). Microsatellite markers, which occur on average every 30kb (Beckman and Weber, 1992) have multiple alleles and may have heterozygosity frequencies of >70%, making them particularly useful for genetic analysis. An additional advantage of microsatellite markers is that they can be readily analysed using the polymerase chain reaction, or PCR (Weber and May, 1989).

The amount of useful information that can be obtained from a polymorphic marker depends on the number of alleles and their relative frequencies in the population. A statistical measure of the informativeness of a marker is provided by its PIC (polymorphism information content), with a PIC value of >0.5 indicating high informativity (Botstein et al., 1980). PIC values take into account all possible allele combinations and allele frequencies in the population. Essentially, the more polymorphic a marker is the higher its PIC value and the more useful information that can be gained from it.

2.1.2 Linkage analysis and genomewide screening

During meiosis, when homologous chromosomes align and pair, one or more recombination events take place between each pair. This means that at some point along the DNA of the two chromosomes, a break occurs and the fragments are exchanged. Recombination events provide information about how close together two loci are. If two loci are close together, there is a small likelihood that recombination will occur between them. In this case, the two loci (e.g. a polymorphic marker and disease gene) would tend to be inherited together

(cosegregate). If, however, they are far apart, there is a much greater chance of a recombination event occurring and they would show less cosegregation.

The degree of linkage is measured in centiMorgans (cM), a percentage measure. Two loci, which show a recombination rate of 1%, are defined as being 1cM apart. A recombination fraction (θ) describes how often any two loci are inherited together. If they are very close together, they invariably cosegregate, and θ approaches 0. A recombination fraction of θ=0.5 means that the two loci are inherited together half of the time, which would be expected if the two loci are completely independent (i.e. on separate chromosomes).

The LOD (logarithm of odds) score method for calculating the probability of genetic linkage was devised by Newton E Morgan in 1955 based on sequential testing procedures. It calculates the logarithm (base 10) of the likelihood that two alleles are linked divided by the likelihood that they are not linked i.e. the observation occurred by chance. Calculations are performed over a range of recombination fractions (θ) between 0-0.5.

$$\text{LOD } (Z) = \log_{10} [L(\theta)/L(0.5)]$$

The θ that gives the highest LOD score is an estimation of the distance in cM between the two markers. A LOD score of >3.0 is taken to be statistically significant as this means that the likelihood of linkage occurring at this distance is 1,000 times greater than occurring by chance. A LOD score of <-2.0 is used to exclude linkage as this as this means it is 100 times more likely that the two alleles are not linked. However, a LOD score of 3.0 actually correlates with a probability of 20:1. This is because of the prior probability that two autosomal loci are linked due to the fact that they must be on one of 22 pairs of chromosomes. The exception is for X-linked disorders where a LOD score of >2.0 is considered to be significant.

Genomewide linkage analysis is a screening process using a large number of microsatellite markers distributed relatively evenly throughout the genome to search for a chromosomal region cosegregating with the disease phenotype. This process involves PCR amplification of the microsatellite markers. One primer in each pair is fluorescently labelled so that the PCR products can be analysed by a fluorescently based detection method.

Multipoint mapping involves the genotyping of each individual of the family in which the disease is segregating with a genomewide set of markers. The ultimate goal of this type of mapping strategy is to locate the disease gene with respect to this marker framework. The genotype data generated is imported into a computer programme (e.g. GENEHUNTER), which calculates LOD scores at each marker interval of the framework map and simultaneously analyse information from a number of polymorphic markers. The result of this type of analysis is typically presented as a likelihood curve plotted against map location. The maximum LOD score on this curve (Zmax) represents the most likely location of the disease gene.

Homozygosity mapping provides a rapid means of mapping autosomal recessive genes in consanguineous families. This strategy assumes that affected individuals within an inbred population will have inherited two copies of the same ancestral mutation, and therefore will be homozygous for the flanking genetic material. Genotype data is analysed using compatible computer programmes such as HOMOZ.

2.1.3 The polymerase chain reaction (PCR)

PCR is the in vitro enzymatic amplification of a defined DNA segment many times so that it constitutes the only detectable DNA (Saiki et al., 1988). In cells, DNA replication begins with a short primer sequence, which is extended by the enzyme DNA polymerase. PCR utilises two primers, which are synthetic DNA sequences (typically 15-30 bp long) designed from existing sequence data, flanking the desired target sequence. PCR involves repeated cycles of denaturing to produce single-stranded DNA, primer annealing, and new strand synthesis by extension of the annealed primer using a thermostable DNA polymerase. Taq polymerase, isolated from Thermus aquaticus (a thermophilic bacterium) is most commonly used (Strachan and Read, 1997). The initial products of the PCR act as templates for subsequent rounds of synthesis with initial exponential amplification of the target sequence. During the early cycles there is exponential amplification, then in later cycles there is linear product accumulation, and eventually a "plateau" is reached. Twenty to thirty cycles will amplify the target sequence about 10^5-fold from 1μg of genomic DNA (Davies and Read, 1992).The primers are the most important determinant of PCR efficiency, and the annealing temperature

depends almost entirely on their sequence. The concentrations of $MgCl_2$ and dNTPs in the PCR mixture are also important for efficient and specific DNA amplification.

2.1.4 Polyacrylamide gel electrophoresis (PAGE)

Polyacrylamide gels are used to separate small DNA fragments (<500bp). A voltage is applied across the gel and acts on the negatively charged DNA. The principle underlying PAGE is that smaller DNA fragments are able to move faster through the gel matrix than larger DNA fragments. PAGE is very sensitive and has a resolving power of up to 1bp. The size of the pores in the gel through which DNA migrates determines the size of the fragment that can be resolved. The pore size can be varied by adjusting the concentrations of polyacrylamide and the cross-linking reagent. Non-denaturing and denaturing polyacrylamide gels can be used to separate double-stranded and single-stranded DNA fragments, respectively. In denaturing PAGE, double-stranded DNA samples are denatured, usually by heating the DNA in a solution containing a chemical denaturant, for example formamide. These samples are then loaded onto polyacrylamide gels also containing a chemical denaturant, such as urea, to ensure that the DNA strands remain single-stranded, and an electric current is applied across the gel. In non-denaturing PAGE, the samples are electrophoresed in the absence of any denaturant.

2.1.5 DNA sequencing

DNA sequencing is a technique used to determine the sequence of bases in a length of DNA. The DNA sequence of a particular gene can indicate the function of the protein product, as well as the effect of a specific mutation, and can point to functional domains that may be present in related genes. The process is similar to PCR; however, there is one additional ingredient added to the thermocycling reaction. A proportion of the dNTPs are dideoxyribonucleotides (ddNTPs). These prevent further elongation of the DNA sequence. If appropriate concentrations of each of the four dNTPs and ddNTPs are included, a series of incompletely elongated chains is produced, each differing by one base pair. The sequence can then be determined by running each reaction (containing the different ddNTP) on a polyacrylamide gel. However, most modern strategies for DNA sequencing used today employ a fluorescent detection system incorporating fluorescently-labelled nucleotides. The

fluorescently-labelled reaction products are then electrophoresed on a DNA sequencer (gel or capillary based systems) which uses a laser detection method.

2.1.6 Mutation screening

Determination of the intron/exon organisation of a gene of interest is the first step toward screening the gene for disease-associated mutations. Once the introns and exons have been identified, primers can be designed to amplify each exon plus a sufficient amount of flanking intronic sequence so that splice donor and acceptor site sequences are included. The amplified PCR products can then be subjected to rapid mutation screening methods, such as single strand conformation polymorphism (SSCP) analysis, where the sample of interest can be compared with the wildtype sequence, or can be sequenced directly.

2.1.7 Single strand conformation polymorphism (SSCP) analysis

Although direct sequencing is the most accurate means of detecting mutations, it can be very time consuming. Other techniques such as SSCP can provide a more rapid approach for screening large numbers of samples for mutations after which sequencing can be carried out if necessary. SSCP exploits the fact that the secondary structure of a particular DNA sequence can be altered by a mutation in that sequence (Orita et al., 1989). This can change the rate of mobility of a single-stranded DNA sequence in a non-denaturing acrylamide gel. Under the correct conditions, such as the appropriate percentage of acrylamide gel and ideal temperature (usually 4°C or 10°C) band shifts are detectable, allowing the differentiation between the normal sequence and an altered sequence. Mutation detection with SSCP analysis is detects approximately 90% of mutations (Fan E et al., 1993). However, this method is limited by the requirement for DNA fragments of usually less than 400bp.

2.1.8 Mitochondrial respiratory chain function

Located on the inner mitochondrial membrane, the respiratory chain is composed of more than 80 peptides organised into 5 enzymatic complexes (I-V). The overall function of the mitochondrial respiratory chain is to produce ATP from the reduction of oxygen to generate energy for cellular function. Electrons generated by donors in intermediary metabolism are received and sequentially transferred through redox groups to final acceptor, oxygen. Free energy generated is then used to pump protons from mitochondrial matrix to intermembrane space. This generates an electrochemical gradient across inner mitochondrial membrane. Proton flux back into mitochondrial matrix through Complex V is then coupled to ATP synthesis.

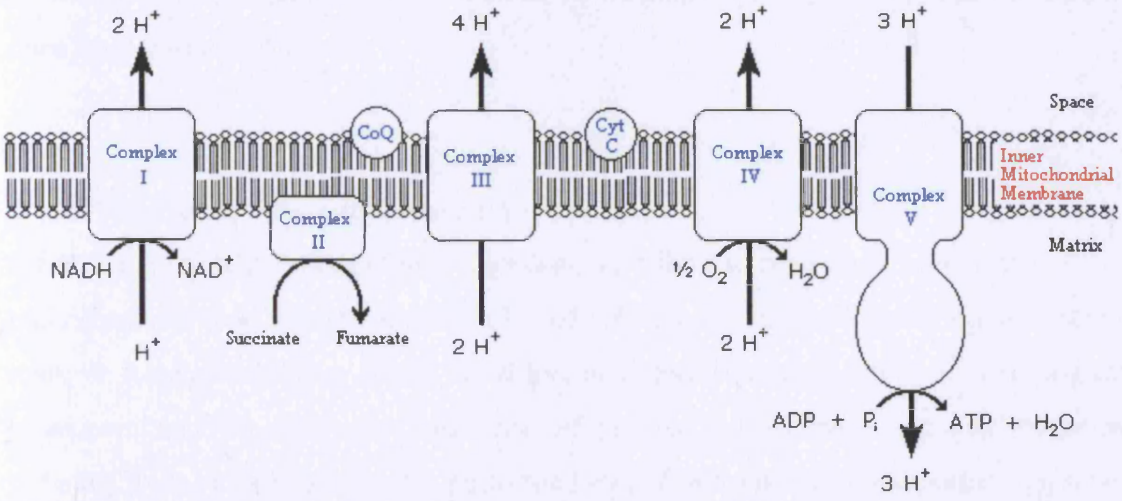

Figure 2.1 Overview of the mitochondrial respiratory chain (modified from metabolic pathways of biochemistry at http://www.gwu.edu/~mpb/oxidativephos.htm)

Diseases associated with defects in respiratory chain function may arise from mutations in mitochondrial DNA or nuclear genes encoding proteins essential for mitochondrial function. The function of individual components of the respiratory chain can be assessed by uncoupling the chain using specific inhibitors to individual complexes. A large number of neurodegenerative and other disorders have now been associated with specific defects in mitochondrial respiratory function (Orth and Schapira, 2001).

2.1.9 Enzyme assays and spectrophotometry

A spectrophotometer measures either the amount of light absorbed or transmitted. All of the mitochondrial enzyme assays utilise differences in absorbance. Light of a given wavelength (lambda = λ) is split and passes along two different paths. The light passes through the "test" cuvette along one route and the "reference" cuvette along the other. The light is then converged and passes through a photomultiplier tube (PM). The difference in absorbance is then measured. The spectrophotometer measures the difference in absorbance between the front and the back cuvettes. Initiation of the majority of mitochondrial enzyme reactions results in the generation of a relative increase in absorbance, compared to the reference, due to the production of increasing amounts of chromophore. This generates an easily interpretable incline on the resulting graph. If the reaction results in a reduction in the amount of chromophore and hence absorbance the positions of the test and reference cuvettes are reversed so that an incline is still produced on the graph, making calculations (i.e. reaction rates) easier to perform.

2.1.10 Muscle biopsies and tissue preparation

As defects in mitochondrial oxidative phosphorylation had been implicated in the pathogenesis of some forms of HSP, affected individuals who had agreed to participate in the research were asked if they would be willing to undergo a muscle biopsy for histological assessment and respiratory chain function assays. Age and sex matched control tissue was obtained from biopsies previously performed on patients who had no abnormal physical signs and normal histological appearance.

Samples of muscle tissue were obtained using open muscle biopsy from the vastus lateralis muscle under local anaesthetic. The majority of the sample was instantly frozen in liquid nitrogen and sent for histological assessment including Trichrome Gomori, Cytochrome oxidase (COX) and succinate dehydrogenase (SDH) staining. Remaining muscle from this sample was then available for respiratory chain function assays and electron microscopy. A small piece of muscle tissue was also placed directly into tissue culture medium for myoblast culture.

2.2 General solutions

Lysis buffer

0.32M Sucrose (BDH)

10mM Tris, pH7.5 (Sigma)

5mM $MgCl_2$ (BDH)

1% Triton X-100 (Sigma)

TE buffer

10mM Tris (Sigma), pH7.5

1mM EDTA (ethylenediaminetetraacetic acid; BDH), pH8.0

10X PCR IV buffer (ABgene)

750mM Tris-HCl (pH8.8 at 25°C)

200mM $(NH_4)_2SO_4$

0.1% Tween-20

This buffer is supplied containing 15mM $MgCl_2$ or with 25mM $MgCl_2$ separately

10X Agarose gel loading buffer

20% Ficoll 40 (Sigma)

0.02% Bromophenol blue (BDH)

0.02% Xylene cyanol (Sigma)

Distilled water

DNA molecular weight marker X, 0.07-12.2kb

20µl DNA molecular weight (1µg μl^{-1}) [Invitrogen]

40µl 10X Agarose gel loading buffer

40µl 0.1M NaCl

140µl TE buffer

20X TAE (Tris Acetate Electrophoresis) buffer (ND)

2.0M Tris-acetate

50mM EDTA

10X TBE (Tris Borate Electrophoresis) buffer (ND)

0.89M Tris-borate, pH8.3

20mM EDTA

10X Denaturing loading buffer

98% Formamide (Sigma)

0.05% Bromophenol blue (BDH)

0.05% Xylene cyanol (Sigma)

Blue dextran loading buffer

50mg/ml blue dextran containing 25mM EDTA (AB)

Diluted 1 in 10 with formamide (Sigma)

20X SSC

3M NaCl

0.3M Sodium citrate (pH7.0)

Denaturing solution

1.5M NaCl (BDH)

0.5M NaOH (BDH) Adjusted to pH12.0

Neutralising solution

1.5M NaCl (BDH)

0.5M Tris (Sigma) Adjusted to pH6.0

2.3 General protocols

2.3.1 DNA extraction from 5ml of whole blood

DNA extractions were performed using a standard phenol-chloroform procedure (Kunkel et al., 1977). This begins with cell lysis using lysis buffer with centrifugation at 8000rpm for 10 minutes at 4°C in a Beckman J2-HS or a Sorvall RC5B centrifuge in a 30ml round-bottom centrifuge tube (Sarstedt) to pellet the cell nuclei. The pellets are then resuspended in 5ml of 0.075M NaCl/0.024M EDTA (pH 8.0), and 250µl SDS [sodium dodecyl sulphate; 10%; (ND)] and 100µl proteinase K (10mg/ml) added to lyse nuclear membranes and to digest proteins, respectively, and incubated overnight at 37°C. Ensuring that no lumps of pellet are visible, then an equal volume of pre-equilibrated phenol saturated with 0.1M Tris, pH7-8 (Rathburn) is added, followed by centrifugation at 8000rpm for 10 minutes at room temperature. The upper aqueous layer was then transferred into a fresh tube and an equal volume of 24:1 chloroform:isoamyalcohol (BDH) added to remove traces of phenol, and centrifuged at 8000rpm for 10 minutes at room temperature. Again, the upper aqueous layer is transferred to a fresh tube, and 10ml of absolute ethanol (BDH) added to precipitate the DNA, which is then spooled onto a sterile loop and dissolved in an appropriate volume of TE buffer (pH7.5) depending on the size of the spooled DNA.

2.3.2 PCR for primers not fluorescently-labelled

A master mix was made up such that each aliquot contained the following (Table 2.1), if 1.5mM Mg^{2+} required for PCR reaction:

Table 2.1 PCR reaction mixture

PCR reaction component	**Volume (µl)**
Forward primer (50pmol μl^{-1}) [Sigma-Genosys]	1.0
Reverse primer (50pmol μl^{-1}) [Sigma-Genosys]	1.0
5mM dNTPs (Abgene)	1.0
Reaction buffer IV (10X) with 15mM $MgCl_2$ (ABgene)	2.5
Red Hot Taq DNA polymerase (0.2 units μl^{-1}; ABgene)	2.0
Distilled water	15.5

Then 200ng of DNA (in a 2µl volume) was added to the appropriate 0.5ml PCR tube (Sarstedt) to give a final volume of 25µl. Amplifications were performed using a touchdown method (Roux, 1995) in a GeneAmp PCR system 9700 (AB), a Techne Genius PCR machine, or Hybaid MBS 0.5G PCR machine (Table 2.2).

Table 2.2 PCR cycle programme

Number of cycles	**Temperature (°C)**	**Time (seconds)**
2	96	30
	Primer-specific temperature + 4	30
	72	30
2	96	30
	Primer-specific temperature + 2	30
	72	30
35	96	30
	Primer-specific temperature	30
	72	30

The PCR conditions for amplifying the microsatellite markers analysed by polyacrylamide gel electrophoresis were individually optimised.

2.3.3 Agarose gel electrophoresis

PCR products mixed with 2µl of agarose gel loading buffer were visualised after electrophoresis alongside a DNA molecular weight marker, in 1X TAE in 2% agarose (BM, GB) gels containing ethidium bromide (Sigma) at 0.5µg ml^{-1}.

2.3.4 Polyacrylamide gel electrophoresis (PAGE)

Amplified microsatellite markers were subsequently size fractionated by denaturing PAGE with denaturing loading buffer in 8% or 10% denaturing polyacrylamide (Amresco or ND) gels (Tables 2.3A and 2.3B), in 1X TBE preheated to approximately 60°C. The amount of PCR product mixed with 2µl of denaturing loading buffer and loaded on the polyacrylamide gels was varied dependent on the strength of the product visible on agarose gel electrophoresis. PAGE was carried out at 50mA for an appropriate length of time such that the different sized alleles that had been amplified could be differentiated on the polyacrylamide gel. The gels were subsequently silver stained and fixed.

Table 2.3 Protocol for making an 8% denaturing acrylamide gel (25ml) using a pre-prepared solution

Gel component	**Volume/gel**
* GenePAGE 8% solution (Amresco)	25.0ml
TEMED (N, N, N', N'-tetramethylethylenediamine; Sigma)	40µl
25% APS (ammonium persulphate, Sigma)	40µl

*GenePAGE 8% solution contains 7.6% (w/v) acrylamide, 0.4% (w/v) bisacrylamide, 7M urea, 0.089M tris, 0.089M boric acid, 2mM EDTA.

2.3.5 Silver staining

Polyacrylamide gels were placed in a fixing solution of 10% ethanol (BDH) and 0.5% glacial acetic acid (BDH) for at least 15 minutes, left in 0.1% silver nitrate (Sigma or BDH) for 5-10 minutes, stained in 1.5% NaOH (BDH), 0.15% formaldehyde (BDH), then in 0.75% sodium carbonate (BDH) for 15 minutes. The gels were thoroughly rinsed in distilled water between each stage. The visualised size-fractionated alleles were given a number and then individuals were assigned a genotype.

2.3.6 Genome wide marker analysis

A genome wide screen was performed using the ABI PRISM Linkage Mapping Set Version 2 (Applied Biosystems) which contains fluorescently labelled primer pairs for the amplification of 384 microsatellite markers, with an average spacing of 10cM. Each marker was amplified individually, however, the markers are arranged into 26 panels each containing non-overlapping sized markers labelled with three different flourophores. Each panel of markers was therefore pooled together, allowing simultaneous electrophoresis and laser detection.

2.3.7 PCR with fluorescently labelled primers

A PCR master mix was made up for each of the primer pairs (table 2.4). 9.2µl of this mix was loaded into 96 well plates (AB gene) and 0.8µl of DNA at 50ng/µl added to each reaction mixture. PCR amplifications were performed in the Hybaid MBS 0.5G PCR machine using the recommended cycle programmes (table 2.5).

Table 2.4 PCR mixture for amplification of fluorescently labelled markers

PCR master mix component	**Volume (µl)**
Primer mix* (Applied Biosystems)	1.0
True Allele PCR premix** (Applied Biosystems)	6.0
Distilled water	2.2

* Contains forward (labelled) and reverse primers combined at 10µM concentration in a solution of 10mM Tris, 1mM EDTA at pH 8.0

** Contains an optimised mixture of AmpliTaq Gold DNA polymerase, buffer, $MgCl_2$ and dNTPs

Table 2.5 Recommended cycle programme for amplification of fluorescently labelled microsatellite markers

Number of cycles	Temperature (^{0}C)	Time (seconds)
1	95	720
10	94	15
	55	15
	72	30
25	89	15
	55	15
	72	30
1	72	600

2.3.8 Genotyping of labelled products

PCR products were checked for successful amplification by electrophoresis in 2% agarose gels. Panels of PCR products were then pooled together and added to a solution containing HiDi formamide and the Gene-scan 500 marker in 96 well plates (table 2.6). This loading mixture was the denatured at 96^{0}C for 3 minutes and immediately cooled on ice, prior to running on the ABI 3100 automated sequencer. The ABI 3100 was set up with a 36cm capillary array loaded with POP4 linear flowable polymer. Samples were added to the capillaries with a 22 second 1Kvolt injection and underwent electrophoresis at 60^{0}C, 100μA for 25 minutes.

Table 2.6 Loading mixture for detection on the ABI3100 automated sequencer

Loading mixture component	Volume (μl)
Pooled PCR products	2.0
4nM Genescan-500* (Applied Biosystems)	0.5
HiDi Formamide (Applied Biosystems)	9.5

* Genescan-500 ROX fragment sizes: 35, 50, 75, 100, 139, 150, 160, 200, 250, 300, 340, 350, 400, 450, 490, 500

2.3.9 Data analysis

Alleles were sized using GeneScanTM Analysis software (Applied Biosystems), with reference to the internal lane size standard, to within 0.01bp accuracy. The data files generated were imported into the Genotyper 3.7 software (Applied Biosystems) and the markers then ordered and genotyped. The resulting microsatellite marker information was then assessed for homozygosity and where appropriate imported into the Genehunter (version 2.1) software which calculates haplotype information and multipoint LOD scores. Two-point LOD scores were also calculated using the subprogram MLINK (version 5.1) of the LINKAGE program package. All programs used for linkage analysis were accessed through the Human Genome Mapping Project (HGMP) website.

2.3.10 PCR product purification

DNA of interest was amplified by PCR in a total volume of 50µl. Of this 5µl was electrophoresed on a 2% agarose gel as described in section 2.4.4. The remaining 45µl of PCR product was then purified using a spin column protocol [QIAquick PCR Purification Kit (QIAGEN) or GENECLEAN Turbo for PCR Kit (QBiogene)] to remove primers, unincorporated nucleotides, and polymerases, and eluted into 20µl with distilled water.

2.3.11 DNA sequencing protocol

3µl of spin purified PCR product was used as a template in each sequencing reaction using the ABI PRISM BigDye Terminator Cycle Sequencing Ready Reaction Kit (AB) [Table 2.7]. The sequencing reaction amplifications were performed using the cycle programme in Table 2.8. Both strands of each PCR product were sequenced.

Table 2.7 Sequencing reaction protocol

Sequencing reaction component	**Volume (µl)**
BigDye Terminator (AB)	2.0
Primer (5pmolμl^{-1})	1.0
Distilled water	4.0
Purified PCR product	3.0

Table 2.8 DNA sequencing cycle programme

Number of cycles	Temperature (°C)	Time
25	96	30 seconds
	50	15 seconds
	60	4 minutes

The sequencing reaction product was then purified using the DyeEx Spin Kit (QIAGEN) according to the recommended protocol to remove unincorporated BigDye™ terminators. The final eluent was then dried on a PCR machine at 60°C. Finally 10µl of Hi-Di formamide (AB) was added to the dried sequencing product before being denatured, cooled, and run on an ABI3100 automated sequencer (capillary injection-based) [AB].

2.3.12 Single strand conformation polymorphism (SSCP) analysis

PCR products were mixed with denaturing loading buffer and electrophoresed in 0.6X TBE usually using 0.55X or 0.6X MD gels (Table 2.9) for an appropriate length of time at 10°C (constant 250V) using BioRad Protean II equipment. DNA was visualised by silver staining.

Table 2.9 Protocol for preparing a 0.55X or 0.6X MD acrylamide gel for SSCP analysis

Component of gel mixture	Volume	
	0.55X	0.6X
2X SequaGel MD (ND)	9.625ml	10.500ml
10X TBE	2.100ml	2.100ml
Distilled water	23.275ml	22.400ml
TEMED (Sigma)	70µl	70µl
25% APS (Sigma)	70µl	70µl

2.3.13 NADH-COQ1 reductase assay (mitochondrial complex I activity)

The NADH-COQ1 assay measures the rate of oxidisation of NADH to NAD^+ by complex 1 of the mitochondrial respiratory chain. Ubiquinone accepts the electrons and is reduced to Ubiquinol. Cyanide inhibits complex IV (cytochrome c oxidase) activity and the Rotenone is added because it specifically inhibits mitochondrial NADH COQ1 reductase to terminate the reaction.

The homogenised muscle or mitochondrial preparation from cultured myoblasts may be used undiluted or diluted (e.g. 1:20) in homogenisation buffer, according to its specific nature. Freeze-thawing the sample a total of 3 times in liquid nitrogen disrupts the mitochondrial membranes, exposing the enzymes in an intact and metabolically active state.
The ubiquinone is supplied at an unknown concentration. To determine the amount of ubiquinone required for the reaction sodium borohydride is used to reduce the ubiquinone to its non-absorbing state. The absorbance change is calculated using the spectrophotometer and the amount of ubiquinone required for each reaction is calculated using the formula 0.3/absorbance change x 20.4µl. The remaining reagents and volumes required for the NADH-COQ1 assay are shown in table 2.10

Table 2.10 NADH-COQ1 assay reaction mixtures

Reagent	**Reference cuvette**	**Test cuvette**
25mM K^+ Phosphate Buffer + 10mM $MgCl_2$, (pH 7.2)	800µl	800µl
5mM NADH (3.6mg/ml)	30µl	30µl
100mM KCN (6.5mg/ml)	10µl	10µl
50mg/ml BSA	50µl	50µl
dd H_2O	100µl	100 - (x + y)µl
Homogenised muscle or mitochondrial preparation	-	xµl
5mM Ubiquinone	-	yµl

X = 5,10 or 15, Y = amount previously calculated

The NADH-COQ1 assay is performed as follows:

1. Select the "NADH Q1 Red" programme on the Hitachi spectrophotometer (Wavelength = 340nm, Temp = 30°C).
2. Set the data scale form -0.05 to 0.25.
3. Set up 6 cuvettes (3 reference & 3 test) loaded with 800µl of buffer, 30µl of NADH, 10µl of KCN & 50µl of BSA. Add 100µl of ddH_2O to the 3 reference cuvettes. Mix (parafilm) and place in the water bath to pre-warm.
4. Add 100µl of pre-warmed ddH_2O - (xµl (homogenised muscle) + yµl (as previously calculated ubiquinone) and xµl of homogenised muscle to one test cuvette, mix thoroughly (parafilm) and load into the back of the spectrophotometer.
5. Load one reference cuvette into the front of the spectrophotometer.
Autozero, start the assay and leave to flatline (for approx ½ minute).
6. Add yµl of ubiquinone to the back test cuvette. The rate is visualised as an increase in absorbance. Leave to run for 3-4 mins or until the absorbance reads 0.2.
7. Add 10µl of Rotenone to both cuvettes (test cuvette first), take out, mix (parafilm) and replace. The rate of reaction should decrease at this point due to inhibition of the Rotenone-sensitive component of the enzyme activity.
8. Leave to run for a further 3-5 minutes to give a linear rate.
9. Stop and scan the trace adding 4 cursor points as shown in the figure below, taking care to avoid the non-linear region of the incline.
10. Calculate the reaction rates between the first and second pair of points and subtract the latter from the former to give the rotenone sensitive rate which is equivalent to complex I activity (figure 2.2).

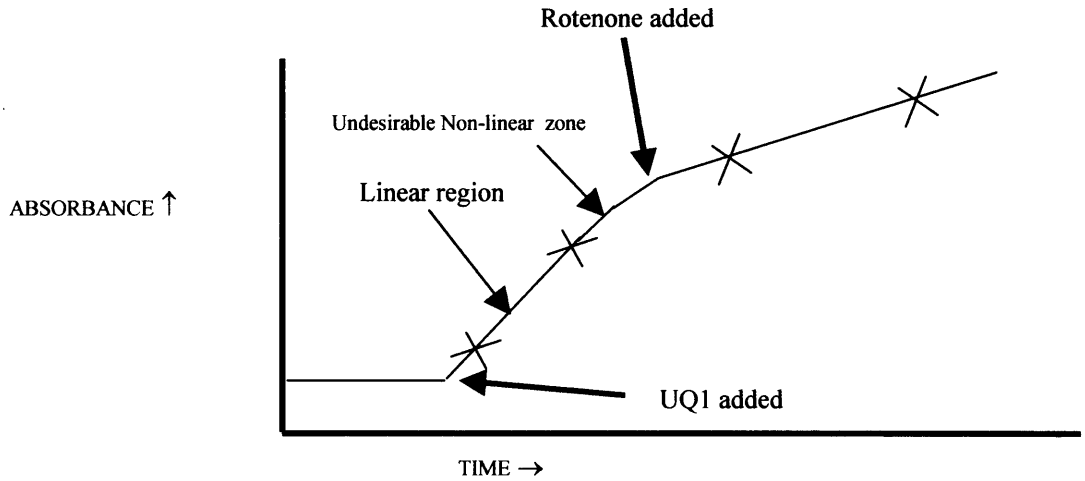

Figure 2.2 Example of graph for calculation of complex I activity

The M extinction coefficient of NADH is 6.22 x 10^3. However, because the contribution of ubiquinone reduction to the absorption at 340nm this means that the true value in the assay is 6.81. The reaction rate is calculated as follows:

$$\text{Rate (nmol/min/mol)} = \left[\frac{\frac{\text{Absorbance change}}{\text{Time}}}{6.81 \times 10^3} \right] \times \frac{1000}{\mu\text{l sample}} \times \frac{1}{1000}$$

2.3.14 Succinate cytochrome C assay (mitochondrial complexes II and III activity)

The succinate cytochrome C assay measures the rate of reduction of cytochrome C. It is performed at 30°C using a wavelength of 550nm. Cyanide inhibits complex IV activity. Antimycin A is used to terminate the reaction, as this is a potent inhibitor of mitochondrial succinate cytochrome C activity. Muscle tissue or mitochondria are prepared as for the NADH-COQ1 assay and freeze thawing is again required to expose the enzymes in a functionally active state. The mitochondrial enzyme is activated prior to its addition to the test cuvette, during which time the fumarate in complex II is replaced by succinate. If the reaction is not initiated prior to its addition, a non-linear graph will be produced as the rate of reaction increases until it reaches its maximum. This makes the desired calculations more difficult. The reagents and volumes required for the succinate cytochrome C assay are shown in table 2.11.

Table 2.11 Succinate cytochrome C assay reaction mixtures

Reagent	**Reference cuvette**	**Test cuvette**
166mM K^+ Phosphate Buffer pH 7.4	600µl	600µl
15mM (K_2) EDTA (6.1mg/ml)	20µl	20µl
2mM Cytochrome C (25mg/ml)	50µl	50µl
100mM KCN (6.5mg/ml)	10µl	10µl
50mg/ml BSA	50µl	50µl
dd H_2O	320µl	320 - (x + y)µl
Homogenised muscle or mitochondrial preparation	-	xµl
500mM NA^+ Succinate (675mg/5ml)	-	yµl
2mM Antimycin A (1mg/ml)	-	10µl

X = 5,10 or 15, Y = 40

The succinate cytochrome C assay is performed as follows:

1. Select the "Succinate Cytochrome C" programme on the Hitachi spectrophotometer. Wavelength = 550nm, temperature = 30°C.
2. Set the data scale at 0-0.4.
3. Load 6 cuvettes with buffer (600µl), EDTA (20µl), cytochrome C (50µl) and ddH_20 (3 ref cuvettes = 320µl : 3 test cuvettes = 320µl - total volume of succinate (y = 40µl) and x, where x = volume of homogenised muscle added e.g. 10µl.
4. Load 3 eppendorfs with identical volumes of (40µl) Na Succinate and (10µl) KCN.
5. Add the chosen volume of homogenised muscle e.g. 10µl, to one of the eppendorfs and place it in the water bath for 5 minutes at 30°C to activate the enzyme.
6. After 4 minutes of the time has elapsed add 10µl of KCN to the reference cuvette. Mix and load both of the cuvettes, (reference - back: test - front) into the spectrophotometer.

7. Autozero the spectrophotometer and start the assay. The trace should be flat-lining as the sample cuvette doesn't contain any substrate or mitochondria.
8. When the full five minutes has elapsed, add the entire contents of the pre-warmed eppendorf (Na succinate, KCN & mitochondria) to the test cuvette and mix.
9. Run the assay for an absorbance change of approx 0.4 then add 10µl of Antimycin A to the test cuvette, mix and run for a further 4-5 minutes. The trace should flat-line from this point.
10. Using the "SCAN TRACE" function, 4 cursor points are plotted as shown on the diagram below. The Rate of Reaction is calculated between the first two points and between the second two points (figure 2.3).

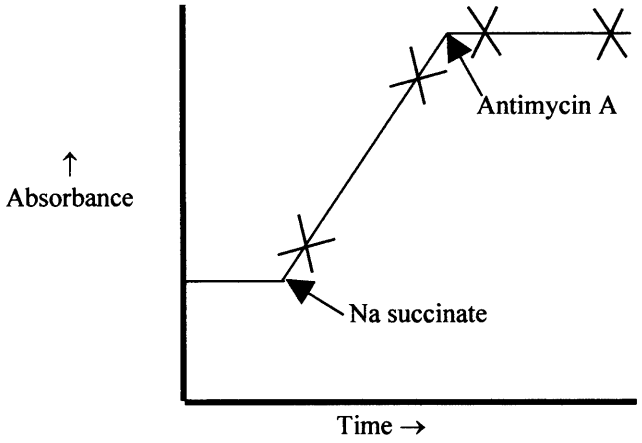

Figure 2.3 Example of graph for calculation of complex II/III activity

The M extinction coefficient of reduced cytochrome c is 19.2×10^3, which gives the answer in moles. The rate of reaction is calculated as follows:

$$\text{Rate (nmol/min/mol)} = \left[\frac{\dfrac{\text{Absorbance change}}{\text{Time}}}{19.2 \times 10^3} \right] \times \frac{1000}{\text{µl sample}} \times \frac{1}{1000}$$

2.3.15 Cytochrome C oxidase assay (mitochondrial complex IV activity)

The cytochrome c oxidase assay measures the rate of oxidation of reduced cytochrome c. Cytochrome c initially comes in its oxidised form and is reduced using an excess of ascorbate. Any residual ascorbate is then removed by dialysis. The molar extinction coefficient for reduced cytochrome c is 19.2 x 10^3 at 550nm. Using this extinction coefficient it can be calculated that 50μM reduced cytochrome c, the required concentration of cytochrome c for the assay, produces an absorbance of 0.96. This is therefore used as a starting point for each reaction. As with complex I and complex II/III assays the mitochondrial enzymes in the sample are released by freeze thawing in liquid nitrogen. Potassium ferricyanide is used to completely oxidise cytochrome c in the reference sample.

The reagents and volumes required for the succinate cytochrome c assay are shown in table 2.12.

Table 2.12 Cytochrome C oxidase assay reaction mixtures

Reagent	Reference cuvette	Test cuvette
0.1M K^+ Phosphate Buffer pH 7	100μl	100μl
Reduced Cytochrome C (50μM)	yμl	yμl
ddH_2O	900 - (x + y)μl	900 - (x + y)μl
Homogenised muscle or mitochondria	-	xμl
0.1M K^+ Ferricyanide	xμl	-

X = 5,10 and 15, Y = amount of reduced cytochrome c to give an absorbance of 0.96

The cytochrome c oxidase assay is performed as follows:

1. Select the "CYTOX" programme on the Hitachi spectrophotometer. Wavelength = 550nm, temperature = 30°C.
2. Load 6 cuvettes (3 test: 3 reference) with buffer (100μl) and the previously calculated desired volume (yμl) of reduced cytochrome c.
3. To the test cuvettes add 900μl of dd H_2O - (xμl of homogenised muscle + yμl of reduced cytochrome c).
4. To the reference cuvettes add 900μl of dd H_2O - (yμl of reduced cytochrome c + xμl of K^+ ferricyanide e.g. 10μl).

5.Pre-warm the cuvettes in the water bath at 30°C.

6. Load one reference cuvette into the back of the spectrophotometer and one test cuvette in the front.

7. Autozero the machine.

8. Add10µl of K^+ Ferricyanide to the back reference cuvette to oxidise the reduced cytochrome c and mix well. The difference in the content of reduced cytochrome c between the test and reference cuvettes is now maximum and the absorbance should read 0.96 ± 0.02.

9. Start the assay.

10. After 30 seconds, take a note of the absorbance (t = 0) and initiate the reaction by adding the mitochondrial enzyme, i.e. xµl of homogenised muscle to the front test cuvette. The sample needs to be added as rapidly as possible and mixed well.

11. Repeat the assay 5 times using different volumes of homogenised muscle sample.

12. The rate is visualised as a decrease in absorbance. Expand the time scale from 0-5 minutes (need a minimum of 3 minutes of running time) and maximise the data scale so that the graph fills the entire screen. The graph is then printed for further calculations (figure 2.4).

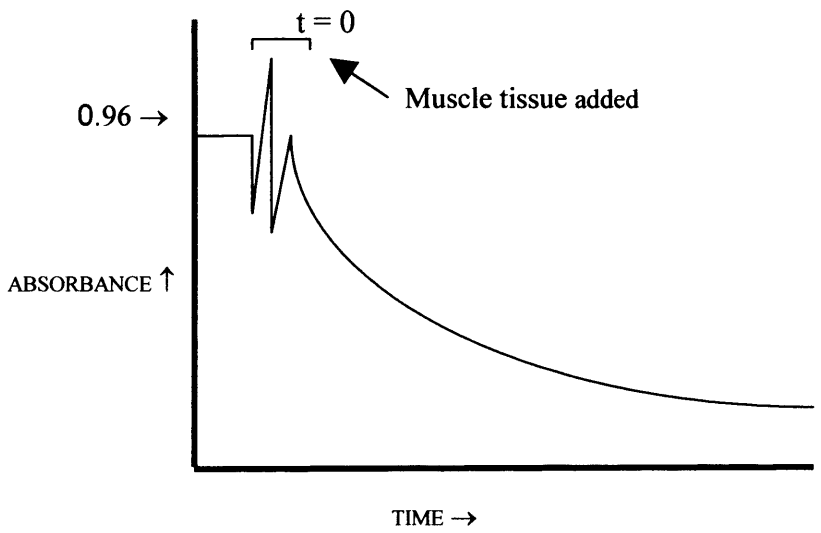

Figure 2.4 Example of a graph for calculation of complex IV activity

Because the reaction is rigorously first order with respect to cytochrome c (i.e. non-linear) it is best to calculate the pseudo first order rate constant k. On the graph draw a tangential straight line as shown and extrapolate the absorbance back to the x-axis, taking care to avoid any artifactually steep initial region of the slope. To give time (t) = 0, take the point that is mid-way during the time taken to add the sample. Draw a line from this point horizontally across the graph and mark along it t = 1, 2 and 3 minutes from the calculated time point t = O using original time scale of the graph as a reference. Draw down to the trace from points t = 1, 2, & 3 and calculate the absorbance values at these times.

Plot : $\ln A_{t=0} - \ln (A_{t=0} - A_{t=n})$ against time (t).

Where ln = the natural log, n = time (mins) and At (absorbance at t= 0) = approx 0.96 (insert value for each individual assay), by entering the absorbance values at t = 0, 1, 2, & 3 and volume in µls of mitoprep (including any dilution in HB) used for each assay in the programme CYTOCALC/cytocal1 (DAN). Cytocal1 automatically draws the graph and gives the k value. The K value (gradient) is the Cytochrome c rate constant and is expressed as the change in absorbance/min/ml. In order to convert this to absorbance/min/µl the value is multiplies by 1000/x (where x is the volume of homogenised muscle in µl used in the assay).

2.3.16 Citrate synthase assay

Citrate synthase is a mitochondrial matrix enzyme. It catalyses the reaction between oxaloacetate (OAA) and acetyl CoA to generate citrate and liberate free thiol groups.

$$\text{Oxaloacetate (OAA)} + \text{Acetyl CoA} \xrightarrow[\text{Synthase}]{\text{Citrate}} \text{Citrate} + \text{CoA-SH}$$

DTNB (5,5-dithio bis-2-nitrobenzoid acid) then binds free thiol groups to produce DTNB-CoA which is yellow and absorbs at 412nm.

$$\text{OAA} + \text{Acetyl CoA}^{-} + \text{DTNB} \xrightarrow[\text{Synthase}]{\text{Citrate}} \text{Citrate} + \text{DTNB-CoA}$$

As it is not part of the mitochondrial respiratory chain its activity is used as a marker for the number of mitochondria in a given sample. Mitochondrial respiratory chain complex enzyme activities are therefore divided by citrate synthase activity to estimate activity independent of the number of mitochondria in each sample. The reagents and volumes required for the citrate synthase assay are shown in table 2.13.

Table 2.13 Citrate synthase assay reaction mixtures

Reagent	Reference cuvette	Test cuvette
200mM Tris (1.2g/50ml) pH8	500µl	500µl
10mM Acetyl CoA	20µl	20µl
10mM DTNB (4mg/ml) + $KHCO_3$	20µl	10µl
Triton-X100	10µl	10µl
ddH_2O	440µl	430µl - xµl
Homogenised muscle or mitochondria	-	xµl
10mM oxaloacetate (7mg/5mls)	-	10µl

X = 5,10 or 15

The citrate synthase assay is performed as follows:

1. Select the citrate synthase assay on the Hitachi spectrophotometer. Wavelength = 412nm, temperature = 30°C.
2. Load 6 cuvettes (3 test: 3 reference) with the four common ingredients (Tris, Acetyl CoA, DTNB and Triton-X100) to each cuvette and pre-warm in the water bath.
3. To the reference cuvettes add 440µl of pre-warmed ddH_2O.
4. To the test cuvettes add 430µl - xµl of pre-warmed ddH_2O and xµl of homogenised muscle or mitochondria.
5. Add 10µl of oxaloacetate to the test cuvette and load both test and reference cuvettes into the spectrophotometer.

The spectrophotometer measures the change in absorbance between the two cuvettes producing an incline on the graph (figure 2.5).

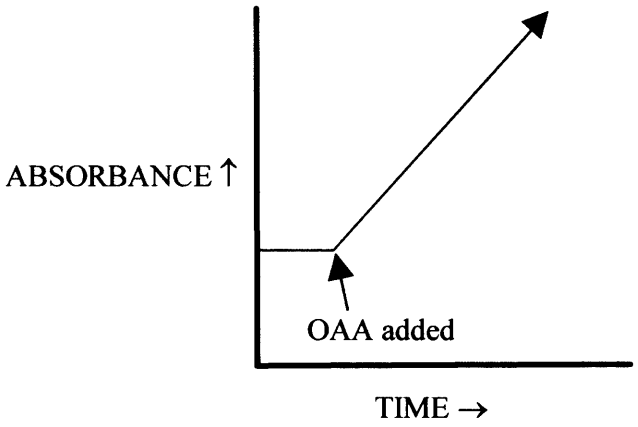

Figure 2.5 Example of a graph for calculation of citrate synthase activity

The M extinction coefficient of DTNB is 13.6 x 10^3. The reaction rate is calculated as follows:

$$\text{Rate (nmol/min/mol)} = \left[\frac{\frac{\text{Absorbance change}}{\text{Time}}}{13.6 \times 10^3} \right] \times \frac{1000}{\mu\text{l sample}} \times \frac{1}{1000}$$

2.3.17 Culture of myoblasts from human muscle

On the day of the muscle biopsy the culture medium is made using the ingredients shown in table 2.14

Table 2.14 Myoblast culture medium

Ingredient	Volume
Dulbecco's modified Eagle's medium + 4.5g/l glucose (Sigma-Aldrich)	500ml
20% Fetal calf serum (GIBCO)	100ml
2μM Uridine	2ml
1μM Sodium pyruvate	5ml
50μg Penicllin + 50μg streptomycin	2.5ml

A trypsinising solution is made by adding 4mls of trypsin to a 100ml bottle of versene (GIBCO).

A dissociation solution is made by dissolving 12,000 digestion units of collagenase (Sigma) and 40mg of bovine serum albumin (fraction V, fatty acid free) in 10mls of culture media. This is filter sterilised using a 0.2μm ministart filter before adding 3.2mls of trypsinising solution and finally making up the volume to 40mls using additional culture media.

Approximately 200mg of skeletal muscle from the biopsy is collected in 10mls of culture media. This is rinsed repeatedly in fresh media to remove excess blood and debris. The muscle is then transferred to a sterile 6cm plate and 5mls of pre-warmed dissociation solution (37^0C) added. The muscle is carefully teased apart using sterile needles then incubated for 15 minutes at 37^0C. After this period 5mls of culture medium is added to halt the reaction before filtering through a cell strainer and centrifuging at 1,000rpm for 10 minutes. The supernatant is discarded and the cells re-suspended in culture medium. Harvested aliquots of suspended cells are transferred to collagen coated plates and incubated at 37^0C (figure 2.6).

Figure 2.6 Cultured human myoblasts on a collagen coated plate

2.3.18 Passaging of cultured myoblasts

Passaging of the cultured myoblast is required once the cells become 70% confluent on the plate to prevent differentiation into mature cells. The media is removed and the plates washed with PBS. 1ml of trypsinising solution is added to the plate which is then incubated at 37^0C for 3 minutes. Once the cells have become detached the reaction is halted by the addition of 9mls of culture medium. This is then centrifuged at 1,000rpm for 10 minutes and the supernatant discarded. The cells are then re-suspended in culture medium and split between two new plates.

2.3.19 Isolation of mitochondria from myoblasts by differential centrifugation

9ml of isolation buffer containing 0.2M sucrose, 0.13M sodium chloride and 1mM Tris HCl (pH7.4) is added to a 1ml suspension of cultured myoblasts. The sample is then homogenized using a motor driven Potter homogeniser. This is then first centrifuged for 10 minutes at 2,500rpm (500g) and the precipitate discarded. The supernatant is centrifuged for a further 15 minutes at 9,500rpm (8,000g). The resulting supernatant is then discarded and the mitochondrial pellet re-suspended in isolation buffer.

Chapter 3

CLINICAL CHARACTERISTICS OF AUTOSOMAL RECESSIVE HSP PATIENTS IN THE UK

3.1 Introduction

The hereditary spastic paraplegias are a clinically and genetically diverse group of disorders. The clinical phenotype is classified as being pure when symptoms and signs are confined to those of a progressive spastic paraparesis. Posterior column dysfunction, with impaired proprioception and vibration sense, and bladder dysfunction are also permitted (Harding, 1984). The phenotype is described as complicated in the presence of additional major neurological or other clinical features. A number of distinct clinical syndromes have been described such as the Troyer and Mast syndromes in the Old Order Amish population.

The diagnosis of HSP is relatively straightforward in the presence of a family history and a progressive spastic paraparesis as the predominant clinical feature. Alternative disorders that should be excluded, as proposed by the Hereditary spastic Paraplegia Working Group are summarised in table 3.1. This is by no means a comprehensive list but highlights some of the more common disorders which may be mistaken for HSP.

Clinical studies to date have mainly focused on the more prevalent autosomal dominant families. Reports on autosomal recessive families are most often in individual families from regions with high rates of consanguinity. Topaloglu and colleagues identified 23 Turkish families, all with early onset autosomal recessive HSP (Topaloglu et al., 1998). Of these 9 families had a pure phenotype and 14 complicated phenotypes with cerbellar ataxia and cognitive impairment being the most frequent additional features. In the largest study to date Coutinho and colleagues assessed 106 affected individuals from 46 families with autosomal recessive HSP from Portugal and Algeria (Coutinho et al., 1999). In this series pure phenotypes were more prevalent than complicated forms (58.7% vs. 41.3%). They proposed a classification into five common phenotypes: (1) pure early onset, (2) pure late onset, (3) complicated with mental retardation, (4) complicated with mental retardation and peripheral neuropathy, and (5) complicated with cerebellar ataxia.

The aim of this study was to identify and characterise UK families with inheritance consistent with autosomal recessive HSP.

Table 3.1 Differential diagnosis of HSP

Category	Disorder	Differentiating clinical features	Diagnostic evaluation
Structural abnormality	Arnold-Chiari malformations	Ataxia	MRI brain
	Cervical spondylotic myelopathy	Upper limb involvement, radiculopathy	MRI spine
	Spinal cord neoplasm	Pain, sensory signs, asymmetric involvement	MRI spine
Inflammatory and degenerative disease	Multiple sclerosis	Exacerbations and remissions, optic neuritis	MRI, CSF examination, VEPs
	Amyotrophic lateral sclerosis	Fasiculations, amyotrophy	EMG
	Spinocerebellar ataxias	Prominent ataxia	Genetic testing
Leukodystrophy	ALD/AMN	Cognitive impairment,	MRI brain, VLCFAs
	MLD	peripheral neuropathy	MRI brain, arylsulphatase
	Krabbe leukodystrophy	Psychomotor regression, peripheral neuropathy	MRI brain, galactocerebrosidase
		Peripheral neuropathy	
Metabolic disorders	Subacute combined degeneration	Peripheral neuropathy, marked dorsal column involvement	Vitamin B12 levels
	Mitochondrial cytopathies	Short stature, retinitis pigmentosa, stroke-like episodes	MRI brain, lactate, muscle biopsy
	Abetalipoproteinaemia	Peripheral neuropathy	Lipoprotein electrophoresis
Infectious diseases	Tertiary syphilis	Subacute course	VDRL, syphilis serology
	Tropical spastic paraparesis	Subacute course	HTLV-1 antibodies
	HIV myelopathy	Subacute course	HIV antibodies
Miscellaneous	DOPA-responsive dystonia	Diurnal variation	Trial of levodopa

ALD = adrenoleukodystrophy; AMN = adrenomyeloneuropathy; MLD = metachromatic leukodystrophy; VLCFA = very long chain fatty acids, HTLV-1 = human T-cell lymphotropic virus type 1, HIV = human immunodeficiency virus (Adapted from Fink et al., 1996)

3.2 Methods

Multi-regional ethical approval was obtained to carry out the clinical, genetic and biochemical studies on autosomal recessive and sporadic HSP cases. Proband patients were initially identified through an established HSP database stored at the Institute of Neurology in London and registered members of the UK familial spastic paraparesis support group. Additional patients were also subsequently identified through the British Neurological Surveillance Unit. Affected individuals and all available at risk family members were assessed including history and a full neurological examination.

Autosomal recessive inheritance was assumed when two or more siblings were affected with unaffected parents (on examination or by history when deceased) or one or more affected sibling in the presence of consanguinity. Diagnostic criteria were those of the Hereditary Spastic Paraplegia Working Group with alternative causes excluded as far as possible with MRI, electrophysiologic evaluation and biochemical testing in at least one affected member of each pedigree as documented in the medical records.

3.3 Results

A total of 20 UK families with autosomal recessive HSP, including 45 affected individuals were identified (figure 3.1). Age of onset ranged from 18 months to 62 years with two thirds of all cases presenting before the age of 20 (figure 3.2). Full details of the clinical characteristics of all affected individuals are presented in table 3.2. An overview of the prevalence of phenotypic characteristics is summarised in table 3.3.

Pedigree 1

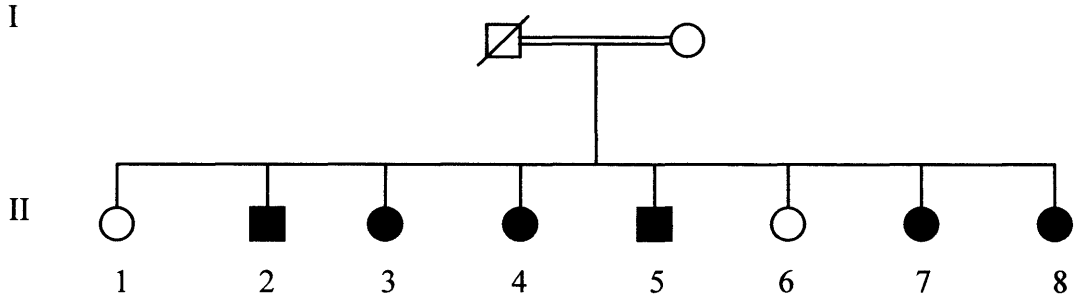

Pedigree 2

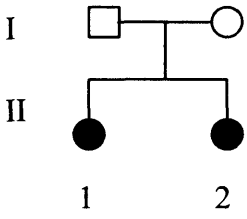

Pedigree 3

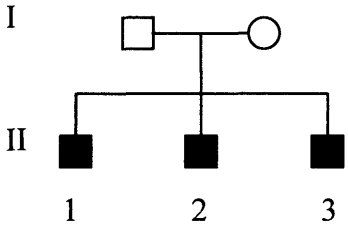

Pedigree 4

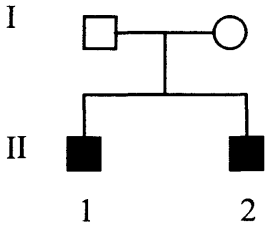

Pedigree 5

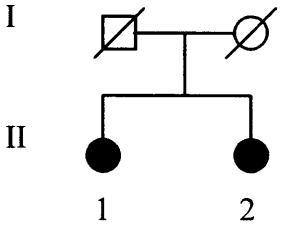

Pedigree 6

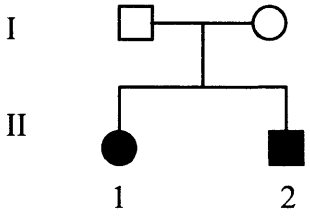

Pedigree 7

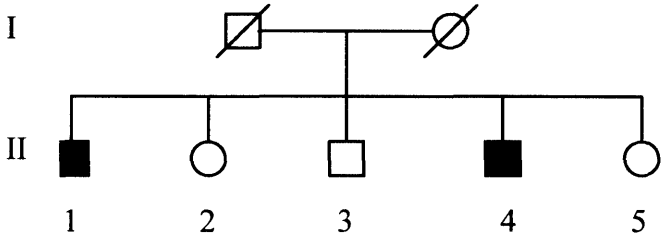

Pedigree 8

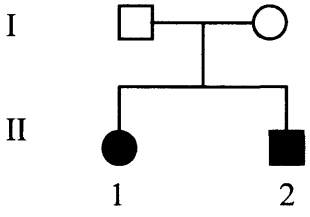

Pedigree 9

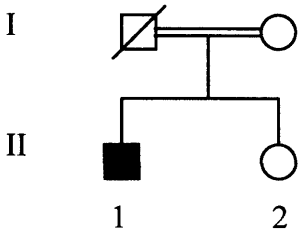

Pedigree 10

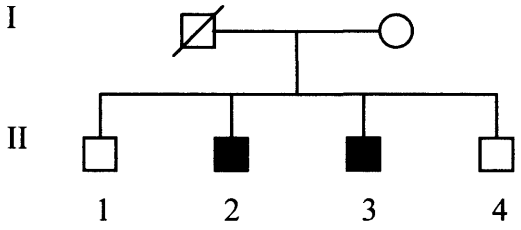

Pedigree 11

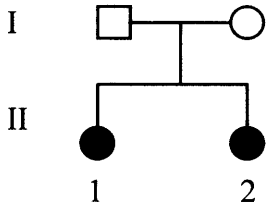

Pedigree 12

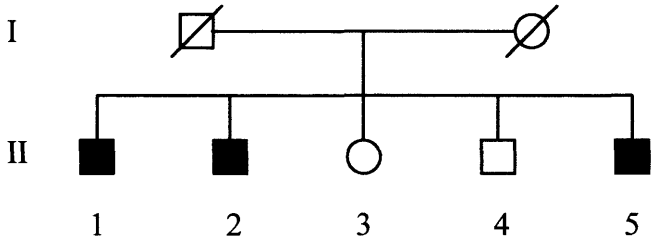

Pedigree 13

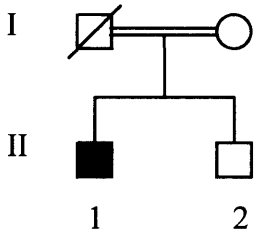

Pedigree 14

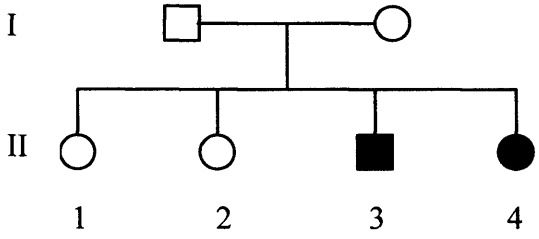

Pedigree 15

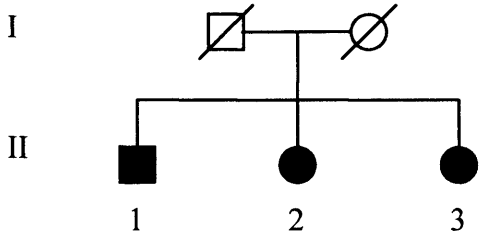

Pedigree 16

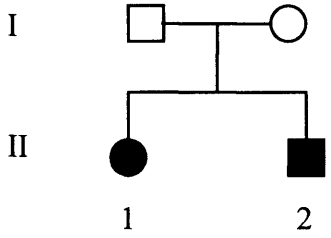

Pedigree 17

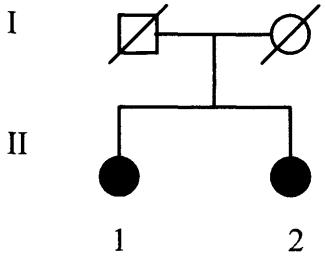

Pedigree 18

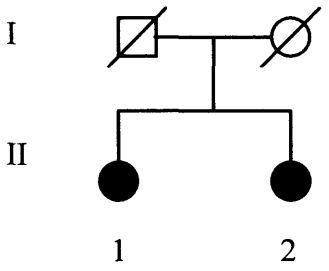

Pedigree 19

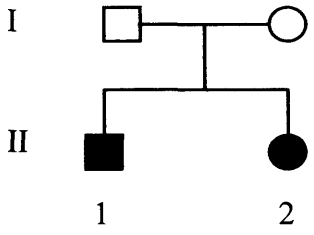

Pedigree 20

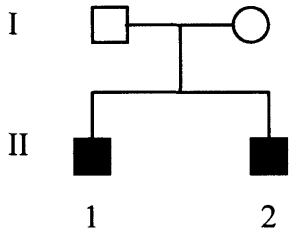

Figure 3.1 Pedigrees of UK families with autosomal recessive HSP

Table 3.2 Clinical characteristics of all autosomal recessive HSP patients

Pedigree	1	1	1	1	1	1	2	2	3	3	3	4	4	5	5	6	6	7	7	8	8	9	10	10	11	11	12	12	12	13	14	14	15	15	15	16	16	17	17	18	18	19	19	20	20
Individual	2	3	4	5	7	8	1	2	1	2	3	1	2	1	2	1	2	1	4	1	2	1	2	3	1	2	1	2	5	1	3	4	1	2	3	1	2	1	2	1	2	1	2	1	2
Phenotpye	p	p	p	p	p	p	c	c	c	c	c	c	c	p	p	c	c	c	c	c	c	c	p	p	c	c	c	c	c	c	c	c	p	p	p	p	p	p	p	p	p	c	c	c	c
Age (years)	53	51	46	45	43	41	23	20	23	18	11	27	24	71	65	32	30	65	61	35	32	43	50	48	23	12	70	63	55	20	34	27	71	68	61	7	5	79	69	51	42	32	30	20	18
Age of onset (years)	8	40	9	14	20	14	16	14	8	14	10	13	16	62	50	21	20	20	16	14	14	5	14	19	11	8	40	52	45	14	21	14	30	50	41	2	2	58	56	33	32	2	2	5	3
Learning difficulties	-	-	-	-	-	-	+	-	+	+	+	+	+	-	-	+	+	-	-	+	+	-	-	-	+	+	-	-	-	-	+	+	-	-	-	-	-	-	-	-	-	-	-	-	-
Dysarthria	-	-	-	-	-	-	+	+	+	-	-	+	+	-	-	+	-	-	-	+	+	+	-	-	-	-	-	+	+	-	+	-	-	-	-	-	-	-	-	-	-	-	-	-	-
Optic atrophy	-	-	-	-	-	-	-	-	-	-	-	-	-	-	-	+	+	-	-	-	-	-	-	-	-	-	-	-	-	-	+	+	-	-	-	-	-	-	-	-	-	-	-	-	-
Nystagmus	-	-	-	-	-	-	-	-	-	-	-	+	-	-	-	+	-	-	-	-	-	-	-	-	-	-	+	+	+	-	-	-	-	-	-	-	-	-	-	-	-	-	-	+	+
Ataxia	-	-	-	-	-	-	-	-	-	-	-	+	+	-	-	-	-	-	-	-	-	+	-	-	-	-	+	+	+	-	-	-	-	-	-	-	-	-	-	-	-	-	-	-	-
Amyotrophy	-	-	-	-	-	-	+	+	+	-	-	-	-	-	-	-	-	-	-	+	+	+	-	-	-	-	-	-	-	+	-	+	-	-	-	-	-	-	-	-	-	-	+	-	-
Extrapyramidal	-	-	-	-	-	-	-	-	-	-	-	-	-	-	-	-	-	-	-	-	-	-	-	-	-	-	-	-	-	-	+	-	-	-	-	-	-	-	-	-	-	-	-	-	-
UL spasticity	-	-	-	-	-	-	+	+	+	-	-	-	-	-	-	+	+	-	-	+	+	+	-	-	-	-	-	-	-	-	-	-	-	-	-	-	-	-	-	-	-	-	-	-	-
UL weakness	-	-	-	-	-	-	+	+	-	-	-	-	-	-	-	+	-	-	-	+	+	-	-	-	-	-	-	-	-	-	-	+	-	-	-	-	-	-	-	-	-	-	-	-	-
UL hyperreflexia	+	-	+	+	+	+	+	+	+	+	-	+	-	-	+	+	+	+	+	+	+	+	+	+	-	-	-	-	-	-	-	-	+	-	-	-	-	-	-	-	-	+	+	-	-
Bladder dysfunction	-	+	+	+	+	-	+	+	+	+	-	+	+	+	+	+	+	-	-	-	+	+	-	-	-	-	-	+	+	-	-	+	+	+	+	-	-	+	-	-	-	+	+	-	-
Pes cavus	-	-	-	-	-	-	-	-	+	+	-	-	-	-	-	-	-	-	-	-	-	+	-	-	-	-	-	-	-	-	+	-	-	-	-	-	-	-	-	-	-	-	-	-	-
Syndacyly	-	-	-	-	-	-	-	-	-	-	-	-	-	-	-	-	-	+	+	-	-	-	-	-	-	-	-	-	-	-	-	-	-	-	-	-	-	-	-	-	-	-	-	-	-
LL spasticity	+	+	+	+	+	+	+	+	+	+	+	+	+	+	+	+	+	+	+	+	+	+	+	+	+	+	+	+	+	+	+	+	+	+	+	+	+	+	+	+	+	+	+	+	+
LL weakness	+	+	+	+	+	+	+	+	+	-	-	+	+	+	+	+	+	+	+	+	+	+	+	+	+	+	+	+	+	+	+	+	+	+	+	+	+	+	+	+	+	+	+	+	+
LL hyperreflexia	+	+	+	+	+	+	+	+	+	+	+	+	+	+	+	+	+	+	+	+	+	+	+	+	+	+	+	+	+	+	+	+	+	+	+	+	+	+	+	+	+	+	+	+	+
Extensor plantars	+	+	+	+	+	+	+	+	+	-	+	+	+	+	+	+	+	+	+	+	+	+	+	+	+	+	-	+	-	+	+	-	+	+	+	+	+	+	+	+	+	+	+	+	+
Impaired pain/temp	-	-	-	-	-	-	-	-	-	-	-	-	-	-	-	-	-	-	-	-	-	+	-	-	-	-	-	-	-	-	-	-	-	-	-	-	-	-	-	-	-	+	+	-	-
Impaired vib/jps	+	+	+	+	+	+	+	+	+	-	-	-	-	+	+	+	-	+	+	-	-	+	-	-	-	-	+	-	-	-	-	-	+	+	+	-	-	+	+	-	-	-	+	-	-
Spatic gait	+	+	+	+	+	+	+	+	+	+	+	+	+	+	+	+	+	+	+	+	+	+	+	+	+	+	+	+	+	+	+	+	+	+	+	+	+	+	+	+	+	+	+	+	+
Mobility	I	I	S	W	S	I	S	I	W	I	I	W	W	W	W	W	S	W	W	W	W	W	S	S	S	I	I	S	I	I	W	I	W	W	S	I	I	S	S	I	I	I	I	S	I

+ present, - absent, I independent, S sticks, crutches or frame, W wheelchairbound

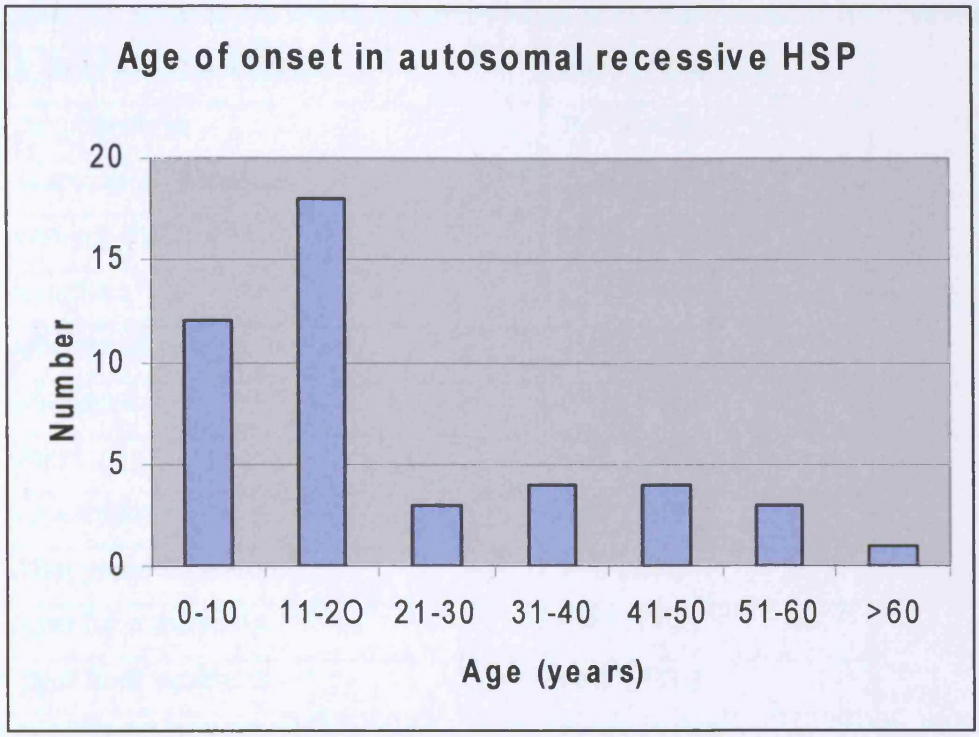

Figure 3.2 Distribution of age of onset in UK autosomal recessive HSP patients

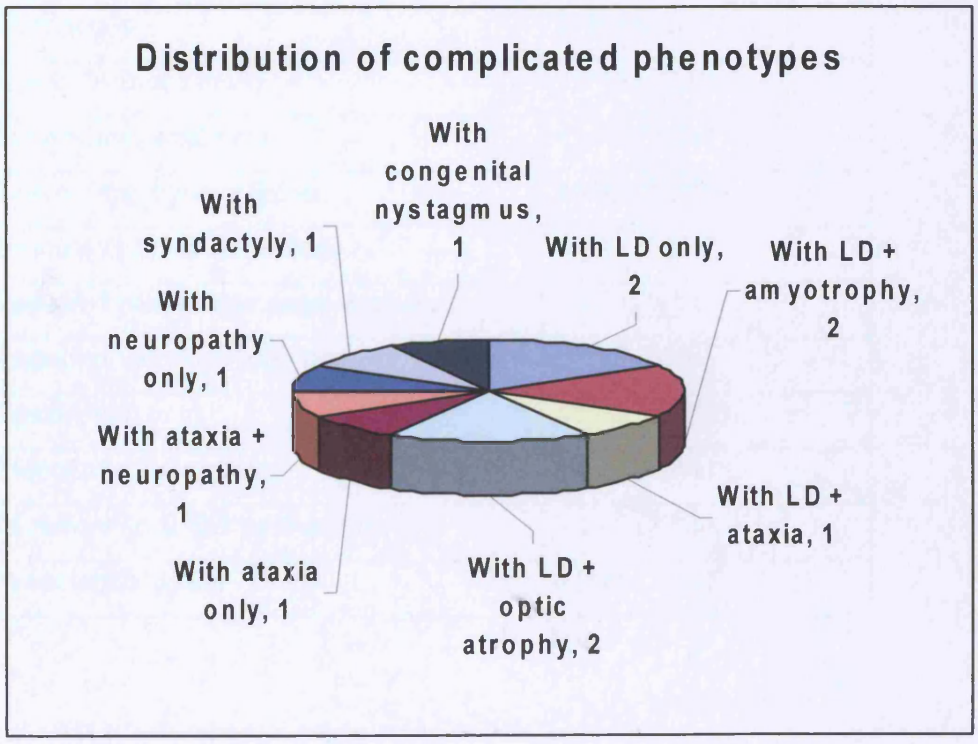

Figure 3.3 Distribution of complicated HSP phenotypes

LD – learning difficulties

Table 3.3 Summary of clinical features in all autosomal recessive HSP patients

CLINICAL FEATURE	PREVELANCE
Pure phenotype	19/45 (42%)
Complicated phenotype	26/45 (58%)
Learning difficulties	14/45 (31%)
Dysarthria	12/45 (27%)
Optic atrophy	4/45 (9%)
Nystagmus	7/45 (16%)
Ataxia	6/45 (13%)
Amyotrophy	9/45 (20%)
Extrapyramidal features	1/45 (2%)
Upper limb spasticity	8/45 (18%)
Upper limb weakness	6/45 (13%)
Upper limb hyperreflexia	23/45 (51%)
Bladder dysfunction	25/45 (56%)
Pes cavus	4/45 (9%)
Syndactyly	2/45 (4%)
Lower limb spasticity	45/45 (100%)
Lower limb weakness	43/45 (96%)
Lower limb hyperreflexia	45/45 (100%)
Extensor plantar responses	41/45 (91%)
Impaired pain/temperature sensation	3/45 (7%)
Impaired vibration/joint position sense	22/45 (49%)
Spastic gait	45/45 (100%)
Independently mobile	18/45 (40%)
Mobile with stick/crutches/frame	12/45 (27%)
Wheelchair bound	15/45 (33%)

In total, 7 families, including 19 affected individuals, were classified as having a pure HSP phenotype. Of these 47% demonstrated upper limb hyperreflexia, 53% reported symptoms of bladder dysfunction and 68% had signs of posterior column dysfunction with impaired vibration and joint position sense. Variability in age of onset and disease severity was noted within affected members of the same family.

The remaining 13 families including 26 affected members were classified as having complicated HSP phenotypes with a variety of additional neurological features. Syndacyly of the second and third toes of both feet was the only significant non-neurological associated feature identified in two affected siblings from one family. Learning disability as documented by an educational psychologist, consultant neurologist or formal IQ testing was the most common additional feature, present in 31% of all patients. Progressive cognitive decline was often suggested although confirmation of this in the form of serial testing could not be established from patient records. Dsyarthria, either spastic or cerebellar in nature, was also a frequent finding occurring in 27% of cases. Marked distal amyotrophy, as distinguished from disuse atrophy, was present in 20% of cases and invariably accounted for any documented upper limb weakness. Cerebellar ataxia occurred in 13% of cases and was usually associated with nystagmus, although in one family two affected siblings with congenital nystagmus and no cerebellar signs were identified. Optic atrophy and extrapyramidal features were relatively rare.

3.4 Discussion

A total of 20 UK families with autosomal recessive HSP were identified for clinical and genetic studies. The use of the database at the Institute of Neurology included only patients who had been seen at the National Hospital for Neurology and DNA stored for research studies. This is likely to have excluded large numbers of patients from outside the south of England. The additional use of the family register from the familial spastic paraparesis support group helped extend the search although only a proportion of patients diagnosed with HSP join the support group and not all complete the survey. The British Neurological Surveillance Unit has provided useful assistance in identifying patients with rare neurological disorders from around the country although not all consultant neurologists participate in this

and it does not attract attention of clinicians working in other areas such as paediatrics and clinical genetics. Some patients may also have already been involved in research studies into HSP and therefore been reluctant to become involved with another group. It is, therefore, not possible to comment on overall prevalence in the UK although such cases are undoubtedly rare.

The majority of autosomal recessive HSP families studied (65%) had complicated phenotypes with a variety of additional neurological features. This is higher than previously reported surveys (Topaloglu et al., 1998; Coutinho et al., 1999). The fact that a significant proportion of cases were contacted through the Institute of Neurology database may have biased this observation, as more straightforward pure cases may not have been referred for a specialist neurogenetic opinion.

The most frequent additional neurological features were learning disability, ataxia and amyotrophy. This is similar to previously reported studies (Topaloglu et al., 1998; Coutinho et al., 1999). However, these complicating features seemed to occur variably in combination both between and within families. Therefore, the division into distinct phenotypic subtypes as suggested by Coutinho and colleagues seems less clear-cut in our group of patients and is unlikely to be helpful in planning genetic linkage studies.

Two thirds of all cases had a disease onset before the age of 20 years which is typical of autosomal recessive disorders. However a number of late onset cases were identified and a variation of age of onset of up to 32 years in members of one family supports the fact that additional environmental or genetic factors influence the disease. However, autosomal dominant inheritance with incomplete penetrance or X-linked inheritance in families where only males are affected cannot be entirely excluded.

Overall, the methods used identified a useful cohort of patients with autosomal recessive HSP for further genetic studies. Further collaboration between neuroscience centres around the UK and the establishment of a national database of HSP families would assist in the generation of more accurate epidemiological data and recruitment of patients for genetic research.

Chapter 4

A CLINICAL AND GENETIC STUDY OF SPG5A LINKED AUTOSOMAL RECESSIVE HSP

4.1 Introduction

In 1994 Hentati and colleagues studied a group of five unrelated Tunisian families with autosomal recessive HSP (Hentati et al., 1994). The phenotype in all affected individuals was an early onset pure form of HSP with bladder dysfunction and mild posterior column sensory impairment. Using a genome wide linkage analysis approach they mapped a 32.8cM region in the pericentromeric area of chromosome 8 co-segregating with the disease in four of the five families with a maximum combined LOD score of 8.77 at marker D8S260. This was the first autosomal recessive HSP locus to be identified and subsequently designated SPG5A. The family excluded from linkage to this locus was clinically indistinguishable from the others demonstrating genetic heterogeneity for this form of HSP.

In 1999, Coutinho and colleagues reported one further consanguineous Algerian family from a total of 23 Algerian and Portuguese pedigrees in which linkage to the SPG5A locus could not be excluded, with a maximum LOD score of 1.96 at marker D8S1797 (Coutinho et al., 1999). Although this was not useful in refining the existing locus it was postulated that SPG5A linked AR HSP was likely to be rare and may be restricted to the North African population.

From the 20 UK autosomal recessive HSP families identified only pedigree 1 (figure 3.1) was of significant size for independent linkage analysis. The phenotype in this family was of a pure early onset form of HSP, similar to those characterised by Hentati and colleagues linked to the SPG5A locus. Linkage analysis was therefore undertaken in this family using markers spanning the SPG5A locus. Linkage to SPG5A was confirmed with peak two point LOD scores of 3.26 at $\theta = 0$ at markers D8S260 and D8S601. Further marker saturation analysis allowed refinement of the existing locus to a 23.6cM interval between markers D8S1051 and D8S1807 with a maximum multipoint LOD score of 4.84 between markers D8S1833 and D8S285. Screening of several candidate genes from within this region did not identify any pathogenic mutations. Muscle biopsy analysis from two affected individuals did not demonstrate any evidence of oxidative phosphorylation defects.

4.2 Material and methods

4.2.1 Subjects

The family was one of twenty autosomal recessive HSP kindred identified through an established database of HSP patients (pedigree 1 in figure 3.1). The parents were Caucasian first cousins. All living members were independently examined by two neurologists. All gave consent to participate in the study which received multi-regional ethical approval.

4.2.2 Genotyping and linkage analysis

Genomic DNA was extracted from whole blood using standard protocols (section 2.3.1). Linkage to the SPG5A locus was initially tested using the polymorphic microsatellite markers D8S260 and D8S601. Amplified PCR products were size fractionated by electrophoresis using 8% polyacrylamide gels (section 2.3.4) and visualised by silver staining (section 2.3.5). Additional marker saturation analysis at the SPG5A locus was performed using established markers based on information from the Marshfield map of chromosome 8.

Pairwise LOD scores were calculated using MLINK and multipoint LOD scores using HOMOZ under the assumption of equal allele frequencies and equal male and female recombination rates. Disease inheritance was presumed to be as an autosomal recessive trait with complete penetrance and an allele frequency of 10^{-4}. For the generation of multipoint LOD scores the family was deconstructed to facilitate computational efficiency.

4.2.3 Muscle biopsy analysis

Open muscle biopsy was performed under local anaesthetic from the left vastus lateralis muscle in two of the affected siblings II:3 and II:7. Muscle was analysed for standard histological and histochemical reactions including sequential cytochrome c oxidase (COX) and succinate dehydrogenase (SDH) reactions. Muscle samples from both patients and seven age matched controls were prepared and assayed as previously described for mitochondrial complex I, II/III, IV and citrate synthase (sections 2.3.13-2.3.16). Respiratory chain complex enzyme activities were all corrected for citrate synthase.

4.2.4 Mutation detection

Primers were designed to amplify the entire coding regions and splice junctions of five genes from within the SPG5A locus; AP3M2, LOC138051, ATP6VH1, SDCBP and TRAM (appendix 2). For each gene DNA was used from the mother (an obligate carrier) and one affected individual. 50µl PCR reactions were performed under optimised conditions (section 2.3.2). Purified PCR products were sequenced using BIGDYE (Applied Biosystems) and analysed on the ABI 3100 genetic analyser (sections 2.3.10 and 2.3.11).

4.3 Results

4.3.1 Clinical analysis

The family was of English ancestry. The parents were first cousins with six of their eight children were affected. Individual I:1 died age 74 of carcinoma of the pancreas and by history had no evidence of gait disturbance or other neurological disorder. Individual II:2 was examined as part of this study. Aged 83 she had no abnormal neurological signs. The main clinical findings of affected individuals are summarised in table 4.1. The phenotype observed was a pure form of HSP with four of the six affected members having some degree of additional bladder dysfunction. All affected individuals also demonstrated evidence of posterior column sensory impairment with varying degrees of diminished vibration sensation and proprioception. Significant variability in age of onset (8-40 years) and rate of disease progression was noted among affected individuals.

Initial investigations in the oldest affected sibling (II:2) included a normal MRI of the brain and spinal cord. A myelogram and CSF examination were also normal. Cortical evoked responses were absent from the legs and bilaterally delayed from the arms. Visual and brainstem evoked potentials were normal. More recently patient II:3 was re-investigated due to the later age of onset and milder phenotype. MRI of the brain and spinal cord was normal apart from the incidental finding of a Rathke's pouch cyst. EMG and nerve conduction studies were normal. Posterior tibial somatosensory evoked potentials were bilaterally absent. A full biochemical screen including white cell enzymes and very long chain fatty acids failed to identify any alternative cause for a spastic paraparesis.

Table 4.1 Clinical characteristics of affected individuals

	Family member					
Characteristic	II:2	II:3	II:4	II:5	II:7	II:8
Age at examination (years)	53	51	46	45	43	41
Age of onset (years)	8	40	9	14	20	14
Bladder dysfunction	-	-	+	++	+	+
Upper limbs:						
Spasticity	-	-	-	-	-	-
Weakness	-	-	-	-	-	-
Hyperreflexia	+	-	+	+	+	+
Posterior column sensory impairment	-	-	-	-	-	-
Lower limbs:						
Spasticity	+++	++	+++	+++	+++	+++
Ankle clonus	-	-	+	+	+	+
Weakness	+	+	++	+++	++	+
Hyperreflexia	+	+	+	+	+	+
Posterior column sensory impairment	+	+	+	+	+	+
Extensor plantar reflexes	+	+	+	+	+	+
Current mobility	I	I	F	W	F	I

+ = present (+mild, ++moderate, +++severe), - = absent.

I = Independent, F = Requires walking frame, W = Wheelchair bound.

4.3.2 Muscle biopsy analysis

Muscle biopsy samples from both affected individuals demonstrated varying degrees of denervation changes. There was a substantial variation in fibre size with an excess of type 1 fibres. Both samples showed numerous small atrophic, angulated fibres which were predominantly type IIb (figure 4.1). No ragged red fibres were seen. Oxidative stains were within normal limits in patient II:3. In patient II:7 no COX negative fibres were present although there were some SDH positive fibres . A small patch of inflammatory infiltration was also noted, although this is unlikely to be of any significance (figure 4.2). Mitochondrial respiratory chain analysis from both patient muscle samples did not demonstrate a significant reduction in mitochondrial function (figure 4.3).

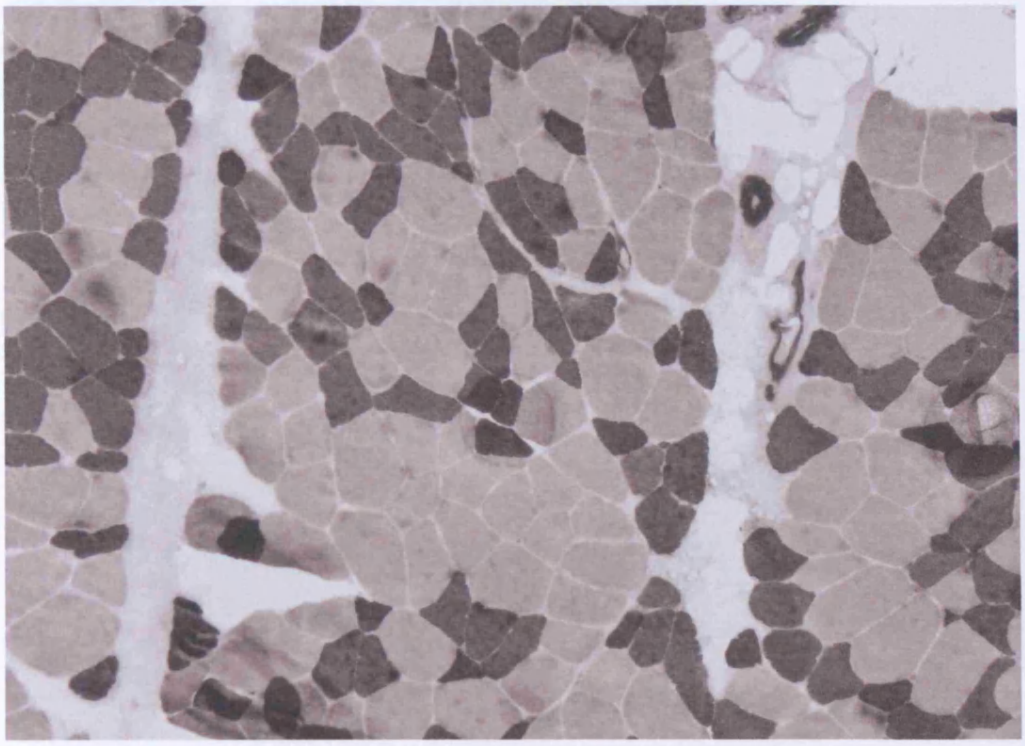

Figure 4.1 ATPase stained muscle biopsy from patient II:3 showing small angulated type IIb fibres

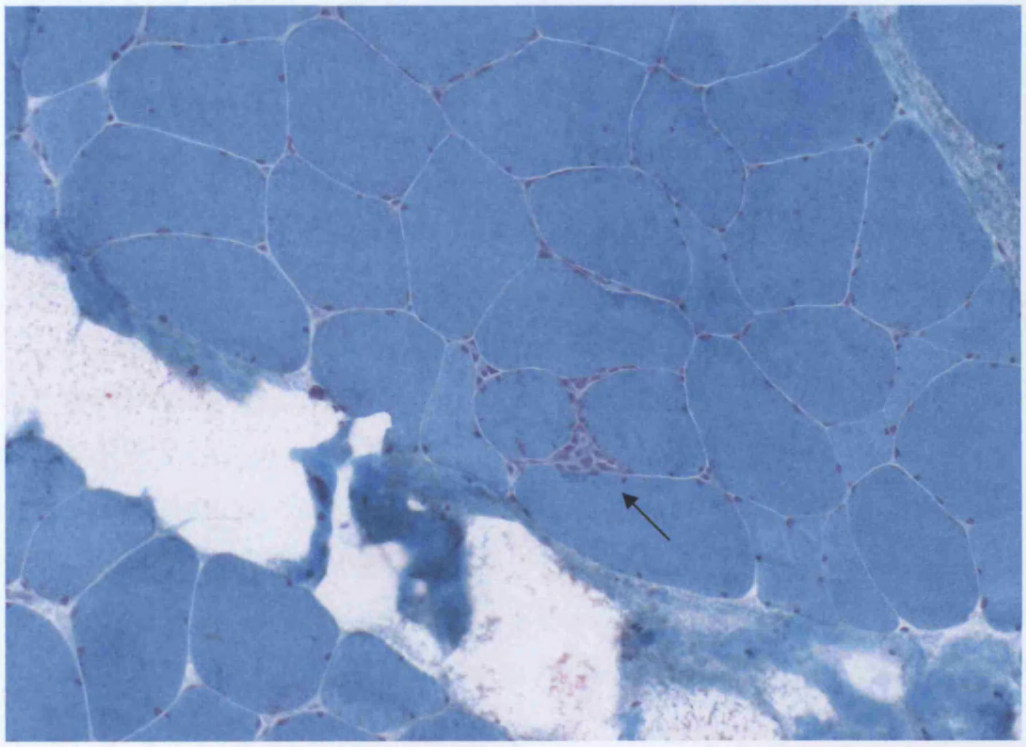

Figure 4.2 Gomori trichrome stained muscle biopsy from patient II:7 showing a small patch of inflammatory infiltration

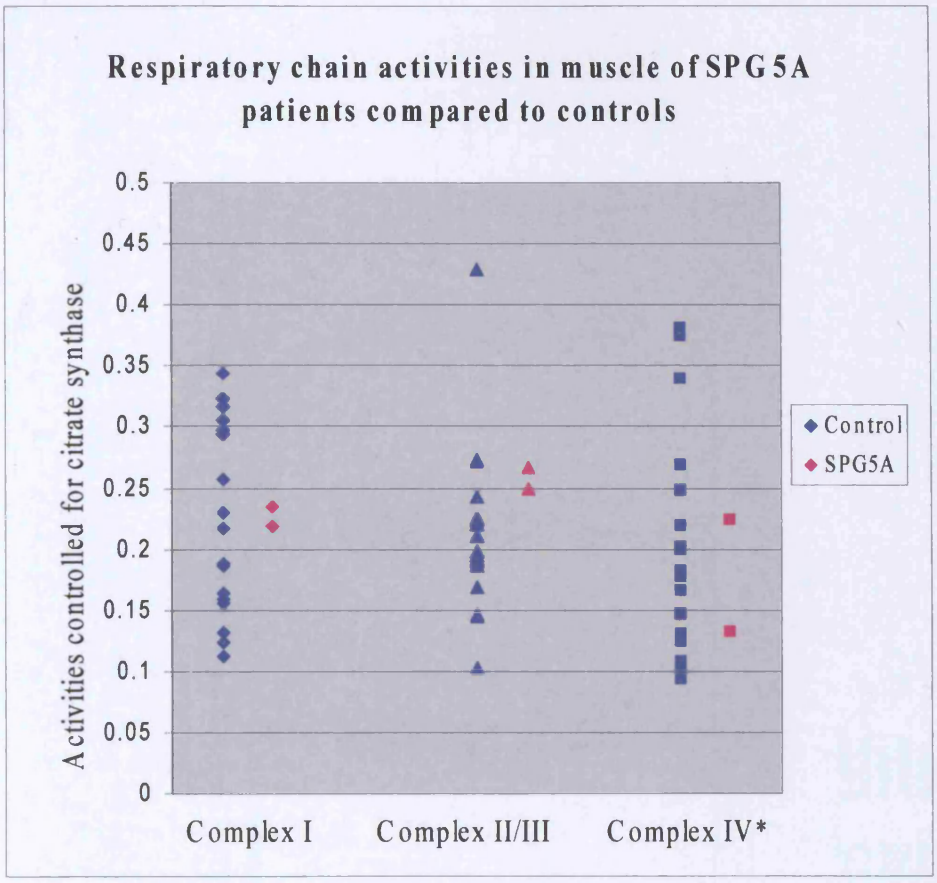

Figure 4.3 Respiratory chain complex activites in SPG5A patients

* 1 x 10^{-1}

4.3.3 Linkage analysis

Analysis of microsatellite markers spanning the SPG7, SPG11, SPG14, SPG15 and SPG 20 loci all generated LOD scores of <-2, excluding linkage. In contrast, two point LOD scores for both D8S260 and D8S601 (LOD score 3.26 at $\theta = 0$) confirmed linkage to the SPG5A locus. Haplotype analysis of additional surrounding markers is shown in figure 4.4. A region of homozygosity co-segregating with the disease in all affected individuals was established between markers D8S589 and D8S543. Multipoint LOD scores across the region were significantly positive with a maximum score of 4.84 between markers D8S1833 and D8S285 (figure 4.5). Loss of homozygosity occurred at markers D8S1051 and D8S1807, reducing the SPG5A locus interval to 23.6cM.

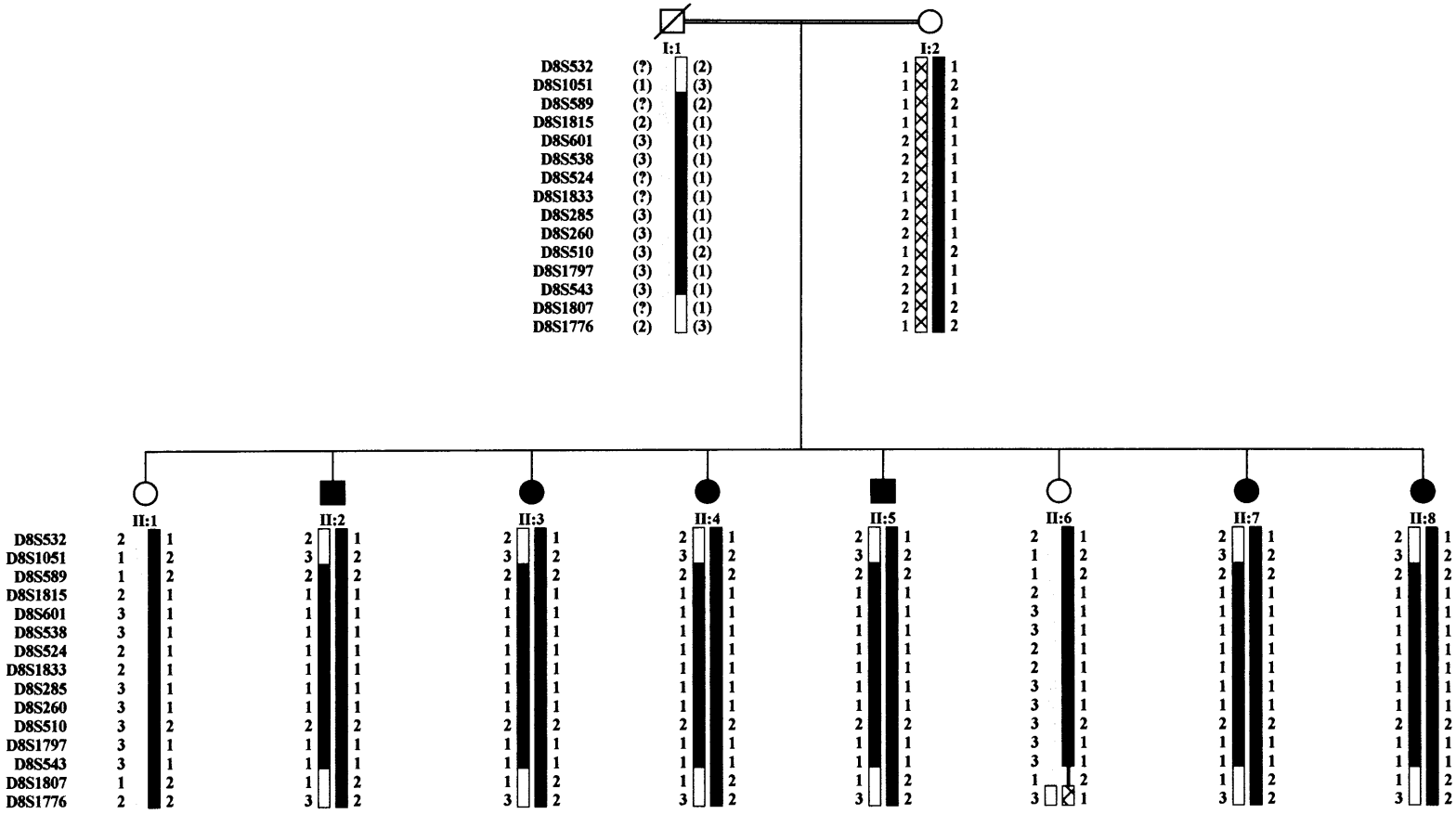

Figure 4.4 Haplotype construction in autosomal recessive HSP family for chromosome 8 markers demonstrating a region of homozygosity in all affected individuals between markers D8S589 and D8S543. Bracketed haplotypes are inferred

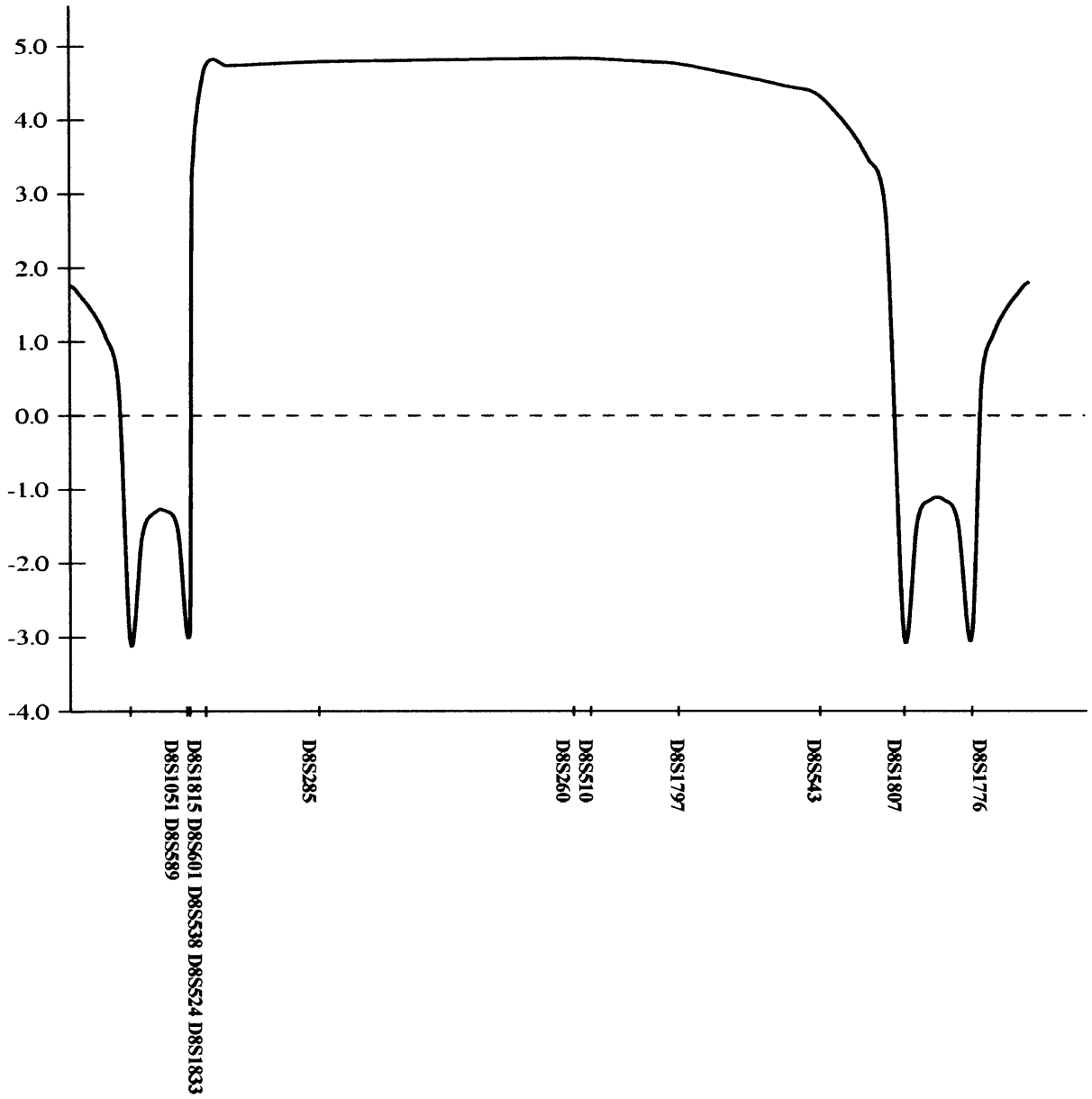

Figure 4.5 Multipoint analysis of all chromosome 8 markers generating a maximum LOD score of 4.84 between markers D8S1833 and D8S285

Of the remaining 19 ARHSP kindred SPG5A linkage was excluded in all but two small families, in which the number of affected individuals was insufficient to generate statistically significant LOD scores.

4.3.4 Mutation screening

Direct sequencing of the entire coding regions and splice junctions of five candidate genes from within the refined SPG5A locus with protein products predicted to play a role in intracellular transport or mitochondrial function (AP3M2, LOC138051, ATP6VH1, SDCBP and TRAM) failed to identify any pathogenic mutations.

4.4 Discussion

Linkage of pure autosomal recessive HSP to a 32.8cM region on chromosome 8 (SPG5A) was initially established by Hentati and colleagues in four out of five Tunisian families (Hentati et al., 1994). A further Algerian family subsequently has also shown probable linkage to this region (Coutinho et al., 1999). We have identified the first English autosomal recessive HSP family conclusively linked to the SPG5A locus, providing evidence that it is not confined to one ethnic group and may account for a significant proportion of cases worldwide.

Clinical features of affected individuals in this family were similar to those previously described with a pure HSP phenotype. Again, posterior column sensory loss was apparent along with symptoms of bladder dysfunction in four of six affected individuals suggesting a possible common phenotype for SPG5A linked HSP. However, within the family the age of onset ranged from 8 to 40 years of age with variability in disease severity and progression suggesting additional environmental or genetic factors may affect the course of the disease.

There have been limited studies of muscle pathology and mitochondrial function in HSP (Hedera et al., 2000; Santorelli et al., 2000b; Piemonte et al., 2001; McDermott et al., 2002). Muscle biopsies from patients with paraplegin mutations have shown evidence of mitochondrial dysfunction, including ragged red fibers, SDH-positive and COX-negative fibers, although in less severely affected individuals only scattered COX-negative fibers may be seen (Casari et al. 1998; McDermott et al 2001). Impairment of oxidative phosphorylation has also been reported in a small number of unlinked autosomal dominant and recessive HSP cases (Santorelli et al., 2000b; Piemonte et al., 2001; McDermott et al., 2002). The muscle biopsy in patient II:7 contained some SDH positive fibers although there were no other indications of mitochondrial dysfunction. This was supported by normal respiratory chain

function assays in both samples. The small patch of inflammatory infiltration seen in patient II:7 is of uncertain significance, although it is unlikely this reflects the underlying pathogenesis of the disease, particularly as it was not seen in the second affected patient.

Genetic linkage analysis in this family has enabled a moderate refinement of the SPG5A locus to a 23.6cM interval at chromosome 8q11.1-q21.2. These findings should prompt investigation of further autosomal recessive HSP families from diverse ethnic groups to assess linkage to SPG5A. Muglia and colleagues have subsequently reported a further potential refinement of the SPG5A locus using combined LOD scores in four small autosomal recessive HSP pedigrees, although in view of the increasingly broad genetic heterogeneity of the disorder this method raises doubts that for each individual family apparent linkage may simply have been observed due to chance (Muglia et al., 2004). The confirmed locus therefore remains large, containing over 250 established genes or partial transcripts.

The fact that muscle biopsy analysis in two affected individuals from this family did not show any histological or biochemical evidence of oxidative phosporylation defects means that a nuclear encoded mitochondrial protein similar to paraplegin is unlikely to play a pathogenic role. The possible function of other recently identified HSP genes in cellular trafficking dynamics highlights proteins with this functionality as candidates from within the refined SPG5A locus. Sequencing of 5 candidate genes; AP3M2, LOC138051, ATP6VH1, SDCBP and TRAM, from within the critical interval failed to identify any coding sequence mutations. This means that these candidates are unlikely to play a causative role in SPG5A linked HSP although mutations in upstream promoter regions or intronic sequence cannot be excluded. The search for further SPG5A linked families to narrow down the critical interval will help to rationalise the candidate gene screening approach to identify the causative gene for this form of HSP.

Chapter 5

A CLINICAL, GENETIC AND BIOCHEMICAL STUDY OF SPG7 MUTATIONS IN HEREDITARY SPASTIC PARAPLEGIA

5.1 Introduction

SPG7 was the first autosomal recessive HSP gene to be characterised. Located on chromosome 16, it comprises 17 exons spanning approximately 52 kb. The protein product, paraplegin, consists of 795 amino acids and localises to mitochondria. It was originally found to share its closest amino acid sequence homology with the yeast mitochondrial metalloproteases Afg3, Rca1 and Yme1 (Casari et al., 1998; Settasatian et al., 1999). These proteins are members of the AAA protein superfamily (ATPase associated with diverse cellular activities) which are found widely in both prokaryotic and eukaryotic cells and play an important role in a variety of cellular activities including cell division, transcription, organelle biogenesis, vesicle transport and enzyme assembly (Patel and Latterich, 1998). More specifically, yeast mitochondrial ATPases are known to possess both proteolytic and chaperone-like activities at the inner mitochondrial membrane where they are involved in the assembly and degradation of proteins in the respiratory chain complex (Pearce, 1999). Mutation of these genes in yeast induces a respiratory chain defect due to a block in the assembly of the subunits into functional enzymes (Paul and Tzagoloff, 1995). Subsequently a number of additional human genes encoding proteins highly homologous to paraplegin such as AFG3L1, AFG3L2 and YME1L1 have been discovered (Kremmidiotis et al., 2001; Banfi et al., 1999; Coppola et al., 2000). The precise function of paraplegin and related proteins in humans remains uncertain.

At the time of this work four SPG7 mutations had been described resulting in either pure or complicated HSP phenotypes. Following linkage to 16q24.3 in a large consanguineous Italian family with a variable complicated phenotype (De Michele et al., 1998), Casari and colleagues discovered a 9.5kb deletion corresponding to the last five exons of the SPG7 gene (Casari et al., 1998). Muscle biopsy analysis from two severely affected individuals from this family revealed characteristic changes of mitochondrial oxidative phosphorylation defects including ragged-red fibres, cytochrome oxidase negative (COX) and succinate dehydrogenase (SDH) positive fibres. Electron microscopy confirmed an accumulation of abnormal mitochondria containing paracrystalline inclusions in a "parking lot" pattern. However, in two less severely affected individuals only a few scattered COX negative fibres were seen. Two additional frameshift mutations, a two base pair deletion in exon 6 in a small Italian family with pure HSP and a single base insertion in exon 17 in a French HSP kindred

with a complicated phenotype including optic, cortical and cerebellar atrophy were also identified. Both families were consanguineous and homozygous for the mutation (Casari et al., 1998). Most recently, McDermott and colleagues detected a heterozygous nine base pair deletion in exon 11 of SPG7 in a father and son both affected by a spastic paraparesis suggesting a possible autosomal dominant mode of inheritance in this family (McDermott et al., 2001).

The aim of this study was to screen a large cohort of autosomal recessive and sporadic HSP cases from Great Britain to estimate the prevalence of SPG7 mutations in this population and further characterise the nature of mitochondrial dysfunction in affected individuals.

5.2 Materials and methods

5.2.1 Subjects

The 20 autosomal recessive HSP kindred previously described and a further 29 sporadic patients with no family history, in whom alternative causes for a spastic paraplegia had been excluded, were identified through an established database of British HSP patients and the British Neurological Surveillance Unit. All individuals gave informed consent to participate in the study, which received multi-regional ethical committee approval.

5.2.2 Genotyping and linkage analysis

Genomic DNA was extracted from whole blood using standard protocols (section 2.3.1). Linkage to the SPG7 locus was investigated in the 20 autosomal recessive HSP families using the polymorphic microsatellite markers D16S413, D16S3023 and D16S303. Amplified PCR products were size fractionated by electrophoresis using 8% polyacrylamide gels (section 2.3.4) and visualised by silver staining (section 2.3.5). Pairwise LOD scores were calculated using MLINK under the assumption of equal allele frequencies and equal male and female recombination rates. Disease inheritance was presumed to be as an autosomal recessive trait with complete penetrance and an allele frequency of 10^{-4}.

5.2.3 Mutation detection

18 pairs of primers were designed, based on chromosome 16 draft sequence data, to amplify the coding region and flanking splice junctions of all 17 exons of the SPG7 gene. 50µl PCR reactions were performed under optimised conditions (table 5.1).

Table 5.1 Primers and conditions for SPG7 PCR reactions

Exon	Forward primer	Reverse primer	Anneal temp. ^{0}C	mM MgCl	PCR product size (bp)
1	5' ATCACGCAGGCGCGGCTTTCAG 3'	5' CTGGGCCTTACAGAGCAGA 3'	60	1.5	270
2	5' AGTCTGCATTGCTTTGGTACT 3'	5' TAGCTGAGGCGATAAGTGTG 3'	57	1.5	228
3	5' GGAGTACACTGTTGTCCTGT 3'	5' ACAGAAATGTAAAGACATCCAG 3'	55	1.5	226
4A	5' AAGCTCTGGATGTCGCCCGT 3'	5' AGGAAATGCTGCCTCCGCTG 3'	57	1.5	193
4B	5' GCGGTTGTCATGAGCCTCCT 3'	5' CTCACTCTCACAGGCTGCCA 3'	57	2.0	241
5	5' GACTGTAGGGTTGCTCGTCT 3'	5' CAGATTACAAAGCCAAGTTAGG 3'	55	1.5	260
6	5' TTGGAAGCCTGCGTCTGTCA 3'	5' GTATTCAGCAAACACAAACCAG 3'	57	1.5	225
7	5' CTGGCATCGTGCTGCTGATT 3'	5' CCCTTCTGGGAGAGGAGGA 3'	57	1.5	257
8	5' AGTGTTGCATTGTCTGCTGC 3'	5' ATGTGTGAAAGGAGCCAGGT 3'	57	2.0	252
9A	5' CCTTGGTGTAGAACTTTGTCT 3'	5' TGTTGGAGAAGCCGGACATG 3'	55	1.5	221
9B	5' GCATCGTCTACATCGATGAG 3'	5' CCTGTTCTGAAAGACATCGG 3'	55	1.5	187
10	5' TCCCTCCTGTGTCCTGAAGG3'	5' CCAGACCACTCAGAGCGAGT 3'	57	1.5	283
11	5' ACCTGTGGCAGTAACTAGGT 3'	5' GCCTTGATGCTGTTTGCGCA 3'	57	1.5	211
12	5' CTCTTAAGCCCTGATAGCAG 3'	5' TCACCTCTCAATACCTGCCT 3'	55	2.0	252
13	5' GTCTCGAACTCCTGTCCTCA 3'	5' AGTCAGCTACAGACACAGGC 3'	60	1.5	300
14	5' ACGGAGACCTCTTAGTCCCA 3'	5' CATGGCATGCACTGGAACAG 3'	55	2.0	321
15	5' ACTGCTCTGCGCCTGCAGT 3'	5' CCTTGTGTGGTAGACCCA 3'	57	1.5	294
16	5' TCTGTGCTTTGGTGCTGGAG 3'	5' ACCGTGGGTGCTGTGTGGA 3'	57	1.5	206
17	5' ACATGCATATGCCTGTTCTTT 3'	5' CTCAGCTGAAAAGCAACTCAG 3'	55	1.5	312

Single strand conformation polymorphism (SSCP) analysis was performed using 0.6% Mutation Detection Enhancement (MDE) gels run at 4-10^{o}C for 10-16 hrs to achieve optimum separation of the strands (section 2.3.12). Mobility shifts were characterised by direct sequencing of purified PCR products using BIGDYE (Applied Biosystems) and analysed on the ABI 3100 genetic analyser (section 2.3.11).

5.2.4 Muscle biopsy analysis

Open muscle biopsies were performed under local anaesthetic from vastus lateralis in two patients with SPG7 mutations. Muscle was analysed for standard histochemical reactions including sequential cytochrome c oxidase (COX) and succinate dehydrogenase (SDH) reactions through the clinical service at the Royal Free Hospital. Muscle samples from both patients, four additional patients with autosomal recessive HSP in whom linkage to SPG7 had been excluded and 19 age-matched controls were also prepared and assayed for mitochondrial complex I, II/III, IV and citrate synthase as previously described (sections 2.3.12-2.3.16). Activities were corrected for citrate synthase. Respiratory chain complex activity was also measured in mitochondrial fragments isolated from cultured myoblasts by differential centrifugation from both patients and nine age–matched controls.

5.3 Results

5.3.1 Genotyping and linkage analysis

Linkage to the SPG7 locus was excluded in 14 of the 20 autosomal recessive HSP kindred (LOD score <-2). The remaining 6 families were not excluded due to the small pedigree size or uninformative markers. One affected individual from each of these families along with the 29 sporadic spastic paraplegia cases were therefore screened for SPG7 mutations.

5.3.2 Mutation detection

Following initial SSCP analysis and sequencing of all mobility shifts, a total of 12 heterozygous sequence changes were identified in the coding regions of the SPG7 gene. Four were previously reported polymorphisms. Three other conserved sequence changes, 120G→A (G40G), 1816 C→T (G605G) and 2283G→A (Q761Q), were also subsequently identified in control samples defining them as novel polymorphisms. The remaining five coding sequence changes were not identified in 200 control chromosomes supporting these as pathogenic mutations. An additional 7 intronic polymorphisms were also identified in patient and control samples during sequencing. A summary of SPG7 polymorphisms and their relative frequencies in patient and control chromosomes is presented in table 5.2.

Table 5.2 Frequency of SPG7 polymorphisms in patients and controls

Location	Nucleotide change	Predicted protein change	Patient Chromosomes (n = 70)	Control Chromosomes (n = 100)
Exon 1	120G→A	G40G	1	1
Intron 4	IVS4 + 12C→T	-	36	56
Intron 7	IVS7 + 5G→A	-	2	3
Intron 7	IVS7 + 17G→C	-	2	2
Intron 7	IVS7 + 38G→A	-	3	5
Intron 10	IVS10 + 19G→A	-	2	5
Exon 11	1507A→G	T503A	2	6
Exon 11	1529C→T	A510V	1	4
Intron 12	IVS12 +13C→T	-	1	4
Intron 13	IVS13 +45G→C	-	14	31
Exon 14	1816C→T	G605G	0	1
Exon 15	2063G→A	R688Q	5	24
Exon 17	2283G→A	Q761Q	2	2
Exon 17	2292C→T	I764I	2	4

In total, six SPG7 mutations were identified, five of which were novel (table 5.3). Two sporadic spastic paraplegia patients (1 and 2) were compound heterozygotes, each possessing two different mutations. A further sporadic patient (3) initially appeared to carry only a single heterozygous mutation, the 9 base pair deletion in exon 11 (1450-1458del9) that had previously been associated with possible autosomal dominant inheritance. Direct sequencing of all the remaining exons in this patient revealed a second sequence change in exon 15, 2026C→T (F676L), which had not produced a visible mobility shift on SSCP under any conditions tested. A new pair of primers containing the sequence change in the first base of the reverse primer were therefore designed and PCR under optimised conditions successfully amplified the patient DNA but none of 100 control samples, supporting this as the second mutation in this patient.

Table 5.3 SPG7 mutations detected

Patient	Location	Nucleotide change	Predicted protein change
1	Exon 1	28G→T	A10S
	Exon 13	1729G→A	G577S
2	Exon 8	1057-1085del29	Frameshift 353-384X385
	Exon 13	1715C→T	A572V
3	Exon 11	1450-1458del9	E,R,R484-486del
	Exon 15	2026T→C	F676L

5.3.3 Clinical characteristics of patients with SPG7 mutations

SPG7 mutations were associated with variably complicated HSP phenotypes in all three patients (table 5.4). Age of onset ranged from 11 to 19 years with slowly progressive deterioration. All demonstrated increased tone in all four limbs, more prominent in the legs, with relatively preserved power. Patients 2 and 3 both had marked cerebellar ataxia with associated dysarthria and cerebellar eye signs. None of the patients had signs of optic atrophy.

MRI brain scans in patients 2 and 3, who had ataxia, showed cerebellar atrophy (figure 5.1). Two small areas of periventricular high T2 signal lesions of uncertain significance were also noted in patient 2. MRI appearances of the spinal cord were normal in all three patients. Electromyogram (EMG), nerve conduction studies (NCS) and visual evoked responses in patients 2 and 3 were also normal.

Table 5.4 Clinical characteristics of patients with SPG7 mutations

Patient	1	2	3
Age (years)	17	51	42
Sex	M	F	M
Age of Onset (years)	11	14	19
Dysarthria	+	+	-
Nystagmus	-	+	+
Bladder dysfunction	-	-	+
Upper Limb			
Spasticity	+	+	+
Weakness	-	-	-
Ataxia	-	+	+
Hyperreflexia	+	+	+
Sensory impairment	-	-	-
Lower Limb			
Pes cavus	+	+	-
Spasticity	+	+	+
Weakness	-	+	+
Ataxia	-	+	+
Hyperreflexia	+	+	+
Sensory impairment	-	+	-
Plantar reflexes	↑↑	↑↑	↑↑
Gait	Spastic	Spastic-ataxic	Spastic-ataxic
Functional status	Independent	Requires stick	Independent
EMG/NCS	Not done	Normal	Normal
MRI Brain	Normal	Periventricular T2 hyperintensity. Cerebellar atrophy	Cerebellar atrophy
MRI Spinal cord	Normal	Normal	Normal

M = male, F = female, + = present, - = absent, ↑↑ = bilaterally extensor

Figure 5.1 Axial T2 MRI brain in patient 3 showing cerebellar atrophy

Both parents of patient 3 had a normal neurological examination as part of this study. The parents of patient 1 were not available, but had previously been examined and felt to be normal. The parents of patient 2 were also not available (mother died, father declined to be involved) but neither had any neurological or gait abnormalities by history.

5.3.4 Muscle biopsy analysis

Muscle biopsies from patients 2 and 3 both showed changes of denervation with limited reinnervation. In each case fibre typing showed a marked excess of type 1 fibres with numerous small, atrophic, angulated fibres, predominantly type II. No ragged-red fibres were seen and, although there were a few scattered COX negative fibres throughout the biopsies, oxidative stains, including SDH, were considered within normal limits for the age of the patients.

Analysis of mitochondrial respiratory chain function in muscle from patients 2 and 3 is shown in figure 5.2. Compared to controls, citrate synthase corrected activities for complex 1 and complex II/III fell below the mean control range in both patients, while complex IV activity appeared relatively preserved. A similar picture was apparent when the two SPG7 mutation patients were compared to other autosomal recessive HSP patients in whom linkage to SPG7 had been excluded, with complex I and complex II/III activities falling below mean controls. However, due to the small sample size in this group confidence intervals for the mean control activities were large and the differences not significant (table 5.5). Respiratory chain function assays on mitochondrial fractions isolated from cultured myoblasts in both SPG7 mutation patients also demonstrated a reduction in citrate synthase corrected complex I activity outside the standard error for mean control rates, although complex II/III and complex IV activities were within the normal range (figure 5.3).

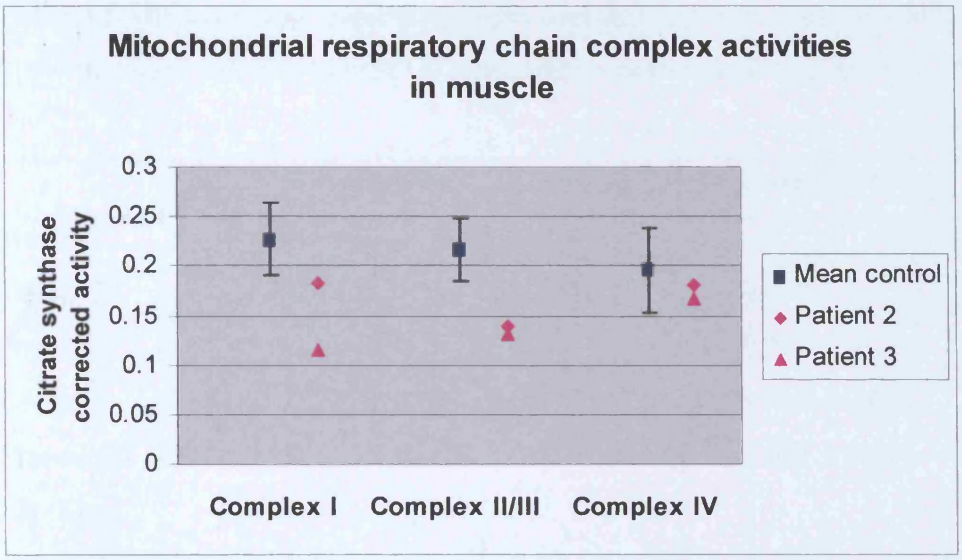

Figure 5.2 Respiratory chain complex activity corrected for citrate synthase in homogenised muscle

* Complex IV activity x 10^1

* Control data expressed as mean +/- 95% CI

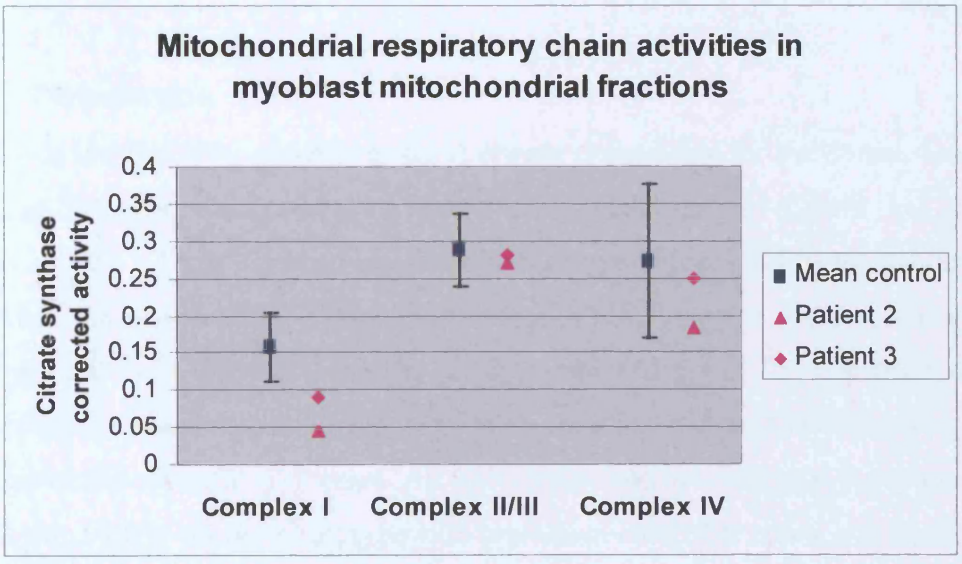

Figure 5.3 Respiratory chain complex activity corrected for citrate synthase in myoblast mitochondrial fractions

* Complex IV activity x 10^1

* Control data expressed as mean +/- 95% CI

Table 5.5 Mitochondrial respiratory chain complex activities corrected for citrate synthase in SPG7 mutation patients, non-SPG7 autosomal recessive HSP patients and controls

	Complex I	Complex II/III	Complex IV
Muscle			
Patient 2	0.182	0.132	0.018
Patient 3	0.15	0.14	0.017
Controls	0.227 ± 0.037	0.217 ± 0.032	0.019 ± 0.004
Non-SPG7 HSP	0.185 ± 0.085	0.211 ± 0.116	0.017 ± 0.116
Myoblast			
Patient 2	0.09	0.27	0.025
Patient 3	0.044	0.28	0.018
Controls	0.158 ± 0.046	0.288 ± 0.046	0.027 ± 0.011

± 95% Confidence Interval

5.4 Discussion

Since the discovery of SPG7 as the first gene responsible for autosomal recessive HSP only four mutations, each in separate families, have been reported (Casari et al., 1998; McDermott et al, 2001). Three occurred in consanguineous pedigrees possessing homozygous mutations, while the most recently reported heterozygous nine base pair deletion in exon 11 (1450-1458del9) was found in the father and son from a family in which possible autosomal dominant inheritance was suggested. We have identified six SPG7 mutations, in three apparently sporadic HSP cases. All were compound heterozygous for two separate mutations. A remarkably similar phenotype with prominent cerebellar ataxia was observed in two of these cases. No mutations were identified in any of the six autosomal recessive HSP patients from families in whom linkage to the SPG7 locus could not be excluded. The distribution of the mutations identified in SPG7 is shown in figure 5.4

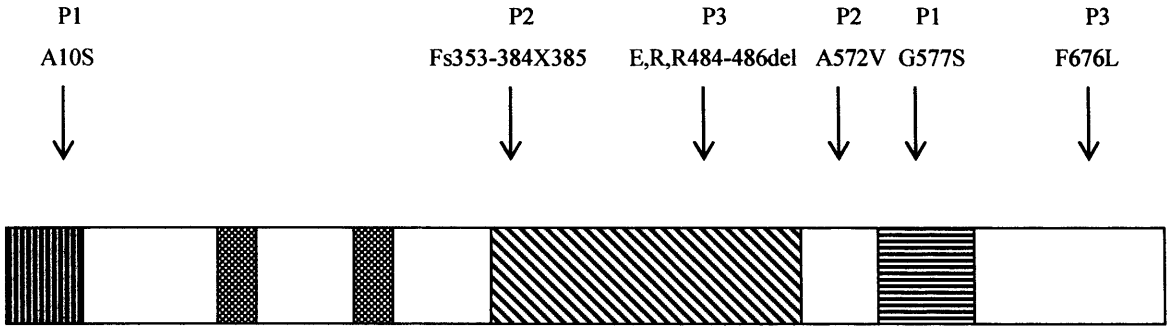

Leader peptide

Transmembrane domains

AAA cassette

Zinc binding domain

P1 = patient 1, P2 = patient 2, P3 = patient 3.

Figure 5.4 Schematic representation of the SPG7 gene showing functional domains and sites of mutations

The two missense mutations in patient 1 occur in highly conserved functional domains. The A10S mutation in exon 1 results in the substitution of a hydrophobic to hydrophilic amino acid residue in the leader peptide of paraplegin, which is essential for targeting of the protein to mitochondria. These short amino acid sequences at the N-terminal of nuclear encoded mitochondrial proteins need to form a basic, amphipathic helix in order to fulfil this function (Lithgow, 2000). The introduction of a hydrophilic amino acid residue into the leader peptide is therefore predicted to disrupt the mitochondrial localisation of paraplegin. The second mutation, G577S, is situated within the conserved zinc-binding motif (HESGH) providing further evidence for the functional significance of this domain in paraplegin.

In patient 2, the missense mutation in exon 13 (A572V), results in an amino acid substitution two residues before the zinc binding domain. Although both are small non-polar, hydrophobic amino acids, modelling of the mutant protein with the prediction program GOR4 (http://npsa-pbil.ibcp.fr/cgi-bin/secpred_gor4.pl) showed an altered conformation in the region of the zinc-binding domain from an alpha helix, random coil, alpha helix pattern to an extended

strand. This alteration in secondary structure is likely to disrupt the functional activity of this domain. The second mutation in patient 2, a 29 base pair deletion in exon 8 (1057-1085del29), is within the AAA cassette involving part of the highly conserved ATP binding motif. It causes a frameshift with a premature stop codon at residue 385, predicted to result in a truncated protein.

The first mutation identified in patient 3 was the nine base pair deletion in exon 11 (1450-1458del9), previously reported as a possible autosomal dominant mutation (McDermott et al., 2001). This is within the AAA cassette, resulting in the loss of three amino acids (E,R,R484-486del). In patient 3 our SSCP analysis also failed to identify a second mutation and it was only by direct sequencing of the remaining SPG7 exons that a further sequence change, 2026C→T (F676L) was detected. This was confirmed as a mutation by allele specific oligonucleotide analysis in 200 control chromosomes.

Neurological examination of the parents of patient 3, both in their 70's and asymptomatic, was entirely normal. Sequencing of the two exons in both parents confirmed the mother carried the nine base pair deletion in exon 11 (figure 5.5) and the father the missense mutation in exon 15. In this case the 1450-1458del9 clearly acts in an autosomal recessive manner with a combination of two heterozygous mutations required to produce the disease phenotype. The second mutation F676L did not occur in an obvious functional domain within paraplegin. It results in substitution of leucine for phenylalanine and this change was not detected in 200 control chromosomes implying it is likely to be pathogenic.

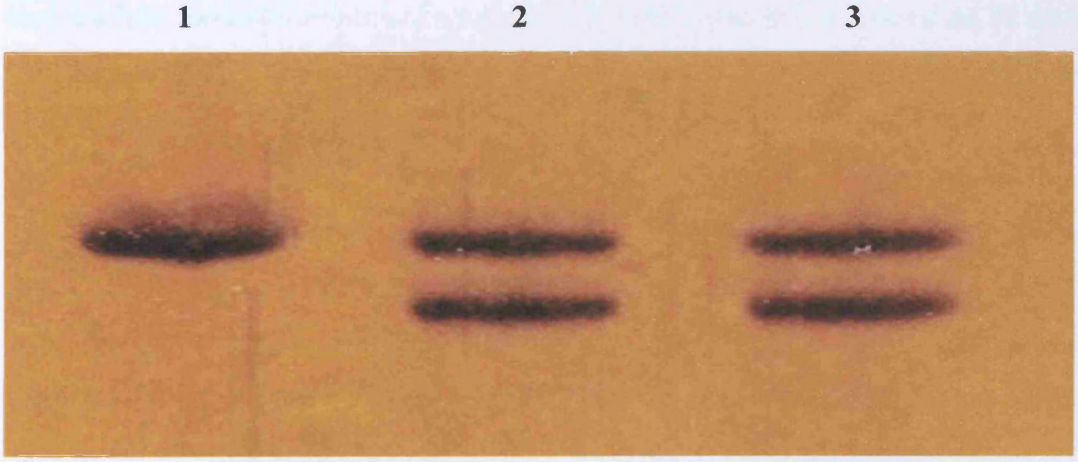

Figure 5.5 8% PAGE gel showing normal SPG7 exon 11 in lane 1 (father) and 9 base pair deletions in lanes 2 (mother) and 3 (patient 3)

Histological analysis of muscle from two patients with confirmed SPG7 mutations failed to demonstrate the previously reported morphological changes associated with oxidative phosphorylation impairment, although both our patients were still ambulatory and are likely to have been less severely affected than previous cases. The absence of these features on muscle biopsy therefore cannot be used to exclude SPG7 as the cause of the disease. The only consistent finding was of denervation changes with an excess of type I fibres which probably reflects longstanding spasticity.

Mitochondrial respiratory chain activities in muscle from patients 2 and 3 did, however, show a reduction in complex I and complex II/III function, when corrected for citrate synthase, compared to controls. Similar results were obtained when respiratory chain complex activities in muscle were compared to other patients with autosomal recessive HSP in whom SPG7 mutations had been excluded, suggesting that this effect may not simply reflect the effect on muscle of longstanding spasticity and reduced mobility. However, due to the small number of non-SPG7 autosomal recessive HSP patients differences between the two groups did not reach statistical significance.

A previous study of respiratory chain function in muscle from HSP patients included two patients with autosomal recessive HSP, in whom SPG7 mutations had been excluded (Piemonte et al., 2001). One of these had characteristic histological changes associated with oxidative phosphorylation impairment and both had isolated complex I deficiencies. A recent study of mitochondrial function in HSP patients in whom both SPG4 and SPG7 mutations had been excluded also demonstrated a reduction in both complex I and complex IV activities (McDermott et al, 2003), suggesting respiratory chain defects may be common to more than one form of autosomal recessive HSP.

The pattern of complex I-III deficiency in skeletal muscle is reminiscent of the pattern of defect found in cardiac tissue from patients with Friedrich's ataxia (FRDA) (Bradley et al., 2000). In FRDA deficiency of frataxin is thought to result in abnormal iron-sulphur cluster formation in respiratory chain proteins, leading to oxidative stress and damage. This pattern of complex I-III deficiency is also seen, for example, in the SOD2 knockout mouse (Melov et al., 1999). It is therefore possible that the pattern of respiratory chain defect in the muscle from patients with SPG7 mutations may represent excess free radical mediated damage. The

fact that only a defect in complex I activity was observed in myoblasts may simply represent the accumulation of oxidative damage in a fixed as opposed to dividing tissue. Subsequently, Atorino and colleagues have also demonstrated complex 1 deficiency in cultured fibroblasts from two of the original patients with the homozygous 9.5kb deletion in SPG7 (Atorino et al., 2003). In addition, they demonstrated that paraplegin forms a complex with a homologous protein AFG3L2 at the inner mitochondrial membrane, which was found to be abnormal in the HSP fibroblasts. The increased sensitivity to oxidative stress was found to be reversed by the exogenous expression of wild-type paraplegin suggesting that the complex I deficiency may directly contribute to the process of neurodegeneration.

Overall SPG7 mutations appear to be a relatively rare cause of HSP, identified in only 3/49 (6%) of patients studied. This figure, however, should be regarded as a minimum estimate as it is likely that SSCP may have failed to detect all mutations. In addition, this study demonstrates that the SPG7 locus is highly polymorphic which means that SSCP would not be an efficient tool for screening for mutations and direct sequencing may be preferable. Elleuch and colleagues recently screened a total of 136 individuals with both pure and complicated autosomal recessive HSP using a combination of denaturation high-performance liquid chromatography and direct sequencing (Elleuch et al., 2006). They identified 47 sequence variations in the SPG7 gene including 6 mutations, 27 polymorphisms and 14 changes with uncertain effects. Of these only one case had compound heterozygous mutations which were definitely causative. The phenotype in this family was also complicated with cerebellar ataxia. 20 further families were found to have a single heterozygous mutation not found in a large control population. Of these four were predicted to produce highly defective proteins suggesting that they were indeed pathogenic. It is therefore possible that large scale deletions, intronic or promoter sequence mutations may be causative in these cases. Overall this study supports a frequency of SPG7 mutations causing autosomal recessive HSP in around 5% of cases.

Unlike many of the more common forms of HSP it is hoped that the underlying pathogenesis involving mitochondrial dysfunction associated with SPG7 mutations may make these cases more amenable to therapeutic interventions than other forms of the disease. A mouse model for paraplegin-associated HSP has also now been developed (Ferreirinha et al., 2004). Paraplegin deficient mice manifest progressive motor impairment with similar pathological

evidence of axonal degeneration, morphologically abnormal mitochondria and impaired respiratory chain function as seen in human patients. Recently, using a gene therapy approach, the intamuscular delivery of paraplegin through an adenoassociated virus vector has been shown to rescue some of the axonal changes seen in paraplegin deficient mice (Pirozzi et al., 2005). Again, this offers hope that similar techniques may be developed for treatment in human patients. However, gene therapy using a variety of vectors remains in the early stages for treating human disease and is limited by both safety issues and the ability to target delivery of the gene to the appropriate areas, in this case the central nervous system. The mouse model does though provide future opportunities for testing drug treatments based on neuroprotection or improving mitochondrial respiratory chain function. Further studies are required to determine the precise function of paraplegin in human mitochondria in health and disease in order to facilitate the development of potentially disease modifying treatments for this type of HSP.

Chapter 6

SPG3A MUTATION SCREENING IN ENGLISH FAMILIES WITH EARLY ONSET AUTOSOMAL DOMINANT HSP

6.1 Introduction

In 1993 Hazan and colleagues mapped the first locus for autosomal dominant HSP (SPG3A) to chromosome 14q (Hazan et al., 1993). Linkage to this region was excluded in further autosomal dominant HSP kindred confirming the genetic heterogeneity of the disease. Following further refinement of the critical interval, Zhao and colleagues screened for mutations in a number of candidate genes in three large SPG3A linked families (Zhao et al., 2001). They identified three separate pathogenic mutations in a gene encoding a novel protein with significant homology to the dynamin family of GTPases, which they named atlastin. The mutations were all situated within the N-terminal region, resulting in the alteration of amino acids in the conserved GTPase domain.

Sequencing of the SPG3A gene in a further 10 early onset autosomal dominant HSP kindred, in which linkage analysis had not been performed, identified a further two families in whom all affected individuals possessed the same R239C mutation found in one of the original linked pedigrees. Although these families were not apparently related a distant founder effect could not be excluded (Zhao et al., 2001). Muglia and colleagues subsequently identified a further SPG3A mutation in an additional autosomal dominant HSP family (Muglia et al., 2002). Again this was situated within the N-terminal region. All the families with SPG3A mutations were noted to have an early onset pure HSP phenotype.

In this study we screened 12 English autosomal dominant HSP families with an early onset pure form of the disease to assess the frequency of mutations in this population.

6.2 Patients and methods

12 autosomal dominant HSP families with an uncomplicated phenotype and age of onset less than 12 years were identified from an existing database of HSP patients. Approval for genetic studies in HSP was obtained from the multi-regional ethics committee and all participants gave informed consent. DNA from index cases from each of the 12 families had previously been screened for spastin mutations using a combination of single stranded conformation polymorphism (SSCP) analysis and

sequencing of any motility shifts (Proukakis et al., 2003). No sequence variations were identified in the SPG4 gene in any of these cases.

DNA was extracted from whole blood using standard techniques (section 2.3.1). The 14 exons and flanking sequences of the SPG3A gene were amplified by the polymerase chain reaction (PCR) using the primers and conditions described previously (Zhao et al., 2001). Sequencing of purified PCR products on both strands was performed using the Big Dye Terminator kit (Applied Biosystems) according to manufacturer's protocols and analysed on the ABI3100 genetic analyser (section 2.3.11). Single strand conformation polymorphism (SSCP) analysis was performed using 0.6% Mutation Detection Enhancement (MDE) gels run at 10°C for 14 hrs to achieve optimum separation of the strands (section 2.3.12).

6.3 Results

Direct sequencing identified a heterozygous C and T at nucleotide 884 of the atlastin full length cDNA resulting in the previously described R239C mutation in the index case from one autosomal dominant HSP family. Co-segregation of the disease with the mutation in all affected members was demonstrated by SSCP analysis of the exon 7 PCR product (figure 6.1) and subsequently confirmed by direct sequencing (figure 6.2). The age of onset of the disease in this family was identical in all affected individuals at 3 years of age with insidious disease progression and increasing disability over many years. The main clinical characteristics of all affected individuals studied are summarised in table 6.1. No further SPG3A mutations were identified in any of the 14 exons or flanking splice sites in affected individuals from the remaining 11 families.

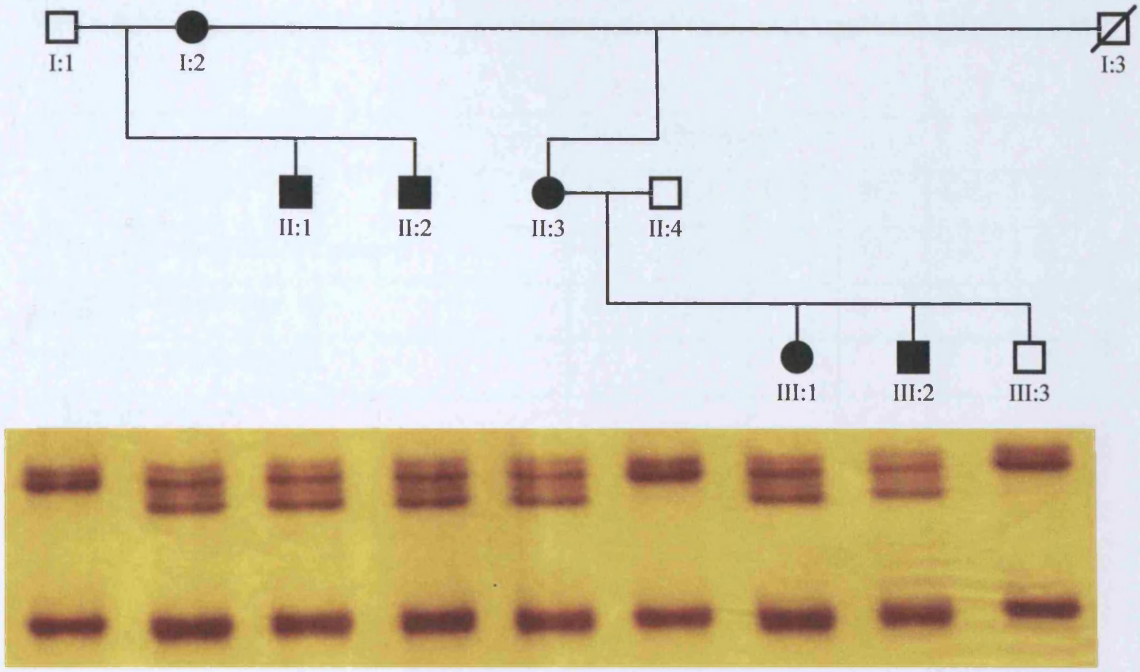

Figure 6.1 Early onset autosomal dominant HSP family with SSCP analysis of exon 7 showing different motility patterns in affected and unaffected individuals

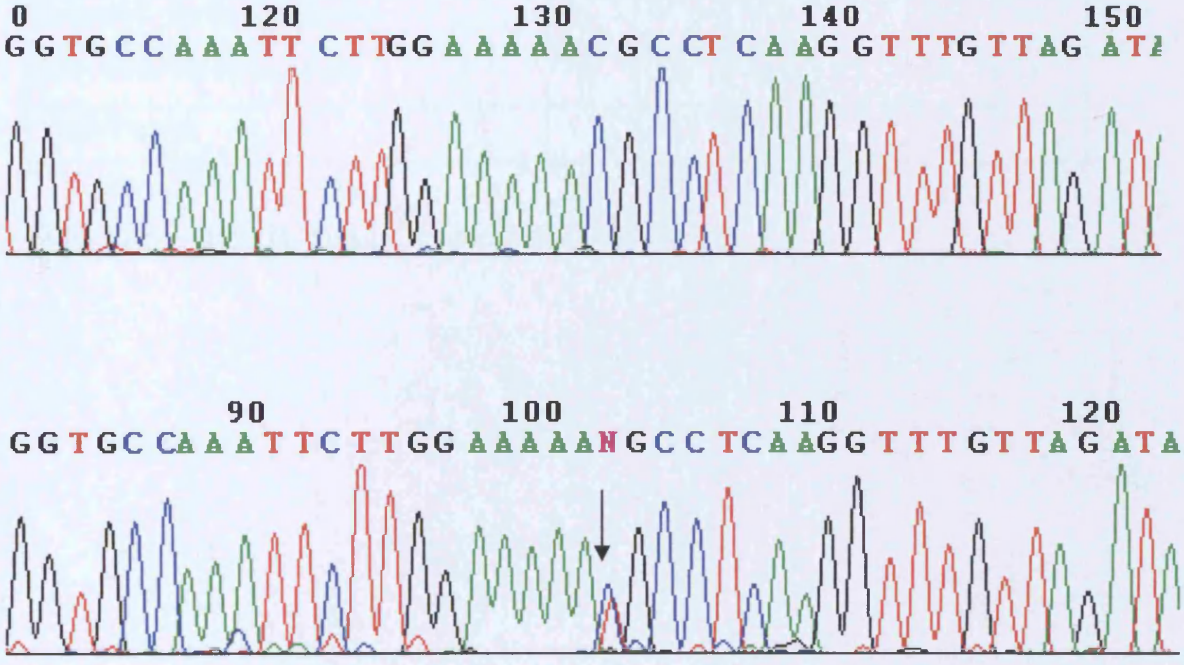

Figure 6.2 Representative SPG3A sequences from normal and affected individuals. The arrow indicates the heterozygous C and T at nucleotide 884 in an affected individual

Table 6.1 Clinical characteristics of affected individuals carrying the R239C mutation

	Family member					
Characteristic	I:2	II:1	II:2	II:3	III:1	III:2
Age at examination (years)	62	40	35	33	14	11
Age of onset (years)	3	3	3	3	3	3
Bladder dysfunction	-	-	-	-	-	-
Upper limbs:						
Spasticity	-	-	-	-	-	-
Hyperreflexia	-	-	-	-	-	-
Lower limbs:						
Spasticity	-	++	+++	+++	+++	+++
Ankle clonus	-	+	+	+	+	+
Weakness	+++	++	++	++	+	+
Hyperreflexia	-	+	+	+	+	+
Sensory impairment	-	-	-	-	-	-
Extensor plantar responses	+	+	+	+	+	+
10m walk time (seconds)	19	13	14	15	12	11
Walking aid	+	-	-	-	-	-

- = absent, + = present (+ mild, ++ moderate, +++ severe)

6.4 Discussion

The identification of the R239C mutation in exon 7 of the SPG3A gene is the first to be confirmed in an English autosomal dominant HSP family, highlighting a widespread prevalence. This particular mutation is the most frequently occurring SPG3A mutations so far described, suggesting either a commonly occurring new mutation or founder effect from a common ancestral mutation.

The phenotype observed in this family was of a uniformly early onset uncomplicated HSP, with all affected members developing gait disturbance from the age of 3 years. This appears to be the commonest phenotypic presentation with SPG3A mutations and when there is little or no disease progression cases may be mistaken for spastic diplegic cerebral palsy (Rainier et al., 2006). However, later onset patients have been reported, in one case associated with the same mutation that was found in an early onset family (Sauter et al., 2004). A complicated phenotype with axonal neuropathy has also been described (Scarano et al., 2005).

Despite the early onset in this family there was clear evidence of insidious disease progression with worsening lower limb weakness and increasing disability with time, suggesting an underlying neurodegenerative rather than neurodevelopmental process. However, the phenotype associated with SPG3A mutations does appear overall to be less severe than those frequently seen with other forms of autosomal dominant HSP where patients may be wheelchair bound after prolonged disease duration (Reid et al., 1999). In this family the disease demonstrated complete penetrance with no apparently asymptomatic individuals carrying the mutation, as has been observed in other forms of autosomal dominant HSP (Patel et al., 2001). Only one family with SPG3A mutations demonstrating incomplete penetrance has so far been described (D'Amico et al., 2004).

Overall SPG3A mutations were identified in affected individuals from only 1/12 (8%) early onset uncomplicated autosomal dominant HSP families from the UK, indicating that even within this specific group of autosomal dominant HSP patients SPG3A mutations appear to be rare. Patients had been previously screened for spastin mutations using a combination of single stranded conformation polymorphism

(SSCP) analysis and sequencing of any motility shifts although it is possible that mutations may have been missed using this screening method and large scale deletions of the spastin gene, which have recently been found to be as common as point mutations (Depienne et al., 2007) would not be detected with this approach. It is therefore still possible that some of these families may harbour undetected spastin mutations causing an early onset HSP phenotype.

Subsequent studies screening for SPG3A mutations in early onset, spastin negative, autosomal dominant HSP patients from different populations have reported a much higher prevalence. Sauter and colleagues identified SPG3A mutations in 38% of such cases (Sauter et al., 2004), while Dürr and colleagues demonstrated a similar prevalence of 39% among European and African families (Dürr et al., 2004). This suggests that either the frequency of SPG3A mutations varies significantly between populations or that due to the smaller numbers studied in our group SPG3A mutations were underrepresented.

The precise function of atlastin in humans and mechanism by which mutations cause disease remain unclear. Dynamins, the proteins most closely associated with atlastin, are known to play a role in a wide variety of vesicle trafficking events (McNiven et al., 2000). The atlastin protein is localised to the Golgi apparatus predominantly in brain, where it is enriched in pyramidal neurons in the cerebral cortex and hippocampus (Zhu et al., 2003). Recently using confocal and electron microscopies, Zhu and colleagues have found that atlastin is highly enriched in vesicular structures within axonal growth cones and axonal branch points in cultured cerebral cortical neurones, suggesting a possible functional role for atlastin in axonal development (Zhu et al., 2006). To support this notion knockout of atlastin expression in these neurones was found to reduce the number of neuronal processes and impair axon formation and elongation during development (Zhu et al., 2006).

Two separate groups have also recently identified that atlastin binds with spastin which is a microtubule severing ATPase involved in axonal transport suggesting that there may be disruption to a common molecular pathway responsible for axonal growth and maintainace underlying these forms of HSP (Sanderson et al., 2006;

Evans et al., 2006). Further studies into the function of atlastin and consequences of mutations should enhance our understanding of the pathogenesis of the disease.

Chapter 7

A NEW LOCUS FOR AUTOSOMAL RECESSIVE HSP, SPG26, MAPS TO CHROMOSOME 12p11.1-12q14

7.1 Introduction

At the time of this work nine autosomal recessive HSP loci had been identified and causative mutations found in three genes; SPG7 (paraplegin), SPG20 (spartin) and SPG21 (maspardin) [Casari et al., 1998, Patel et al., 2002; Simpson et al., 2003]. SPG7 was the first autosomal HSP gene to be characterised. The protein product of the SPG7 gene, paraplegin, is a member of the AAA protein superfamily (ATPase associated with diverse cellular activities). Paraplegin localises to the mitochondria and is highly homologous to a number of yeast mitochondrial metalloproteases , which are known to possess both proteolytic and chaperone-like activities at the inner mitochondrial membrane where they are involved in the assembly and degradation of proteins in the respiratory chain complex (Pearce, 1999). SPG7 mutations may result in either pure or complicated HSP phenotypes. Muscle biopsy analysis of patients with SPG7 mutations may show histological evidence of mitochondrial dysfunction and recently biochemical studies have shown specific defects in mitochondrial respiratory chain function (Casari et al., 1998; McDermott et al., 2001).

Mutations in the SPG20 and SPG21 genes have so far only been identified in the Old Order Amish population in association with well-characterised complicated HSP phenotypes, the Troyer and Mast syndromes (Patel et al., 2002; Simpson et al., 2003). The protein product of SPG20, spartin, contains a MIT domain and is thought to play a role in cellular trafficking (Ciccarelli et al., 2003). Similarly maspardin, the product of the SPG21 gene, has been shown to localise to transportation vesicles and may play a role in protein transportation or sorting (Simpson et al., 2003).

The remaining autosomal recessive HSP loci have been mapped to chromosomes 8q11.1-q21.2, SPG5A (Hentati et al., 1994; Wilkinson et al., 2003); 15q13-q15, SPG11 (Martinez Murillo et al., 1999; Shibasaki et al., 2000), 3q27-q28, SPG14 (Vazza et al., 2000), 14q22-q24, SPG15 (Hughes et al., 2001); 1q24-q32, SPG23 (Blumen et al., 2003); 13q14, SPG24 (Hodgkinson et al., 2002) and 6q23-q24.1, SPG25 (Zortea et al., 2002).

We identified a large consanguineous Kuwaiti family with autosomal recessive HSP, complicated by distal amyotrophy, dysarthria and intellectual impairment for further genetic analysis.

7.2 Materials and methods

7.2.1 Subjects

A large consanguineous family comprising of five affected and seven unaffected siblings with a complicated HSP phenotype were identified through the medical genetics services in Kuwait. The parents were first cousins and of Bedouin ancestry. All individuals gave informed consent to participate in the study, which received ethical committee approval.

7.2.2 Genotyping and linkage analysis

Genomic DNA was extracted from whole blood using standard protocols (section 2.3.1). Genome wide linkage analysis, using parents and affected individuals only, was performed with the ABI linkage marker set (version 2) with an ABI 3100 genetic analyser and Genotyper software (version 3.7) [sections 2.3.6-2.3.9]. Marker saturation analysis was performed using microsatellite markers based on information from the Marshfield genetic map of chromosome 12. Amplified PCR products were size fractionated by electrophoresis using 8% polyacrylamide gels (section 2.3.4) and visualised by silver staining (section 2.3.5). Multipoint LOD scores were calculated using GENEHUNTER (version 2.1) under the assumption of equal allele frequencies and equal male and female recombination rates. Disease inheritance was presumed to be as an autosomal recessive trait with complete penetrance and an allele frequency of 10^{-4}. The pedigree was deconstructed to aid computational efficiency.

7.2.3 Sequencing of the KIF5A gene

The 28 exons and flanking splice junctions of the KIF5A gene were amplified using the primers and reaction conditions described previously (Reid et al., 2002). Sequencing of purified PCR products was performed using the Big Dye Terminator kit (Applied Biosystems) according to manufacturer's protocols and analysed on the ABI3100 genetic analyser (section 2.3.11).

7.3 Results

7.3.1 Clinical analysis

The clinical characteristics of this family were initially reported by Farag and colleagues in 1994 (Farag et al., 1994). The family were subsequently re-assessed as part of this study by two independent neurologists in Kuwait (E Samilchuck and R Khan) and additional investigations carried out. A uniform early onset of disease between 6 and 11 years of age was noted. At the time of examination all affected individuals had signs of a progressive spastic paraparesis with distal amyotrophy in both upper and lower limbs. Four of the five were dysarthric. All demonstrated mild to moderate intellectual impairment with reduced verbal and performance IQ, although it is unclear whether this represents progressive cognitive decline, static learning disability or secondary to other factors associated with their physical disability. The clinical characteristics of affected individuals are summarised in table 6.1. Neurological examination of the parents and remaining siblings was unremarkable. Routine biochemical studies and neurophysiological testing including nerve conduction velocities and EEG were within normal limits. MRI of the brain in one of the affected individuals was unremarkable.

Table 7.1 Clinical characteristics of affected individuals

Affected individual	**1**	**2**	**3**	**4**	**5**
Age at examination (years)	42	39	36	30	22
Age of onset (years)	6	6	6	6	11
Dysarthria	+++	+++	+++	+++	-
Distal amyotrophy	+++	+	+++	+++	+++
Lower limb spasticity	+++	+++	+++	++	+
Ankle clonus	+	+	+	-	-
Lower limb hyperreflexia	+++	+++	+++	+++	+
Plantar response	↑↑	↑↑	↑↑	↓↓	↓↓
Gait	Spastic-ataxic	Spastic	Spastic	Spastic	Spastic
Emotional lability	+	+++	+	+++	-
IQ Verbal Performance	 55 61	 55 72	 52 73	 48 73	 73 64

- absent, + mild, ++ moderate, +++ severe. ↑↑ bilaterally extensor, ↓↓ bilaterally flexor

7.3.2 Genotyping and linkage analysis

Following the genome wide scan a region of homozygosity was identified on chromosome 12 flanked by markers D12S345 and D12S326. Marker saturation analysis demonstrated a 22.8cM region of homozygosity co-segregating with the disease in all affected individuals flanked by markers D12S59 and D12S1676 (figure 7.1). Multipoint LOD scores across the region were significantly positive with a maximum score of 5.1 between markers D12S1686 and D12S1702 (figure 7.2).

A database search of the region identified approximately 400 known or predicted genes including KIF5A, in which a missense mutation (A767G) has previously been described in a family with an uncomplicated autosomal dominant form of HSP. Direct sequencing of all 28 exons and splice junctions of the KIF5A gene in parents and affected individuals did not reveal any pathogenic mutations.

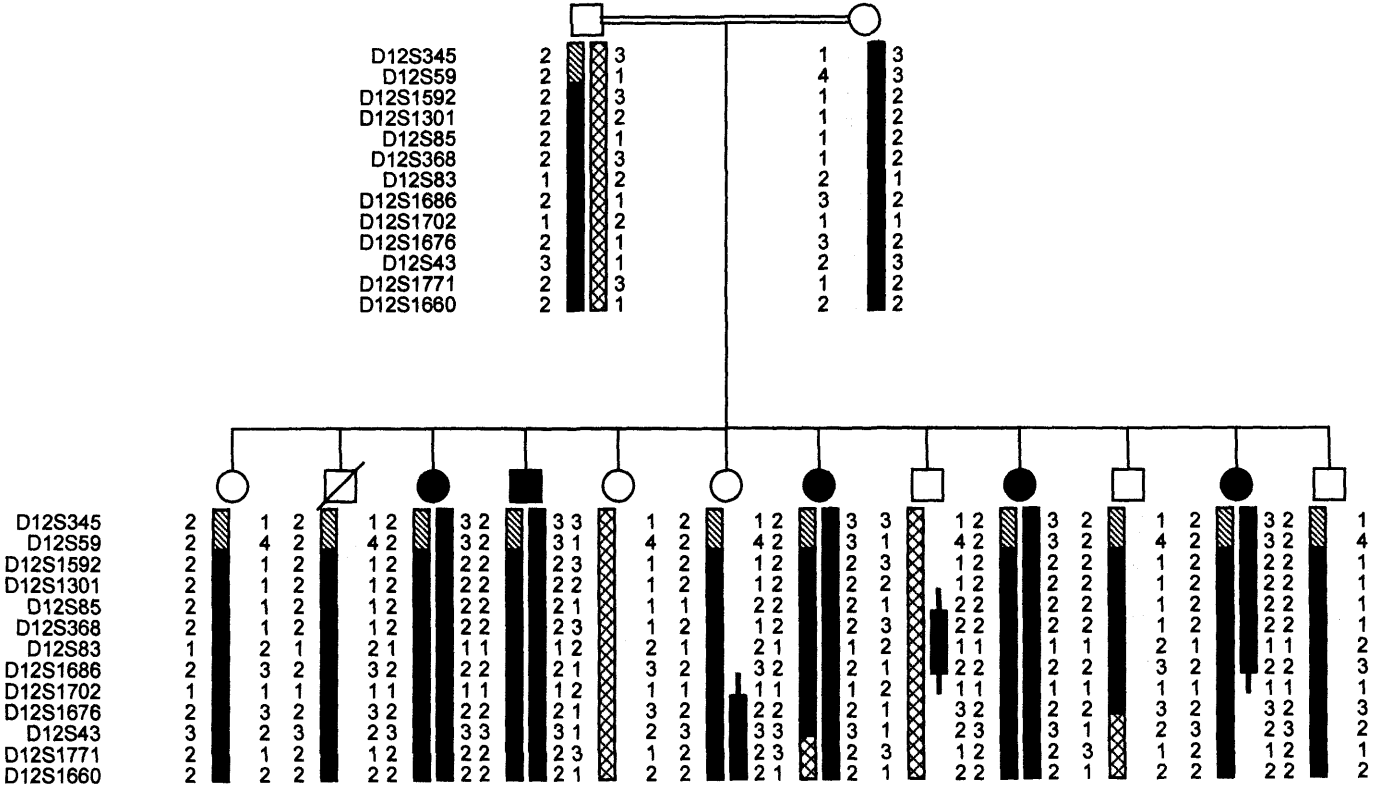

Figure 7.1 Haplotype construction in the Bedouin family for chromosome 12 markers demonstrating a region of homozygosity in all affected individuals flanked by markers D12S59 and D12S1676

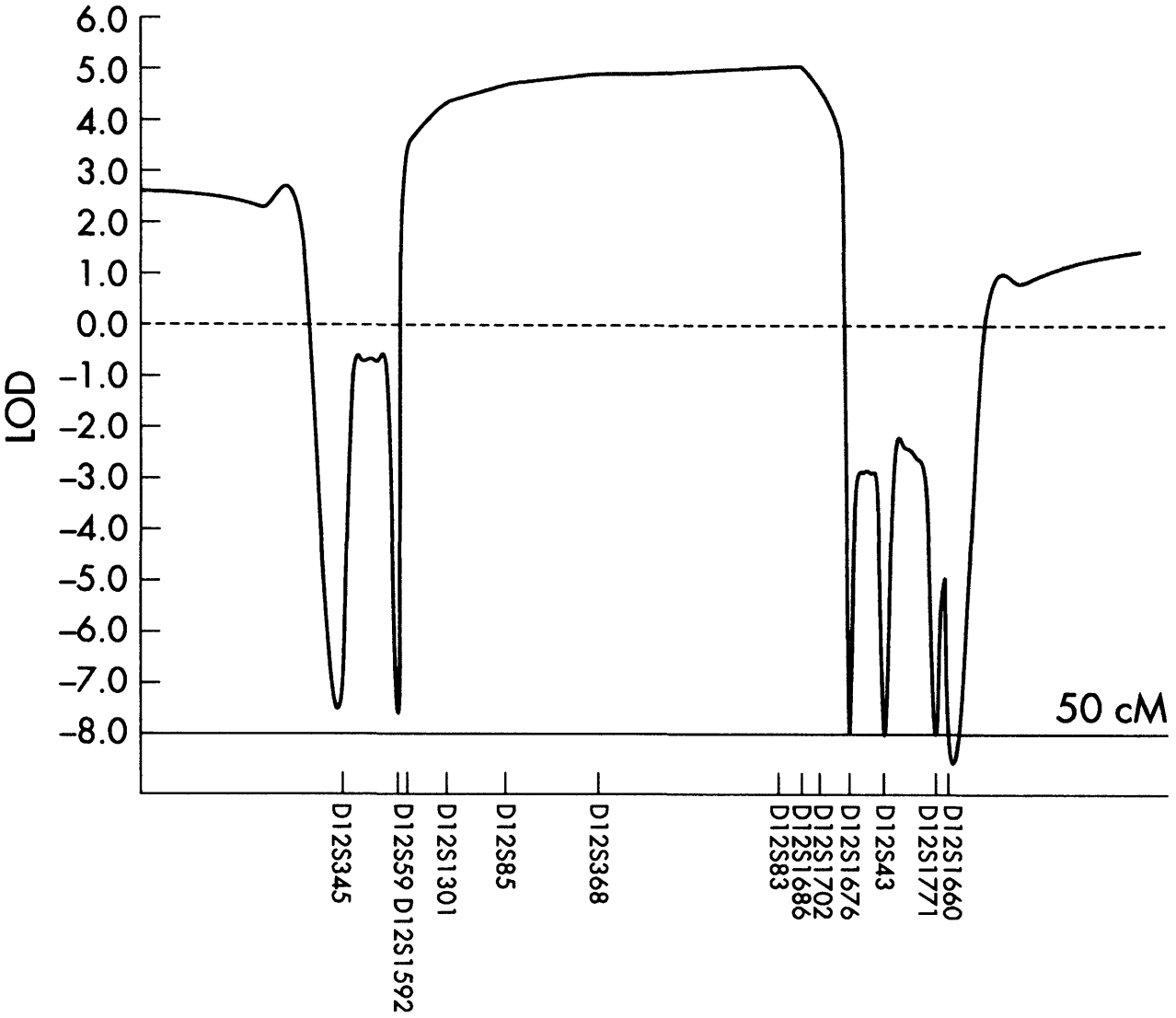

Figure 7.2 Multipoint LOD scores for markers situated across the SPG26 locus, flanked by markers D12S59 and D12S1676

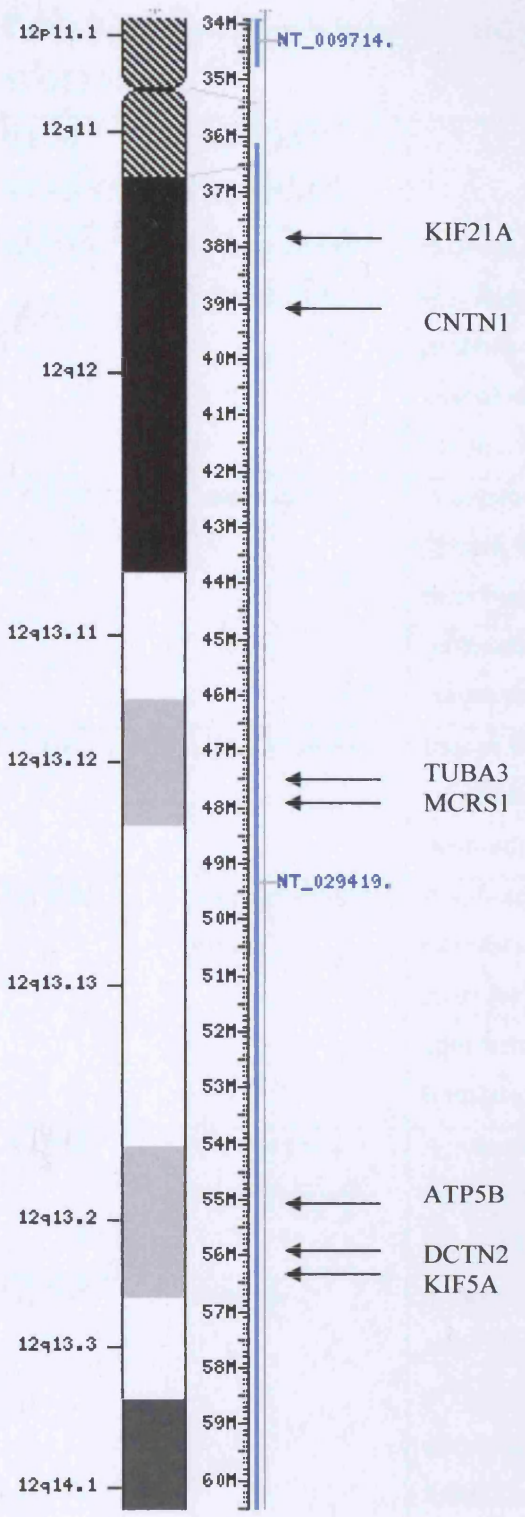

Figure 7.3 Representation of the SPG26 locus showing the position of KIF5A and other potential candidate genes

Table 7.2 Potential candidate genes and predicted protein functions from within the SPG12 locus

GENE SYMBOL	PROTEIN PRODUCT	FUNCTION
KIF21A	Kinesin family member 21A	Belongs to a family of kinesin motor proteins. Neurons use kinesin and dynein microtubule-dependent motor proteins to transport essential cellular components along axonal and dendritic microtubules. Mutations in KIF5A cause a form of autosomal dominant HSP (SPG10)
CNTN1	Contactin 1	A member of the immunoglobulin superfamily. It is a glycosylphosphatidylinositol-anchored neuronal membrane protein that functions as a cell adhesion molecule. It may play a role in the formation of axon connections.
TUBA3	Alpha 3 tubulin	Part of the tubulin superfamily of microtubule constituents. Expressed predominantly in differentiated neuronal cells.
MCRS1	Microspherule protein 1	A subset of the p78 proteins. Escorts fragile X mental retardation protein-containing silent ribonucleoparticles from the nucleus and nucleolus to the somato-dendritic compartment where it might participate in neuronal translation regulation.
ATP5B	ATP synthase beta polypeptide	A subunit of mitochondrial ATP synthase. Mutations in the nuclear encoded mitochondrial protein paraplegin cause a form of autosomal recessive HSP
DCTN2	Dynactin 2	A subunit of dynactin, which binds to both microtubules and cytoplasmic dynein. It is involved in a diverse array of cellular functions, including ER-to-Golgi transport, movement of lysosomes and endosomes, spindle formation, chromosome movement, nuclear positioning and axonogenesis. Mutations in dynactin 1 are associated with a familial form of motor neurone disease.

7.4 Discussion

Linkage to a 22.8cM region on chromosome 12 has been established in this consanguineous Kuwaiti family with a complicated HSP phenotype. Although this region contains the KIF5A gene in which a missense mutation has previously been described in a single family with a pure autosomal dominant form of HSP (Reid et al., 2002), the fact that no pathogenic mutations were identified in affected individuals in any of the exons, or flanking splice junctions of KIF5A in affected individuals from this pedigree is strongly supportive of a further causative gene in this region. The different mode of inheritance and complicated phenotype with dysarthria, distal amyotrophy and cognitive impairment in our family would further support this hypothesis, although upstream promoter sequence or intronic mutations and large scale deletions of KIF5A cannot be entirely excluded.

We have therefore concluded that this region on chromosome 12p11.1-12q14 represents a novel locus for autosomal recessive HSP, SPG26. This study should prompt the investigation of additional autosomal recessive HSP families for linkage to this region on chromosome 12, which may aid in the refinement of this currently large locus. Ribai and colleagues have recently identified a consanguineous Spanish family with a complicated HSP phenotype including ataxia and congenital cataracts putatively linked to the SPG26 locus (Ribai et al., 2005). Following genome wide linkage analysis in this family they identified a region of homozygosity flanked by markers D12S1617 and D12S1702 which overlaps the SPG26 locus and, although maximal multipoint LOD scores only reached 2.53, would potentially reduce the candidate interval slightly from 23cM to 20cM.

Based upon the proposed functions of the genes so far identified in the various forms of HSP, a variety of different underlying pathogenic mechanisms have been proposed including the disrupted development of the corticospinal tracts, mitochondrial dysfunction and defects in subcellular transportation and sorting processes (Crosby and Proukakis, 2002; Reid, 2003). A number of potential candidate genes have been identified based on these principles (table 7.2). This may provide an alternative approach to screening while the locus remains so large.

Following the report of the SPG26 locus four further new HSP loci have been described, demonstrating the marked genetic heterogeneity of the condition. Meijer and colleagues mapped a pure autosomal recessive HSP family to 10q22.1-q24.1 (SPG27), which partially overlaps the existing SPG9 locus (Meijer et al., 2004). Bouslam and colleagues mapped a further pure autosomal recessive HSP family from Morocco to chromosome 14q21.3-q22.3 (SPG28) and excluded mutations in the SPG3A gene located within this interval (Bouslam et al., 2005). Orlacchio and colleagues identified linkage to chromosome 1p31.1-p21.1 (SPG29) in a Scottish family with autosomal dominant HSP complicated by deafness and hiatus hernia (Orlacchio et al., 2005). They failed to identify any pathogenis mutations in the SNX7 gene encoding one of the sorting nexin proteins involved in various aspects of intracellular transport. Most recently, Klebe and colleagues have mapped a family of Algerian origin with a complicated form of autosomal recessive HSP including mild ataxia and a sensory neuropathy to chromosome 2q37.3. They excluded linkage to this locus in 10 additional European and North African families with autosomal recessive HSP (Klebe et al., 2006).

The identification of the causative gene in SPG26 and theses additional HSP loci should hopefully enhance our understanding of the pathogenic mechanisms underlying this heterogeneous disorder.

Chapter 8

GENERAL DISCUSSION

8.1 Identification of HSP families

The aim of this project was to study the clinical, genetic and biochemical features of autosomal recessive HSP, predominantly in the UK population. In total 20 families, comprising of 46 affected individuals, with inheritance consistent with autosomal recessive HSP were identified. One of the main limiting factors was the ascertainment of sufficient numbers of patients with a rare neurological illness and, in particular, families with a significant number of affected individuals for linkage analysis. The now well-established FSP support group in the UK has helped to facilitate this process through a family database and the neurological disease surveillance unit established by the Association of British Neurologists provides an additional resource for the study of rare neurological disorders. However, further co-operation between research groups around the UK and beyond, such as the Clinical and Genetic Analysis of Cerebellar Ataxias and Spastic Paraplegias study group (SPATAX) will be vital in coordinating future research efforts.

8.2 Phenotypes in autosomal recessive HSP patients

Of the 20 autosomal recessive families identified, only one was of sufficient size for linkage analysis. Neurological assessment of affected individuals in this group confirmed the clinical heterogeneity of the disorder, with widespread variability in phenotypes between and even within families. Overall the majority of autosomal recessive HSP patients (58%) were found to have a complicated phenotype with a variety of additional neurological features. The commonest additional neurological features were learning difficulties (31%), dysarthria (27%) and distal amyotrophy (20%). Due to the marked genetic heterogeneity of autosomal recessive HSP combining the different small families for genome wide linkage analysis would only be feasible if a common rare phenotype were shared between them to suggest an allelic association.

8.3 Confirmation and refinement of the SPG5A locus

Linkage analysis in the large consanguineous autosomal recessive HSP family (figure 3.1, pedigree 1) confirmed linkage to the previously described SPG5A locus (Hentati et al., 1994). The phenotype of a pure, early onset form of HSP was identical to those described in the original study. This represented the first family outside of Africa conclusively linked to the SPG5A locus. Marker saturation of the area allowed refinement of the critical interval for SPG5A to a 23.6cM region on chromosome 8q. Sequencing of 5 candidate genes (AP3M2, LOC138051, ATP6VH1, SDCBP and TRAM) from within the critical interval failed to identify any coding sequence mutations. This means that these candidates are unlikely to play a causative role in SPG5A linked HSP although mutations in upstream promoter regions, intronic sequence or large scale deletions cannot be excluded. The fact that muscle biopsy analysis in two affected individuals from this family did not show any histological or biochemical evidence of oxidative phosporylation defects means that a nuclear encoded mitochondrial protein such as paraplegin is unlikely to play a pathogenic role. The search for further SPG5A linked families to narrow down the critical interval will help to rationalise the candidate gene screening approach to identify the causative gene for this form of HSP.

8.4 SPG7 mutation screening in autosomal recessive and sporadic HSP patients

Of the 20 autosomal recessive HSP families linkage to the SPG7 locus was excluded in 14, including the large family linked to the SPG5A locus. One affected individual from each of the remaining families along with 29 sporadic spastic paraplegia cases were screened for SPG7 mutations using a combination of SSCP and sequencing of mobility shifts. Using this approach two of the sporadic cases were found to be compound heterozygotes for novel SPG7 mutations. In a third sporadic case SSCP identified only the previously reported the 9 base pair deletion in exon 11 (1450-1458del9) that had previously been associated with possible autosomal dominant inheritance. Direct sequencing of all the remaining exons in this patient revealed a second sequence change in exon 15, 2026C→T (F676L), which had not produced a visible mobility shift on SSCP under any conditions tested. The sensitivity of SSCP in

detecting sequence changes under optimised conditions has been reported at up to 95% (Miterski et al., 2000), although as in this case mutations may not be apparent in the form of motility shifts and therefore it is possible that the frequency of SPG7 mutations in this group may have been higher than detected. In particular the high number of polymorphisms in the SPG7 gene may mask additional changes. Direct sequencing of the entire coding region and splice junctions remains the most effective method of identifying mutations, although is more expensive and time consuming.

8.5 Genotype-phenotype correlations with SPG7 mutations

Both pure and complicated HSP phenotypes have previously been reported in association with SPG7 mutations (Casari et al., 1998; McDermott et al., 2001). Our three patients with compound heterozygote SPG7 mutations all had variable complicated phenotypes with two of the three showing marked cerebellar ataxia. The variability in phenotype may be explained by the functional domains of the paraplegin protein affected by the mutations, with both the ataxic patients having large deletions disrupting the AAA cassette. Additional genetic and environmental factors may also contribute to the phenotypic manifestations.

8.6 Oxidative phosphorylation defects with SPG7 mutations

Muscle biopsies were obtained from two of the patients with SPG7 mutations. Unlike in previous reports (Casari et al., 1998; McDermott et al., 2001) no clear histological changes of oxidative phosphorylation defects were identified in our patients. This is relatively common in neurodegenerative disorders associated with mutations in nuclear encoded mitochondrial proteins (Orth and Schapira 2001) and therefore histological changes in muscle biopsies cannot be reliably used to detect patients with SPG7 mutations. Mitochondrial respiratory chain function assays on muscle tissue confirmed a reduction in complex I-III activity, compared to controls, in both patients demonstrating for the first time the biochemical abnormality underlying this form of HSP. This pattern of complex I-III deficiency has also been reported in Friedrich's ataxia and the SOD2 knockout mouse (Melov et al., 1999). It is therefore possible that the pattern of respiratory chain defect in the muscle from patients with SPG7

mutations may represent excess free radical mediated damage. The fact that only a defect in complex I activity was observed in myoblasts may simply represent the accumulation of oxidative damage in a fixed as opposed to dividing tissue. Complex 1 deficiency has also subsequently been demonstrated in cultured fibroblasts from patients with SPG7 mutations to support these findings (Atorino et al., 2003).

8.7 SPG3A mutation screening in early onset pure autosomal dominant HSP

Following the identification of the SPG3A gene, encoding the novel protein atalstin, in autosomal dominant HSP families (Zhao et al., 2001) we reviewed the database for autosomal dominant cases in which spastin mutations had previously been excluded. In view of the fact that all the affected individuals originally described had an early onset pure form of HSP, the screening process was refined to include only those with an onset before the age of 12 years and an uncomplicated phenotype. DNA from one affected member of the 12 families selected was sequenced for mutations in the entire coding sequence and adjacent splice junctions of the SPG3A gene. The previously described R239C mutation was the only pathogenic mutation identified in one of the twelve families. Overall this indicated that in the UK population studied, even within the early onset uncomplicated cases SPG3A mutations were relatively uncommon but provided further evidence of a commonly occurring mutation site. This could represent either a mutation hotspot or a founder effect from a commonly occurring ancestral mutation. This theory could be tested by haplotype analysis of families across the world with the R239C mutation.

Subsequent studies have identified a number of additional SPG3A mutations have been described in different populations and expanded the SPG3A phenotype (Tessa et al., 2002; Abel et al., 2004; Hedera et al., 2004; D'Amico et al., 2004). In one large study looking at the same group of early onset pure HSP families in whom spastin mutations had been excluded, Dürr and colleagues identified SPG3A mutations in 12 out of 31 families (39%) from Europe and Africa (Dürr et al., 2004). This suggests that either the frequency of SPG3A mutations within this population is significantly

higher or that due to the smaller numbers studied in our group SPG3A mutations were underrepresented.

8.8 Mapping of the SPG26 locus

Following the original description of a Kuwaiti family of Bedouin origin with a complicated autosomal recessive HSP phenotype (Farag et al., 1994) a follow-up clinical study was performed and DNA obtained for linkage analysis. Using a genome wide linkage analysis approach a region of homozygosity was identified on chromosome 12 flanked by markers D12S345 and D12S326. Marker saturation analysis of this region demonstrated a 22.8cM region of homozygosity co-segregating with the disease in all affected individuals flanked by markers D12S59 and D12S1676. Multipoint LOD scores across the region were significantly positive with a maximum score of 5.1 between markers D12S1686 and D12S1702. This region included the KIF5A gene, in which a missense mutation (A767G) has previously been described in a family with an uncomplicated autosomal dominant form of HSP (Reid et al., 2002). Although this was felt unlikely to be responsible for this form of HSP in view of the different mode of inheritance and complicated phenotype this had to be excluded. Direct sequencing of all 28 exons and splice junctions of the KIF5A gene in parents and affected individuals failed to reveal any pathogenic mutations.

The 22.8cM interval at chromosome 12p11.1-12q14 was therefore confirmed as a new locus for autosomal recessive HSP, designated SPG26. Unfortunately the interval is large, containing over 400 known or predicted genes, and the identification of further SPG26 linked cases to refine the locus further is likely to be necessary to identify the gene responsible for this form of HSP. A further consanguineous Spanish family with a complicated HSP phenotype including ataxia, congenital cataracts has been putatively linked to the SPG26 locus (Ribai et al., 2005) although maximal multipoint LOD scores only reached 2.53 and cannot therefore confidently reduce the critical interval. A number of interesting candidate genes are however located within this region, including DCTN2 (DCTN1 mutations have previously been identified in a hereditary form of motor neurone disease) and if the locus size cannot be reduced a candidate gene screening approach may be applied.

8.9 Recently identified HSP loci and genes

At the time of examination (October 2007) 38 loci have now been registered at the HUGO database (http://www.genenames.org/) and mutations in 15 causative genes have so far been identified (table 8.1).

Table 8.1 Current genetic classification of HSP

SPG locus	Chromosomal location	Inheritance	Gene product	Phenotype
SPG1	Xq28	X-linked	L1CAM	Complicated
SPG2	Xq22	X-linked	PLP/DM20	Pure and complicated
SPG3	14q11-q21	AD	Atlastin	Pure
SPG4	2p22-p21	AD	Spastin	Pure and complicated
SPG5	8q11.1-q21.2	AR	-	Pure
SPG6	15q11.1	AD	NIPA1	Pure
SPG7	16q24.3	AR	Paraplegin	Pure and complicated
SPG8	8q24	AD	Strumpellin	Pure
SPG9	10q23.3-q24.2	AD	-	Complicated
SPG10	12q13	AD	KIF5A	Pure
SPG11	15q13-q15	AR	-	Pure and complicated
SPG12	19q13	AD	-	Pure
SPG13	2q24-q34	AD	HSP60	Pure
SPG14	3q27-q28	AR	-	Complicated
SPG15	14q22-q24	AR	-	Complicated
SPG16	Xq11.2	X-linked	-	Pure and complicated
SPG17	11q12-q14	AD	BSCL2	Complicated
SPG18	Reserved	-	-	-
SPG19	9q33-q34	AD	-	Pure
SPG20	13q12.3	AR	Spartin	Complicated
SPG21	15q22.3	AR	Maspardin	Complicated
SPG22	Reserved	-	-	-
SPG23	1q24-q32	AR	-	Complicated
SPG24	13q14	AR	-	Pure
SPG25	6q23-q24.1	AR	-	Complicated
SPG26	12p11.4-q14	AR	-	Complicated
SPG27	10q22.1-q24.1	AR	-	Pure
SPG28	14q21.3-q22.3	AR	-	Pure
SPG29	1p31.1-p21.1	AD	-	Complicated
SPG30	2q37.3	AR	-	Complicated
SPG31	2p11.2	AD	REEP1	Pure and complicated
SPG32	14q12-q21	AR	-	Complicated
SPG33	Reserved	-	-	-
SPG34	Reserved	AD	-	-
SPG35	Reserved	AR	-	-
SPG36	12q23-q24	AD	-	-
SPG37	8p21.2-q13.3	AD	-	Pure
SPG38	Reserved	AD	-	Complicated

8.9.1 SPG27

In 2004 Meijer and colleagues reported a large French Canadian family in which 7 of 14 siblings had a pure form of HSP with an age of onset form 25 to 45 years (Meijer et al., 2004). All affected individuals had moderate to severe lower limb spastic paraparesis with hyperreflexia, extensor plantar responses, and spastic bladders. There was also moderate to severe decrease of vibration sense in the feet. Two individuals had dysarthria and one was wheelchair-bound. Nerve conduction studies showed normal sensory and compound muscle action potentials, but somatosensory-evoked potentials were delayed in the two patients studied. Two-point parametric linkage analysis identified a putative disease locus (SPG27) on chromosome 10q22.1-q24.1 (maximum lod score of 4.49 at markers D10S580 and D10S1765). The critical disease locus spans approximately 26 Mb between markers D10S606 and D10S1758 and partially overlaps with the SPG9 locus. However, the authors noted that SPG9 is autosomal dominant and has a complicated phenotype.

8.9.2 SPG28

In 2005 Bouslam and colleagues reported a consanguineous Moroccan family in which 3 members had pure spastic paraplegia with distal sensory loss in the lower limbs and mild upper limb involvement (Bouslam et al., 2005). Age at onset ranged from 6 to 15 years. The patient with earliest onset also had pes cavus and scoliosis. Genome wide linkage analysis identified a 6.7cM candidate disease locus between markers D14S58 and D14S1064 on chromosome 14q21.3-q22.3 (SPG28). No mutations were identified in the SPG3A or the GCH1 gene, both of which map to this interval.

8.9.3 SPG29

In the same year Orlacchio and colleagues reported a large Scottish family in which 19 members were affected with a complicated form of autosomal dominant HSP (Orlacchio et al., 2005). The mean age of onset was 15.2 years. Other features included sensorineural hearing impairment and neonatal hyperbilirubinemia without kernicterus. Six patients had urinary urgency due to detrusor muscle hyperactivity and thirteen patients had a hiatus hernia. Genome wide linkage analysis in this family identified a 22.3-cM disease locus on chromosome 1p31.1-p21.1 (SPG29) flanked by

markers D1S2889 and D1S248 with a maximum multipoint lod score of 7.80 at D1S2865.

8.9.4 SPG30

In 2006 Klebe and colleagues reported a consanguineous family of Algerian origin with autosomal recessive HSP complicated by cerebellar ataxia and peripheral neuropathy (Klebe et al., 2006). They identified linkage to a 5.1cM interval on chromosome 2q37.3 (SPG30) with a maximum multipoint lod score of 3.8 between markers D2S2338 and D2S2585. Direct sequencing excluded mutations in the coding regions of the STK25 gene.

8.9.5 SPG31 (REEP1)

Later that year Züchner and colleagues at Duke University Medical Center mapped a further HSP locus in two large pure autosomal dominant HSP families to an 8.8Mb region between markers D2S139 and D2S2181 at chromosome 2p12 (SPG31) with a combined two point LOD score of 4.7 at marker D2S2951 (Züchner et al., 2006). They then sequenced the entire coding sequence and flanking splice sites of nine candidate genes and identified pathogenic mutations in the REEP1 gene in both families. Four further REEP1 mutations were identified out of a total of ninety additional HSP families screened giving a prevalence of 6.5% in their population studied. This would imply that mutations in REEP1 are the third most common cause for HSP behind spastin and atlastin.

REEP1 was found to be expressed in a variety of tissues including spinal cord. It localises to mitochondria and due to the conserved protein domains it is predicted to be a mitochondrial membrane protein with chaperone-like activity similar to the heat-shock proteins. Although the precise function of REEP1 has yet to be determined this adds further evidence to the role of defective mitochondrial function in the pathogenesis of some forms of HSP.

8.9.6 SPG32 and SPG37

Earlier this year Stevanin and colleagues mapped a further complicated autosomal recessive HSP locus to a 30cM region on chromosome 14q12-q21 (SPG32). The phenotype in affected individuals was complicated by mild mental retardation and imaging showed cerebellar atrophy and brainstem dysraphia (Stevanin et al., 2007a).

Also this year Hanein and colleagues reported a large French family with pure autosomal dominant HSP with an age of onset ranging from 8 to 60 years. Genome wide linkage analysis identified a further HSP locus at chromosome 8p21.2-q13.3 (SPG37) between markers D8S1839 and D8S1795 with a maximum LOD score of 4.2 at marker D8S601 (Hanein et al., 2007). Screening of two candidate genes encoding kinesin family member 13B and neuregulin failed to identify any pathogenic mutations.

8.9.7 Further HSP loci

In the past year a further four HSP loci have been reserved on the Human Gene Nomenclature Database (HUGO) confirming the vast genetic heterogeneity of HSP. It is hoped that the identification of these and other additional HSP genes will add to the understanding of the molecular pathogenesis of this disorder.

8.9.8 KIAA0196 (Strumpellin)

Following the original mapping of the SPG8 locus to chromosome 8q24, Valdmanis and colleagues have recently identified three mutations in the KIAA0196 gene from within this region in six SPG8 linked HSP families (Valdmanis et al., 2007). Three families from North American and one British family all possessed the same V626F mutation. The KIAA0196 gene encodes a 1,159 amino acid protein containing a spectrin repeat domain (Strumpellin). The spectrin repeat domain is found in the spectrin, dystrophin and actin family of proteins where they play a role in binding the cell membrane to the cytoskeletal network. The stability of this connection is important for intracellular transport processes suggesting that disruption of axonal transport may also play a role in this form of HSP although further work is still required to further elucidate the function of this novel protein.

8.9.9 KIAA1840 (Spatacsin)

Also this year Stevanin and colleagues identified ten different mutations in the KIAA1840 gene in twelve autosomal recessive HSP families with thin corpus callosum linked to SPG11 (Stevanin et al., 2007b). KIAA1840 encodes a novel protein (Spatacsin) whose function remains unknown although it has been found to be expressed ubiquitously throughout the nervous system.

8.10 Common molecular mechanisms in the pathogenesis of HSP

Advances in the identification of causative genes have increased our understanding of a number of overlapping molecular mechanisms underlying the various forms of HSP (Crosby and Proukakis, 2002; Reid 2003). Disruption of the corticospinal pathways, manifesting in a spastic paraparesis, may result from either abnormal initial development or subsequent neurodegeneration.

With mutations in the L1CAM and PLP genes the failure of appropriate neuronal migration during development or subsequent myelination results in infantile onset disease usually affecting multiple systems. The role of mitochondrial respiratory chain dysfunction in neurodegenerative disorders is well established and mutations in paraplegin, Hsp60 and REEP1 all provide supportive evidence for this mechanism in HSP. Hsp60 and REEP 1 are thought to play a chaperone-like role at the mitochondrial membrane. Recent studies have demonstrated that paraplegin is involved in ribosome assembly in mitochondria. Paraglegin forms hetero-oligomeric complexes with subunits of the homologous Afg3l2 protein to generate protease activity. This then regulates ribosome assembly and translation by controlling proteolytic maturation of a ribosomal subunit (Rugarli and Langer, 2006). In yeast complementation studies paraplegin deficient cells result in the formation of homo-oligomeric Afg3l2 complexes which are proposed to possess altered substrate specificity. This may explain the selective degeneration of certain axons within the central nervous system and why in particular paraplegin mutations tend to manifest as complicated phenotypes. It is however also likely that the terminal ends of the longest axons are particularly vulnerable to defects in energy metabolism.

Defective cellular trafficking and transport appears to be a major factor underlying neurodegeneration in HSP. Spastin, atlastin, NIPA1, KIF5A, spatacsin, spartin and maspardin all have proposed functions in various pathways associated with intracellular transport processes, particularly those involving microtubule dynamics and vesicle transport. Using a yeast two-hybrid approach Reid and colleagues have identified that spastin interacts with CHMP1B a protein associated with the endosomal sorting complex required for transport-III (Reid et al., 2005). Recent studies have also identified that spastin and atlastin are binding partners indicating a possible common molecular pathway (Zhu et al., 2006; Evans et al., 2006).

Quite how abnormalities in these processes lead to neurodegeneration in HSP remains uncertain. The endocytic pathway plays an important role in the regulation of membrane associated receptors, with receptor regulation being dependent on a balance between degradation in the lumenal compartment of the multivesicular body or lysosome versus recycling back to the plasma membrane (Katzmann et al., 2002). Abnormalities of sorting in the endocytic pathway may therefore result in receptor up or down regulation. Defective endocytic transport could therefore cause multiple abnormalities in plasma membrane receptor levels and consequent abnormalities in a variety of signalling pathways such as apoptosis. The terminal ends of the longest axons might be particularly vulnerable to this process, because downstream pathways might already be working at near threshold levels in such an extreme environment (Reid et al., 2005). It is also possible that abnormalities in endosomal trafficking might directly perturb downstream signalling, independent of plasma membrane receptor levels. Neuronal maintenance is dependent on neurotrophic survival factors released by innervation targets. These survival factors signal by activation of cognate receptors on the neuronal presynaptic membrane (Sofroniew et al., 2001). In at least some neurones nerve growth factor signalling can be conveyed in specialized early endosomes that are transported to the neuronal cell body by retrograde axonal transport (Delcroix et al., 2003). Failure of trafficking of the signalling endosome could therefore lead to neurodegeneration, again with neurones with very long axons could be particularly vulnerable to abnormalities of this type of process (Reid et al., 2005). The fact that these are highly energy dependent processes may also explain a common mechanism associated with mitochondrial respiratory chain dysfunction.

Similar mechanisms have also been proposed in other motor neurone degenerative disorders. For example, Alsin, the protein mutated in a hereditary form of motor neurone disease is thought to be involved in membrane-proximity activities of GTPases that modulate microtubule assembly and cellular transport in neuronal cells (Yang et al., 2001). Another hereditary form of motor neurone disease associated with bulbar and spinal muscular atrophy had recently been found to be due to mutation in the p150Glued subunit of dynactin, a microtubule motor protein essential for retrograde axonal transport (Puls et al., 2005). Defective intracellular transport processes have also been implicated in the pathogenesis of a number of other neurodegenerative disorders such as Alzheimer's disease (Kins et al., 2006) and Huntington's disease (Cowan and Raymond 2006).

8.11 Genetic testing in HSP

To date 11 of the causative genes associated with different forms of HSP have now been discovered and this has opened up the possibility of diagnostic testing for patients. Spastin mutations account for up to 40% of all cases of autosomal dominant HSP and have also been identified in a number of apparently sporadic cases. Spastin gene screening is now available in the UK as diagnostic test with the potential for screening asymptomatic at risk family members and prenatal diagnosis (Hedera et al., 2001). These possibilities, however, have to be considered in the context of a condition for which there is currently no disease modifying treatment and which may vary considerably in disease severity. At the present time genetic testing for other forms of HSP is available as a research tool only. In view of the fact that most mutations are unique to each individual family sequencing of entire genes is the most reliable method of detection and cost is likely to be prohibitive for the less common forms of the disease. This method also fails to identify large scale deletions, which in the case of spastin may be as common as point mutations (Depienne et al., 2007).

8.12 Animal models and future treatment possibilities in HSP

The ultimate goal in the advances in molecular genetics and understanding the pathological mechanisms underlying neurodegeneration in HSP is the development of disease modifying treatments. The development of animal models of neurodegenerative diseases is one method of trying to achieve this. In 2003 the Drosphila homologue of the human spastin gene (Dspastin) was identified (Kammermeier et al., 2003), allowing the development of an insect model of HSP by either overexpression or knockout of the gene, producing adult onset locomotor impairment and neurodegeneration. Like the human protein, Dspastin regulates synaptic microtubule networks (Sherwood et al., 2004). Overexpression leads to decreased microtubule stability, whereas loss of Dspastin leads to enhanced microtubule stability (Roll-Mecak and Vale, 2005). Recently Orso and colleagues have demonstrated that the administration of the microtubule targeting drug vinblastine significantly attenuates the phenotype observed in Drosphila models of spastin-associated HSP (Orso et al., 2005), giving hope that treatment with Vinca alkaloid drugs may modify disease in human patients. However, these drugs are extremely toxic which may limit the progress onto human trials. The development of safer treatments based on regulating microtubule function therefore represents the most likely way forward in terms of drug therapies.

A mouse model for paraplegin-associated HSP has also now been developed. Paraplegin deficient mice manifest progressive motor impairment with similar pathological evidence of axonal degeneration, morphologically abnormal mitochondria and impaired respiratory chain function as seen in human patients (Ferreirinha et al., 2004). Recently, using a gene therapy approach, the intamuscular delivery of paraplegin through an adenoassociated virus vector has been shown to rescue some of the axonal changes seen in paraplegin deficient mice (Pirozzi et al., 2005). Again, this offers hope that similar techniques may be developed for treatment in human patients. However, gene therapy using a variety of vectors remains in the early stages for treating human disease and is limited by both safety issues and the ability to target delivery of the gene to the appropriate areas, in this case the central nervous system. The mouse model does though provide future opportunities for

testing drug treatments based on neuroprotection or improving mitochondrial respiratory chain function.

8.13 Future research directions in HSP

The past few years have seen an exponential rise in our understanding of the genetic basis and molecular mechanisms underlying the various forms of HSP. Common molecular themes are evolving in the pathogenesis of HSP and other neurodegenerative disorders. There are, however, still a large number of HSP loci for which the causative gene remains undiscovered and much work remains to be done to increase our understanding of precisely how defects in axonal transport and mitochondrial respiratory chain dysfunction result in selective neurodegeneration of the corticospinal tracts. The search also continues for additional genetic and environmental factors accounting for the marked variability in age of onset and disease progression so frequently observed among families with HSP. Cellular and animal models for some forms of HSP have now been developed and this is likely to be the first step towards establishing safe and effective disease modifying treatments, although such advances are still likely to be many years away.

REFERENCES

Abel A, Fonknecten N, Hofer A, et al. Early onset autosomal dominant spastic paraplegia caused by novel mutations in SPG3A. Neurogenetics 2004;5:239-243

Ashley-Koch A, Bonner ER, Gaskell PC, et al. Fine mapping and genetic heterogeneity in the pure form of autosomal dominant familial spastic paraplegia. Neurogenetics 2001;3:91-97

Atorino L, Silvestri L, Koppen M, et al. Loss of m-AAA protease in mitochondria causes complex I deficiency and increased sensitivity to oxidative stress in hereditary spastic paraplegia. J Cell Biol 2003;163:777-787

Banfi S, Bassi MT, Andolfi G, et al. Identification and characterization of AFG3L2, a novel paraplegin-related gene. Genomics 1999;59:51-58

Beckman JS, Weber JL Survey of human and rat microsatellites. Genomics 1992;12:627-631

Behan WM, Maia M. Strumpell's familial spastic paraplegia: genetics and neuropathology. J Neurol Neurosurg Psychiatry 1974; 37:8-20

Blumen SC, Bevan S, Abu-Mouch S, et al. A locus for complicated hereditary spastic paraplegia maps to chromosome 1q24-q32. Ann Neurol 2003;54:796-803

Bonneau D, Rozet J-M, Bulteau C, et al. X-linked spastic paraplegia (SPG2): clinical heterogeneity at a single locus. J Med Genet 1993;30:381-384

Botstein D, White RL, Skolnick M, Davis RW. Construction of a genetic linkage map in man using restriction fragment length polymorphisms. Am J Hum Genet 1980;2:314-331

Boulloche J, Aicardi J. Pelizaeus-Merzbacher disease: clinical and nosological study. J Child Neurol 1986;1:233-239

Bouslam N, Benomar A, Azzedine H, et al. Mapping of a new form of pure autosomal recessive spastic paraplegia (SPG28). Ann Neurol 2005;57:567-571

Bradley JL, Blake JC, Chamberlain S, et al. Clinical, biochemical and molecular genetic correlations in Friedreich's ataxia. Hum Mol Genet 2000;9:275-282

Bruyn RP, van Dijk JG. Clinically silent dysfunction of dorsal columns and dorsal spinocerebellar tracts in hereditary spastic paraparesis. J Neurol Sci 1994;125:206-211

Burden-Gulley SM, Pendergast M, Lemmon V. The role of cell adhesion molecule L1 in axonal extension, growth cone motility, and signal transduction. Cell Tissue Res 1997;290:415-422

Bürger J, Fonknechten N, Hoeltzenbein M, et al. Hereditary spastic paraplegia caused by mutations in the SPG4 gene. Eur J Hum Genet 2000 8:771-776

Byrne PC, McMonagle P, Webb S, et al. Age-related cognitive decline in hereditary spastic parapaeris linked to chromosome 2p. Neurology 2000;54:1510-1517

Cailloux F, Gauthier-Barichard F, Mimault C, et al. Genotype-phenotype correlation in inherited brain myelination defects due to proteolipid protein gene mutations. Eur J Hum Genet 2000;8:837-845

Campuzano V, Montermini L, Molto MD, et al. Friedreich's ataxia: autosomal recessive disease caused by an intronic GAA repeat expansion. Science 1996;2271:1423-1427

Cartlidge NE, Bone G. Sphincter involvement in hereditary spastic paraplegia. Neurology 1973;23:1160-1163

Casari G, De Fusco M, Ciarmatori S, et al. Spastic paraplegia and OXPHOS impairment caused by mutations in paraplegin, a nuclear-encoded mitochondrial metalloprotease. Cell 1998;93:973-983

Cavanagh NP, Eames RA, Galvin RJ, Brett EM, Kelly RE. Hereditary sensory neuropathy with spastic paraplegia. Brain 1979;102:79-94

Charvin D, Cifuentes-Diaz C, Fonknechten N, et al. Mutations of SPG4 are responsible for a loss of function of spastin, an abundant neuronal protein localized in the nucleus. Hum Mol Genet 2003;12:71-78

Ciccarelli Fd, Proukakis C, Patel H, et al. The identification of a conserved domain in both spartin and spastin, mutated in hereditary spastic paraplegia. Genomics 2003;81:437-441

Claes S, Devriendt K, Van Goethem G, et al. Novel syndromic form of X-linked complicated spastic paraplegia. Am J Med Genet 2000;94:1-4

Coppola M, Pizzigoni A, Banfi S, et al. Identification and characterization of YME1L1, a novel paraplegin-related gene. Genomics 2000;66:48-54

Coutinho P, Barros J, Zemmouri R, et al. Clinical heterogeneity of autosomal recessive hereditary spastic paraplegia: analysis of 106 patients in 46 families. Arch Neurol 1999;56:943-949

Cowan CM, Raymond LA. Selective neuronal degeneration in Huntington's disease. 2006;75:25-71

Crook R, Verkkoniemi A, Perez-Tur J, et al. A variant Alzheimer's disease with spastic paraparesis and unusual plaques due to deletion of exon 9 of presenelin 1. Nat Med 1998;4:452-455

Crosby AH, Proukakis C. Is the transportation highway the right road for hereditary spastic paraplegia? Am J Hum Genet 2002;71:1009-1016

Crosby AH. Disruption of cellular transport: a common cause of neurodegeneration? Lancet Neurol 2003;2:311-331

Cross HE, McKusick VA. The Troyer syndrome: a recessive form of spastic paraplegia with distal muscle wasting. Arch Neurol 1967a;16:478-488

Cross HE, McKusick VA. The Mast syndrome: a recessively inherited form of presenile dementia with motor disturbances. Arch Neurol 1967b;16:1-13

Cruz Martinez A, Tejada J. Central motor conduction in hereditary motor and sensory neuropathy and hereditary spastic paraplegia. Electromyogr Clin Neurophysiol 1999;6:331-335

D'Amico A, Tessa A, Sabino A, et al. Incomplete penetrance in an SPG3A-linked family with a new mutation in the atlastin gene. Neurology 2004;62:2138-2139

Davies KE, Read AP. Genes and Markers. In: Molecular Basis of Inherited Disease, IRL Press at Oxford University Press 1992;1-14

De Michele G, De Fusco M, Cavalcanti F, et al. A new locus for autosomal recessive hereditary spastic paraplegia maps to chromosome 16q24.3. Am J Hum Genet 1998;63:135-139

Delcroix JD, Valletta JS, Wu C, et al. NGF signaling in sensory neurons: evidence that early endosomes carry NGF retrograde signals. Neuron 2003;39:69-84

Depienne C, Fedirko E, Forlani S, et al. Exon deletions of SPG4 are a frequent cause of hereditary spastic paraplegia. J Med Genet 2007;44:281-284

Dunne JW, Heye N, Dunne SL. Treatment of chronic limb spasticity with botulinum toxin A. J Neurol Neurosurg Psychiatry 1995;58:232-235

Dürr A, Brice A, Serdaru M, et al. The phenotype of "pure" autosomal dominant spastic paraplegia. Neurology 1994;44:1274-1277

Dürr A,Davoine C-S, Paternotte C, et al. Phenotype of autosomal dominant spastic paraplegia linked to chromosome 2. Brain 1996;119:1487-1496

Dürr A, Camuzat A, Colin E, et al. Atlastin 1 mutations are frequent in young-onset autosomal dominant spastic paraplegia. Arch Neurol 2004;61:1867-1872

Elleuch N, Depienne C, Benomar A, et al. Mutation analysis of the paraplegin gene (SPG7) in patients with hereditary spastic paraplegia. Neurology 2006;66:654-659

Ellis D, Malcolm S. Proteolipid gene dosage effect in Pelizaeus-Merzbacher disease. Nat Genet 1994;6:333-334

Errico A, Ballabio A, Rugarli EI. Spastin, the protein mutated in autosomal dominant hereditary spastic paraplegia, is involved in microtubule dynamics. Hum Mol Genet 2002;11:153-163

Evans K, Keller C, Pavur K, et al. Interaction of two hereditary spastic paraplegia gene products, spastin and atlastin, suggests a common pathway for axonal maintenance. Proc Natl Acad Sci U S A 2006;103:10666-10671

Fan E, Levin DB, Glickman BW, Logan DM. Limitations in the use of SSCP analysis. Mutat Res 1993;288:85-92

Farag TI, el-Badramany MH, al-Shakawy S. Troyer syndrome: report of the first "non-Amish" sibship and review. Am J Med Genet 1994;53:383-385

Ferreirinha F, Quattrini A, Pirozzi M, et al. Axonal degeneration in paraplegin-deficient mice is associated with abnormal mitochondria and impairment of axonal transport. J Clin Invest 2004;113:231-242

Figlewicz DA, Bird TD. "Pure" hereditary spastic paraplegias: The story becomes complicated. Neurology 1999;53:5-7

Fink JK, Sharp G, Lange B, et al. Autosomal dominant hereditary spastic paraparesis, type 1: clinical and genetic analysis of a large North American family. Neurology 1995;45:325-331

Fink JK, Wu C-TB, Jones SM, et al. Autosomal dominant familial spastic paraplegia: Tight linkage to chromosome 15q. Am J Hum Genet 1995;56:188-192

Fink JK. The hereditary spastic paraplegias: Nine genes and counting. Arch Neurol 2003;60:1045-1049

Fonknechten N, Mavel, D, Byrne P, et al. Spectrum of SPG4 mutations in autosomal dominant spastic paraplegia. Hum Mol Genet 2000; 9:637-644

Fontaine B, Davoine CS, Dürr A, et al. A new locus for autosomal dominant pure spastic paraplegia, on chromosome 2q24-q34. Am J Hum Genet 2000;66:702-707

Fransen E, Lemmon V, Van Camp G, et al. CRASH syndrome: clinical spectrum of corpus callosum hypoplasia, retardation, adducted thumbs, spastic paraparesis and hydrocephalus due to mutations in one single gene, L1. Eur J Hum Genet 1995;3:273-284

Fransen E, Vits L, Van Camp G, Willems PJ. The clinical spectrum of mutations in L1, a neuronal cell adhesion molecule. Am J Med Genet 1996;64:73-77

Gates PC, Paris D, Forrest SM, Williamson R, McKinlay Gardener RJ. Friedreich's ataxia presenting as adult-onset spastic paraparesis. Neurogenetics 1998;1:297-299

Gencic S, Abuelo D, Ambler M, Hudson LD. Pelizaaeus-Merzbacher disease: an X-linked neurologic disorder of myelin metabolism with a novel mutation in the gene encoding proteolipid protein. Am J Hum Genet 1989;45:435-442

Gisbert S, Santos N, Damen R, et al. Autosomal dominant familial spastic paraplegia: Reduction of the FSP1 candidate region on chromosome 14q to 7cM and locus heterogeneity. Am J Hum Genet 1995;56:183-187

Goldstein LSB, Yang Z. Microtubule-based transport systems in neurons: the roles of kinesins and dynamins. Annu Rev Neurosci 2000;23:39-71

Griffiths I, Klugmann M, Anderson T, et al. Axonal swellings and degeneration in mice lacking the major proteolipid of myelin. Science;280:1610-1613

Hanein S, Dürr A, Ribai P, et al. A novel locus for autosomal dominant "uncomplicated" hereditary spastic paraplegia maps to chromosome 8p21.1-q13.3. Hum Genet 2007;122:261-273

Hansen JJ, Durr A, Cournu-Rebeix I, et al. Hereditary spastic paraplegia SPG13 is associated with a mutation in the gene encoding the mitochondrial chaperonin Hsp60. Am J Hum Genet 2002;70:1328-1332

Harding AE. Hereditary "pure" spastic paraplegias. In: The hereditary ataxias and related disorders. Edinburgh: Churchill Livimgstone, 1984:191-213

Hardin AE. Hereditary spastic paraplegias. Semin Neurol 1993;13:333-336

Hazan J, Lamy C, Melki J, et al. Autosomal dominant familial spastic paraplegia is genetically heterogeneous and one locus maps to chromosome 14q. Nat Genet 1993; 5:163-167

Hazan J, Fontaine B, Bruyn RPM, et al. Linkage of a new locus for autosomal dominant familial spastic paraplegia to chromosome 2p. Hum Mol Genet 1994;3:1569-1573

Hazan J, Fonknehten N, Mavel D, et al. Spastin, a new AAA protein is altered in the most frequent form of autosomal dominant spastic paraplegia. Nat Genet. 1999;23:296-303.

Hedera P, Rainier S, Alvarado D, et al. Novel locus for autosomal dominant hereditary spastic paraplegia on chromosome 8q. Am J Hum Genet 1999a;64:563-569

Hedera P, DiMauro S, Bonilla E, et al. Phenotypic ananlysis of autosomal dominant hereditary spastic paraplegia linked to chromosome 8q. Neurology 1999b;53:44-50

Hedera P, DiMauro S, Bonilla E, Wald JJ, Fink JK. Mitochondrial analysis in autosomal dominant hereditary spastic paraplegia. Neurology 2000;55:1591-1592

Hedera P, Williamson JA, Rainier S, et al. Prenatal diagnosis of hereditary spastic paraplegia. Prenat Diagn 2001;21:202-206

Hedera P, Fenichel GM, Blair M, Haines JL. Novel mutation in the SPG3A gene in an African American family with an early onset of hereditary spastic paraplegia. Arch Neurol 2004;61:1600-1603

Hentati A, Pericak-Vance MA, Hung WY, et al. Linkage of pure autosomal recessive familial spastic paraplegia to chromosome 8 markers and evidence of genetic locus heterogeneity. Hum Mol Genet 1994;3:1263-1267

Hentati A, Pericak-Vance MA, Lennon F, et al. Linkage of a locus for autosomal dominant familial spastic paraplegia to chromosome 2p markers. Hum Mol Genet 1994;3:1867-1871

Hodgkinson CA, Bohlega S, Abu-Amero SN, et al. A novel form of autosomal recessive pure hereditary spastic paraplegia maps to chromosome 13q14. Neurology 2002;59:1905-1909

Hughes CA, Byrne PC, Webb S, et al. SPG15, a new locus for autosomal recessive complicated HSP on chromosome 14q. Neurology 2001;56:1230-1233

Joosten EA, Gribnau AA. Immunocytochemical localization of cell adhesion molecule L1 in developing rat pyramidal tract. Neurosci Lett 1998;100:94-98

Jouet M, Rosenthal A, Armstrong G, et al., X-linked spastic paraplegia (SPG1), MASA syndrome and X-linked hydrocephalus result from mutations in the L1 gene. Nat Genet 1994;7:402-407

Jouet M, Moncla A, Paterson J, et al. New domains of neural cell adhesion molecule L1 implicated in X-linked hydrocephalus and MASA syndrome. Am J Hum Genet 1995;56:1304-1314

Juhola MK, Shah ZH, Grivell LA, Jacobs HT. The mitochondrial inner membrane AAA metalloprotease family in metazoans. FEBS Lett 2000;481:91-95

Katzmann DJ, Odorizzi G, Emr SD. Receptor downregulation and multivesicular-body sorting. Nat Rev Mol Cell Biol 2002;3:893-905.

Kins S, Lauther N, Szodorai A, Beyreuther K. Subcellular trafficking of the amyloid precursor protein gene family and its pathogenic role in Alzheimer's disease. Neurodegener dis 2006;3:218-226

Kjellin K. Familial spastic paraplegia with amyotrophy, oligophrenia and central retinal degeneration. Arch Neurol 1959;1:133-140

Klebe S, Azzedine H, Dürr A, et al. Autosomal recessive spastic paraplegia (SPG30) with mild ataxia and sensory neuropathy maps to chromosome 2q37.3. Brain 2006;129:1456-1462

Krammermeier L, Spring L, Stierwald M, Burgunder JM, Reichert H. Identification of the Drosphila melanogaster homolog of the human spastin gene. Dev Genes Evol 2003;213:412-415

Kremmidiotis G, Gardner AE, Settasatian C, et al. Molecular and functional analyses of the human and mouse genes encoding AFG3L1, a mitochondrial metalloprotease homologous to the human spastic paraplegia protein. Genomics 2001;76:58-65

Rugarli EI, Langer T. Translating m-AAA protease function in mitochondria to hereditary spastic paraplegia.Trends Mol Med 2006;12:262-269

Lindsey JC, Lusher ME, McDermott CJ, et al. Mutation analysis of the spastin gene (SPG4) in patients with hereditary spastic paraparesis. J Med Genet 2000;37:759-765

Lison M, Kornbrut B, Feinstein A, et al. Progressive spastic paraparesis, vitiligo, premature graying, and distinct facial appearance: a new genetic syndrome in 3 sibs. Am J Med Genet 1981;9:351-357

Lithgow T. Targeting of proteins to mitochondria. FEBS Lett 2000;476:22-26.

Lo Nigro C, Cusano R, Scaranari M, et al. A refined physical and transcriptional map of the SPG9 locus on 10q23.3-q24.2. Eur J Hum Genet 2000;8:777-782

Lorrain M. Contribution a l'étude de la paraplégie spasmodique familial. Paris: Steinheil,1898

Lyons GM, Sinkjaer T, Burridge JH, Wilcox DJ. A review of portable FES-based neural orthoses for the correction of foot drop. IEEE Trans Neural Syst Rehabil Eng 2002;10:260-279

Meythaler JM, Steers WD, Tuel SM, et al. Intrathecal baclofen in hereditary spastic paraparesis. Arch Phys Med Rehabil 1992;73:794-797

McDermott CJ, Dayaratne RK, Tomkins J, et al. Paraplegin gene analysis in hereditary spastic paraparesis (HSP) pedigrees in northeast England. Neurology 2001;56:467-471.

McDermott CJ, Shaw PJ. Hereditary spastic paraplegia. Int Rev Neurobiol 2002;53:191-204

McDermott CJ, Taylor RW, Hayes C, et al. Investigation of mitochondrial function in hereditary spastic paraparesis. Neuroreport 2003;14:485-488

McDermott CJ, grierson AJ, Wood JD, et al. Hereditary spastic paraparesis: Disrupted intracellular transport associated with spastin mutation. Ann Neurol 2003;54:748-759

McLeod JG, Morgan JA, Reye C. Electrophysiological studies in familial spastic paraplegia. J Neurol Neurosurg Psychiatry 1977;40:611-615

McMonagle P, Webb S, Hutchinson M. The prevalence of "pure" autosomal dominant hereditary spastic paraparesis in the island of Ireland. J Neurol Neurosurg Psychiatry 2002;72:43-46

McNiven MA, Cao H, Pitts KR, Yoon Y. The dynamin family of mechanoenzymes: pinching in new places. Trends Biochem Sci 2000;69:150-160

Meijer IA, Hand CK, Cossette P, Figlewicz DA, Rouleau GA. Spectrum of SPG4 mutations in a large collection of North American families with hereditary spastic paraplegia. Arch Neurol 2002;59:281-286

Meijer IA, Cossette P, Roussel J, et al. A novel locus for pure recessive hereditary spastic paraplegia maps to 10q22.1-10q24.1. Ann Neurol 2004;56:579-582

Melov S, Coskun P, Patel M, et al. Mitochondrial disease in superoxide dismutase 2 mutant mice. Proc Natl Acad Sci U S A 1999;96:846-851

Miterski B, Krüger R, Wintermeyer P, Epplen JT. PCR/SSCP detects reliably and efficiently DNA sequence variations in large scale screening projects. Comb Chem High Throughput Screen 2000;3:211-218

Muglia M, Magariello A, Nicoletti G, et al. Further evidence that SPG3A gene mutations cause autosomal dominant hereditary spastic paraplegia. Ann Neurol 2002;51:794-795

Muglia M, Criscuolo C, Magariello A, et al. Narrowing of the critical region in autosomal recessive spastic paraplegia linked to the SPG5 locus. Neurogenetics 2004;5:49-54

Mukamel M, Weitz R, Metzker A, Varsano I. Spastic paraparesis, mental retardation and cutaneous pigmentation disorder. A new syndrome. Am J Dis Child 1985;139:1090-1092

Murillo FM, Kobayashi H, Pegoraro E, et al. Genetic localization of a new locus for recessive familial spastic paraparesis to 15q13-15. Neurology 1999;53:50-56

Nakamura A, Izumi K, Umehara F, et al. Familial spastic paraplegia with mental impairment and thin corpus callosum. J Neurol Sci 1995;131:35-42

Neerup Jensen L, Gerstenberg T, Kallestrup EB, et al. Urodynamic evaluation of patients with autosomal dominant pure spastic paraplegia linked to chromosome 2p. J Neurol Neurosurg Psychiatry 1998;65:693-696

Nicholls RD, Knepper JL. Genome organization, function, and imprinting in Prader-Willi and Angleman syndromes. Ann Rev Genomics Hum Genet 2001;2:153-175
Ochoa GC, Slepnev VI, Neff L, et al. A functional link between dynamin and the actin cytoskeleton at podosomes. J Cell Biol 2000;150:377-389

Okuda B, Iwamoto Y, Tachibana H. Hereditary spastic paraplegia with thin corpus callosum and cataract: a clinical description of two siblings. Acta Neurol Scand 2002;106:222-224

Orita M, Suzuki Y, Sekiya T, Hayashi K. Rapid and sensitive detection of point mutations and DNA polymorphisms using the polymerase chain reaction. Genomics 1989;5:874-879

Orlacchio A, Kawarai T, Rogaeva E, et al. Clinical and genetic study of a large Italian family linked to the SPG12 locus. Neurology 2002;59:1395-1401

Orlacchio A, Kawarai T, Gaudiello F, et al. New locus for hereditary spastic paraplegia maps to chromosome 1p31.1-1p21.1. Ann Neurol 2005;58:423-429

Orso G, Martinuzzi A, Rossetto MG, et al. Disease-related phenotypes in Drosphila model of hereditary spastic paraplegia are ameliorated by treatment with vinblastine. J Clin Invest 2005;115:3026-3034

Orth M, Schapira AHV. Mitochondria and degenerative disorders. Am J Med Genet 2001;106:27-36

Patel H, Hart PE, Warner T, et al. Silver syndrome is not linked to any of the previously established autosomal dominant hereditary spastic paraplegia loci. Am J Med Genet 2001a;102:68-72

Patel H, Hart PE, Warner T, et al. The Silver syndrome variant of hereditary spastic paraplegia maps to chromosome 11q12-q14, with evidence for genetic heterogeneity within this subtype. Am J Hum Genet 2001b;69:209-215

Patel H, Cross H, Proukakis C, et al. SPG20 is mutated in Troyer syndrome, an hereditary spastic paraplegia. Nat Genet 2002;31:347-348

Patel S, Latterich M. The AAA team: related ATPases with diverse functions. Trends Cell Biol 1998;8:65-71

Paul MF, Tzagoloff A. Mutations in RCA1 and AFG3 inhibit F1-ATPase assembly in Saccharomyces cerevisiae. FEBS Lett 1995;373:66-70

Pearce DA. Hereditary spastic paraplegia: mitochondrial metalloproteases of yeast. Hum Genet 1999;104:443-448.

Pelosi L, Lanzillo B, Perritti A, et al. Motor and somatosensory evoked potentials in hereditary spastic paraplegia. J Neurol Neurosurg Psychiatry 1991;54:1099-1102

Piemonte F, Casali C, Carrozzo R, et al. Respiratory chain defects in hereditary spastic paraplegias. Neuromuscul Disord 2001;11:565-569

Pirozzi M, Quattrini A, Andolfi G, et al. Intramuscular viral delivery of paraplegin rescues peripheral axonopathy in a model of hereditary spastic paraplegia. J Clin Invest 2006;116:202-208

Pitts KR, Yoon Y, Krueger EW, McNiven MA. The dynamin-like protein DLP1 is essential for normal distribution and morphology of the endoplasmic reticulum and mitochondria in mammalian cells. Mol Biol Cell 1999;10:4403-4417

Polo JM, Calleja J, Combarros O, Berciano J. Hereditary ataxias and paraplegias in Cantabria, Spain. An epidemiological and clinical study. Brain 1991;114:855-866.

Polo JM, Calleja J, Combarros O, Berciano J. Hereditary "pure" spastic paraplegia: a study of nine families. J Neurol Neurosurg Psychiatry 1993;56:175-181

Proukakis C, Hart PE, Cornish A, Warner TT, Crosby AH. Three novel spastin (SPG4) mutations in families with autosomal dominant hereditary spastic paraplegia. J Neurol Sci 2002;201:65-69

Proukakis C, Auer-Grumbach M, Wagner K, et al. Screening of patients with hereditary spastic paraplegia reveals seven novel mutations in the SPG4 (spastin) gene. Hum Mutat 2003;21:170

Puls I, Oh SJ, Sumner CJ, et al. Distal spinal and bulbar muscular atrophy caused by dynactin mutation. Ann Neurol 2005;57:687-694

Rainier S, Bui M, Jones SM, Fink JK. Chromosome 15q linked autosomal dominant hereditary spastic paraplegia: new mapping information and candidate gene analysis. J Hum Genet Suppl 2000;67:391

Rainier S, Hedera P, Alvarado D, et al. Hereditary spastic paraplegia linked to chromosome 14q11-q21: reduction of the SPG3 locus interval from 5.3 to 2.7 cM. JMG 2001;38:e39

Rainier S, Chai J-H, Tokarz D, Nicholls RD, Fink JK. NIPA1 gene mutations cause autosomal dominant hereditary spastic paraplegia (SPG6). Am J Hum Genet 2003;73:967-971

Rainier S, Sher C, Reish O, Thomas D, Fink JK. De novo occurrence of novel SPG3A/atlastin mutation presenting as cerebral palsy. Arch Neurol 2006;63:445-447

Reid E. The hereditary spastic paraplegias. J Neurol 1999;246:995-1003

Reid E, Dearlove AM, Whiteford ML, Rhodes M, Rubinsztein DC. Autosomal dominant spastic paraplegia: refined SPG8 locus and further genetic heterogeneity. Neurology 1999;53:1844-1859

Reid E, Dearlove AM, Rhodes M, et al. A new locus for autosomal dominant "pure" hereditary spastic paraplegia mapping to chromosome 12q13, and evidence for further genetic heterogeneity. Am J Hum Genet 1999;65:757-763

Reid E, Dearlove AM, Osborn O, et al., A locus for autosomal dominant "pure" hereditary spastic paraplegia maps to chromosome 19q13. Am J Hum Genet 2000;66:728-732

Reid E, Escayg A, Dearlove AM, et al. The spastic paraplegia SPG10 locus: narrowing of critical region and exclusion of sodium channel gene SCN8A as a candidate. J Med Genet 2001;38:65-67

Reid E, Kloos M, Ashley-Koch A, et al. A kinesin heavy chain (KIF5A) mutation in hereditary spastic paraplegia (SPG10). Am J Hum Genet 2002;71:1189-1194

Reid E. Science in motion: common molecular pathological themes emerge in the hereditary spastic paraplegias. J Med Genet 2003;40:81-86

Reid E, Connell J, Edwards TL, et al. The hereditary spastic paraplegia protein spastin interacts with the ESCRT-III complex-associated endosomal protein CHMP1B. Hum Mol Genet 2005;14:19-38

Ribai P, Stevanin G, Trefouret S, et al. Extension of the SPG26 phenotype in a Spanish family and refinement of its locus on chromosome 12. JMG 2005;e-letter

Rocco P, Vainzof M, Froehner SC., et al. Brazilian family with pure autosomal dominant spastic paraplegia maps to 8q: analysis of muscle beta 1 syntrophin. Am J Med Genet 2000;92:122-127

Roll-Mecak A, Vale RD. The Drosphila homologue of the hereditary spastic paraplegia protein, spastin, severs and disassembles microtubules. Curr Biol 2005;15:650-655

Rossini PM, Cracco JB. Somatosensory and brainstem auditory evoked potentials in neurodegenerative system disorders. Eur Neurol 1987;26:176-188

Saiki RK, Gelfand DH, Stoffel S, et al. Primer-directed enzymatic amplification of DNA with a thermostable DNA polymerase. Science 1988;239:487-491

Salinas S, Carazo-Salas RE, Proukakis C, et al. Human spastin has multiple microtubule-related functions. J Neurochem 2005;95:1411-1420

Santorelli FM, Patrono C, Fortini D, et al. Intrafamilial variability in hereditary spastic paraplegia associated with an SPG4 mutation. Neurology 2000a;55:702-705

Santorelli FM, Piemonte F, Carrozzo R, et al. OXPHOS and mtDNA alterations in a family with spastic paraparesis. Acta Neurol Scand 2000b;101:255-258

Sauter S, Mitterski B, Klimpe S, et al. Mutation analysis of the spastin gene (SPG4) in patients in Germany with autosomal dominant hereditary spastic paraplegia. Hum Mutat 2002;20:127-132

Sauter SM, Engel W, Neumann LM, Kunze J, Neesen J. Novel mutations in the Atlastin gene (SPG3A) in families with autosomal dominant hereditary spastic paraplegia and evidence for late onset forms of HSP linked to the SPG3A locus. Hum Mutat 2004;23:98

Saugier-Veber P, Munnich A, Bonneau D, et al. X-linked spastic paraplegia and Pilizaeus-Merzbacher disease are allelic disorders at the proteolipid protein locus. Nat Genet 1994;6:257-262

Scarano V, Mancini P, Criscuolo C, et al. The R495W mutation in SPG3A causes spastic paraplegia associated with axonal neuropathy. J Neurol 2005;252:901-903

Schachner M. Cell surface recognition and neuron-glia interactions. Ann NY Acad Sci 1991;633:105-112

Schapira AH, Cooper JM, Dexter D, et al. Mitochondrial complex I deficiency in Parkinson's disease. J Neurochem 1990;54:823-827

Seeligmuller AS. Sklerose der Seintenstrange des Rückenmarks bei vier Kindern derselben Familie. Dtsch Med Wschr 1876;2:185–186

Seri M, Cusano R, Forabosco P, et al. Genetic mapping to 10q23.3-q24.2, in a large Italian pedigree, of a new syndrome showing bilateral cataracts, gastroesophageal reflux and spastic paraparesis with amyotrophy. Am J Hum Genet 1999;64:586-593

Settasatian C, Witmore SA, Crawford J, et al. Genomic structure and expression analysis of the spastic paraplegia gene, SPG7. Hum Genet 1999;105:139-144
Sherwood NT, Sun Q, Xue, M, Zhang B, Zinn K. Drosphila spastin regulates synaptic microtubule networks and is required for normal motor function. PloS Biol 2004;2:e429

Shibasaki Y, Tanaka H, Iwabuchi K, et al. Linkage of autosomal recessive hereditary spastic paraplegia with mental impairment and thin corpus callosum to chromosome 15q13-15. Ann Neurol 2000;48:108-112

Silva MC, Coutinho P, Pinheiro CD, Neves, JM, Serrano. Hereditary ataxias and spastic paraplegias: methodological aspects of a prevalence study in Portugal. J Clin Epidemiol 1997;50:1377-1384

Silver JR. Familial spastic paraplegia with amyotrophy of the hands. J Neurol Neurosurg Psychiatry 1966;29:135-144

Simpson MA, Cross H, Proukakis C, et al. Maspardin is mutated in Mast syndrome, a complicated form of hereditary spastic paraplegia associated with dementia. Am J Hum Genet 2003;73:1147-1156

Sofroniew MV, Howe CL, Mobley WC. Nerve growth factor signaling, neuroprotection, and neural repair. Annu Rev Neurosci 2001;24:1217-81

Sridharan R, Radhakrishnan K, Ashok PP, Mousa ME. Prevalence and pattern of spinocerebellar degenerations in northeastern Libya. Brain 1985;108:831-843

Starling A, Rocco P, Cambi F, et al. Further evidence for a fourth gene causing X-linked pire spastic paraplegia. Am J Med Genet 2002;111:152-156

Stevanin G, Paternotte C, Coutinho P, et al. A new locus for autosomal recessive spastic paraplegia (SPG32) on chromosome 14q12-q21. Neurology 2007;68:1837-1840

Stevanin G, Santorelli FM, Azzedine H, et al. Mutations in SPG11, encoding spatacsin, are a major cause of spastic paraplegia with thin corpus callosum. Nat Genet 2007;39:366-372

Strachan T, Read AP. Applications of PCR. In: Human Molecular Genetics. Bios Scientific Publishers. 1997;134-136

Strümpell A. Beitrage zur pathologie des Ruckenmarks. Archiv für Psychiatrie und Mervenkrankheiten 1880;10:676-717

Strümpell A. Ueber die hereditare spastiche spinalparalyse. Deutsche zeitschrift für Nervenfeilkunde 1893;4:173-188

Svenson IK, Ashley-Koch AE, Gaskell PC, et al. Identification and expression analysis of spastin gene mutations in hereditary spastic paraplegia. Am J Hum Genet 2001;68:1077-1085

Tallaksen CM, Guichart-Gomez E, Verpillat P, et al. Subtle cognitive impairment but no dementia in patients with spastin mutations. Arch Neurol 2003;60:1113-1118

Tamagaki A, Shima M, Tomita R, et al. Segregation of a pure form of spastic paraplegia and NOR insertion into Xq11.2. Am J Med Genet 2000;94:5-8

Tessa A, Casali C, Damiano MD, et al. An additional family carrying a new atlastin mutation. Neurology 2002;59:2002-2005

Topaloglu H, Pinarli G, Erdem H, et al. Clinical observations in autosomal recessive spastic paraplegia in childhood and further evidence for genetic heterogeneity. Neuropaediatrics 1998;29:189-194

Ueda M, Katayama Y, Kamiya T, et al. Hereditary spastic paraplegia with a thin corpus callosum and thalamic involvement in Japan. Neurology 1998;51:1751-1754

Valdmanis PN, Meijer IA, Reynolds A, et al. Mutations in the KIAA0196 gene at the SPG8 locus cause hereditary spastic paraplegia. Am J Hum Genet 2007;80:152-161

Valente EM, Brancati F, Caputo V, et al. Novel locus for autosomal dominant pure hereditary spastic paraplegia (SPG19) maps to chromosome 9q33-q34. Ann Neurol 2002;51:681-685

Vazza G, Zortea M, Boaretto F, et al. A new locus for autosomal recessive spastic paraplegia associated with mental retardation and distal motor neuropathy, SPG14, maps to chromosome 3q27-q28. Am J Hum Genet 2000;67:504-509

Webb S, Patterson V, Hutchinson M. Two families with autosomal recessive spastic paraplegia, pigmented maculopathy and dementia. J Neurol Neurosurg Psychiatry 1997;63:628-632

Weber JL, May PE. Abundant class of human DNA polymorphisms which can be typed using the polymerase chain reaction. Am J Hum Genet 1989;44:388-396
Weber JL. Informativeness of human (dC-dA)n.(dG-dT)n polymorphisms. Genomics 1990;7:524-530

White KD, Ince PG, Lusher M, et al. Clinical and pathologic findings in hereditary spastic paraparesis with spastin mutation. Neurology 2000;55:89-94

Wilkinson PA, Crosby AH, Turner C, et al. A clinical and genetic study of SPG5A linked autosomal recessive hereditary spastic paraplegia. Neurology 2003;61:235-238

Wilson RK, Chen C, Avdalovic N, Burns J, Hood L. Development of an automated procedure for fluorescent DNA sequencing. Genomics 1990;6:626-634

Windpassinger C, Wagner K, Petek E, Fischer R, Auer-Grumbach M. Refinement of the "Silver syndrome locus" on chromosome 11q12-q14 in four families and exclusion of eight candidate genes. Hum Genet 2003;114:99-109

Windpassinger C, Auer-Grumbach M, Irobi J, et al. Heterozygous missense mutations in BSCL2 are associated with distal hereditary motor neuropathy and Silver syndrome. Nat Genet 2004;36:271-276

Yang Y, Hentati A, Deng HX, et al., The gene encoding alsin, a protein with three guanine-nucleotide exchange factor domains, is mutated in a form of recessive amyotrophic lateral sclerosis. Nat Genet 2001;29:160-165

Yip AG, Dürr A, Marchuk DA, et al. Meta-analysis of age at onset in spastin-associated hereditary spastic paraplegia provides no evidence for a correlation with mutational class. J Med Genet 2003;40:e106

Yool DA, Edgar JM, Montague P, Malcolm S. The proteolipid protein gene and myelin disorders in man and animal models. Hum Mol Genet 2000;9:987-992

Zhao X, Alvarado D, Rainier S, et al. Mutations in a newly identified GTPase cause autosomal dominant hereditary spastic paraplegia. Nat Genet 2001;29:326-331

Zhu PP, Patterson A, Lavoie B, et al. Cellular localization, oligomerization, and membrane association of the hereditary spastic paraplegia 3A (SPG3A) protein atlastin. J Biol Chem 2003;278:49063-49071

Zhu PP, Soderblom C, Tao-Cheng JH, Stadler J, Blackstone C. SPG3A protein atlastin-1 is enriched in growth cones and promotes axon elongation during neuronal development. Hum Mol Genet 2006;15:1343-1353

Zortea M, Vettori A, Trevesian CP, et al. Genetic mapping of a susceptibility locus for disc herniation and spastic paraplegia on 6q23.3-q24.1. J Med Genet 2002;39:387-390

Züchner S, Wang G, Tran-Viet KN, et al. Mutations in the novel mitochondrial protein REEP1 cause hereditary spastic paraplegia type 31. Am J Hum Genet 2006;79:365-369

PUBLICATIONS ARISING FROM THIS WORK

Wilkinson PA, Simpson MA, Bastaki L, Patel H, Reed JA, Kalidas K, Samilchuk E, Khan R, Warner TT, Crosby AH. A new locus for autosomal recessive complicated hereditary spastic paraplegia (SPG26) maps to chromosome 12p11.1-12q14. J Med Genet 2005;42:80-82

Wilkinson PA, Crosby AH, Turner C, Bradley LJ, Ginsberg L, Wood NW, Schapira AH, Warner TT. A clinical, genetic and biochemical study of SPG7 mutations in hereditary spastic paraplegia. Brain 2004;127:973-980

Wilkinson PA, Hart PE, Patel H, Warner TT, Crosby AH. SPG3A mutation screening in English families with early onset autosomal dominant hereditary spastic paraplegia. J Neurol Sci 2003;216:43-45

Wilkinson PA, Crosby AH, Turner C, Patel H, Wood NW, Schapira AH, Warner TT. A clinical and genetic study of SPG5A linked autosomal recessive hereditary spastic paraplegia. Neurology 2003;61:235-238

Proukakis C, Auer-Grumbach M, Wagner K, Wilkinson PA, Reid E, Patton MA, Warner TT, Crosby AH. Screening of patients with hereditary spastic paraplegia reveals seven novel mutations in the SPG4 (Spastin) gene. Hum Mutat 2003;21:170

APPENDIX 1

SPG5A Map Details

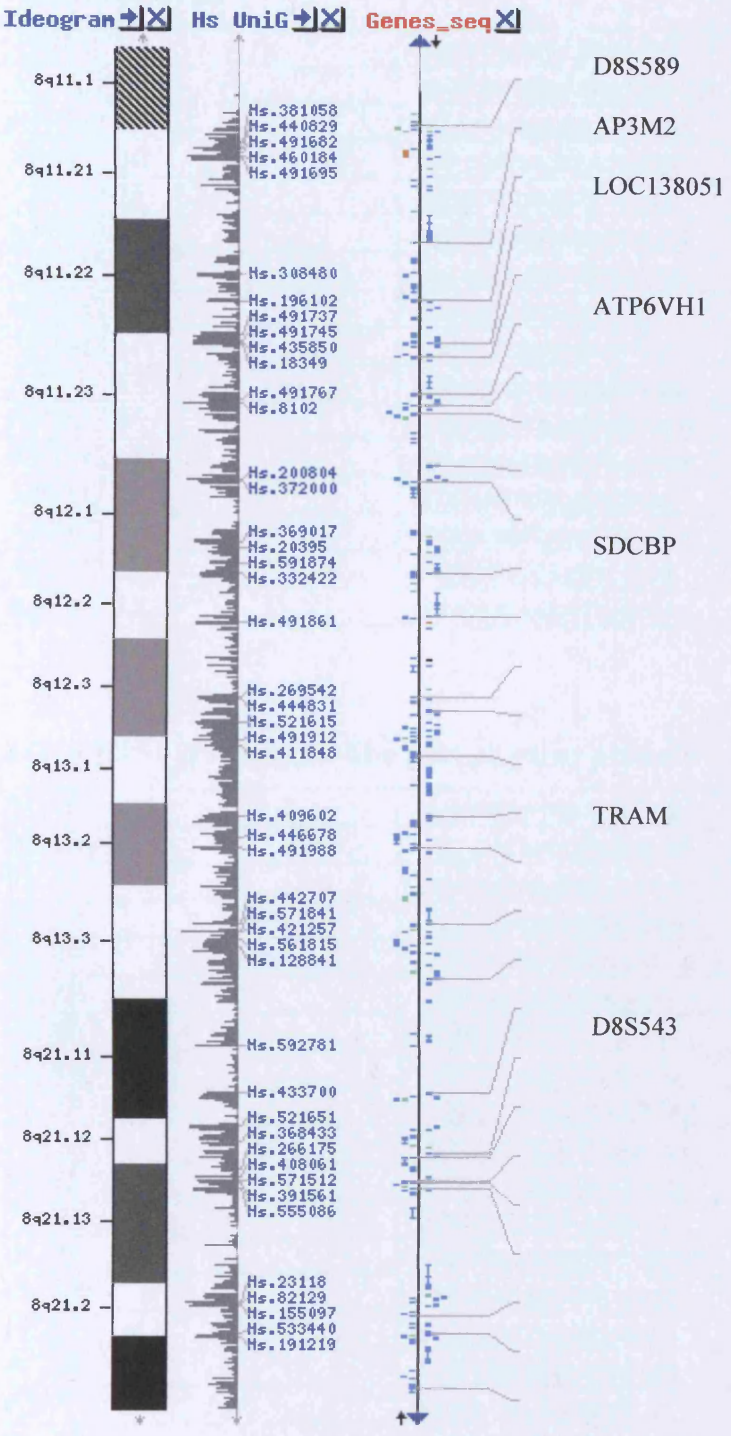

APPENDIX 2

Primers for SPG5A candidate genes

AP3M2 primers

AP3M2 1F	gagtcctgaggctttcagac
AP3M2 1R	tacacaatggaaacaggactac
AP3M2 2F	acagtatctgagtgatcaatg
AP3M2 2R	tgtgcgacactcgactaagc
AP3M2 3F	ggtgttctgtggtttctagag
AP3M2 3R	aagcattatatgaaagaggtc
AP3M2 4F	cagagaagtattcagtaatcg
AP3M2 4R	tactctgtctttccagcagc
AP3M2 5F	tgctttcctgaaagcactgc
AP3M2 5R	tcttaatcaccacagatacgg
AP3M2 6F	ccagtgcacgaatgaaatgac
AP3M2 6R	caaggtctagagtctacacag
AP3M2 7F	atgcaggattctgctgtaac
AP3M2 7R	tgcgccatatggcagaaagc
AP3M2 8F	aacagttaggcgacctgctc
AP3M2 8R	tgacctaggagacaggctg

LOC138051 (Paraplegin-like protein gene) primers

PL 1F	Gcctaaagcagctcttcgtg
PL 1R	Ctggaccaccagtgagaatc
PL 2F	Tcaaagccagctgctaccac
PL 2R	Ggtgtaaaggtcactcgaac
PL 3F	Acttgtcaataactatgtttc
PL 3R	Tcttctgatggtgcagagc
PL 4F	Gtgatgactctttcctgctg
PL 4R	Tgctcctaggtcttgatactg
PL 5F	Ctgtgagaaggccaagctag
PL 5R	Taagtctccgactctagctg
PL 6F	Tcaccgttagtggatccgag
PL 6R	Tatccggttgattggtgctg
PL 7F	acactcaaccagctgctggtgg
PL 7R	Tgtctcgcagcaatctacgc
PL 8F	Caggtgctgatgttgctaat
PL 8R	Ttgagtgactgcagcgagc
PL 9F	Tccacctctgcggcgtcg
PL 9R	Cgagctccgtcagaggag
PL 10F	Cagcgcgaccagcctgag
PL 10R	Ggtgcacttgggcgctgc

ATP6VH1 primers

ATP6VH1 1F	Agtgatcacgatattcataatc
ATP6VH1 1R	Atgcaaaagcatatgactgtc
ATP6VH1 2F	Aatccaggtctgtctgatgc
ATP6VH1 2R	Agcaagaaaactggaagtcac
ATP6VH1 3F	Actgaagttccattgaaatgtg
ATP6VH1 3R	Tgctgctactgtgaggtatg
ATP6 VH1 4F	Aggttgagaagtggtgcac
ATP6VH1 4R	Agcctggacaacatagtgag
ATP6VH1 5F	gagtgttaagaaattgtgtagc
ATP6VH1 5R	tagcttaaaagaacacggatg
ATP6VH1 6F	gtaagctgatacattaggata
ATP6VH1 6R	ctaactggaggtgaccatgg
ATP6VH1 7F	attccagtaggtaatctgac
ATP6VH1 7R	atgtcaaggagagatgcttg
ATP6VH1 8F	tctagctgcttgttattgctg
ATP6VH1 8R	atattcaccaagactctatgg
ATP6VH1 9F	gtctctgaatccatcacatg
ATP6VH1 9R	aacgtattttagtggactctcttg
ATP6VH1 10F	ggagtactgtcagattcttata
ATP6VH1 10R	tcaaccacattagtcagcaag
ATP6VH1 11F	caggaagatatcttcattatac
ATP6VH1 11R	agttcctttgctaacctactc
ATP6VH1 12F	gagctgcctgcttacaaactg
ATP6VH1 12R	gcaagtgagagtttgcagac
ATP6VH1 13F	atatatgacagtgcataatgtg
ATP6VH1 13R	aacagtgttcactcttaact

Syndecan binding protein gene (SBP) primers

SBP 1F	tcaatttctatgacattagag
SBP1R	tataagtagaatgcatgttac
SBP2F	gtaagtatagcatattgttag
SBP 2R	tcttggattccttatatgagc
SBP 3F	aatacgcagaagcccataatg
SBP 3R	tgtgagttagccacaaagag
SBP 4F	actgagtaagttccagttat
SBP 4R	taatcacttattatgtaagag
SBP 5F	cgtatcatagtagtggtaaatg
SBP 5R	gactataaggctcatcaataac
SBP 6F	atccaatatggcaacatttatg
SBP 6R	ctgcagcagaacatggcac
SBP 7F	tctttaccaagactggcatag
SBP 7R	ttaagtcacatgaccatatgc
SBP 8F	acaggtgctaaattggaattg
SBP 8R	tcctcatgcagcatatgctc

TRAM primers

TRAM 1F	gtgagcagctgggaagagc
TRAM 1R	gcctgcacctcagggactg
TRAM 2F	gtgcttcgatttagggacag
TRAM 2R	catggatgagatctctgacg
TRAM 3F	tgtttccataactatgttgtac
TRAM 3R	cagattatggagagctagtac
TRAM 4F	gtactagctctccataatctg
TRAM 4R	tagcagagtttctaatcttag
TRAM 5F	tgcaacctggtatgggacc
TRAM 5R	gattaatagtgacatgaccatg
TRAM 6F	tattgtatggaatgatgacac
TRAM 6R	atggaggaagggcaaacatg
TRAM 7F	ctgggcaacatagcaagac
TRAM 7R	agacaggtcagcatactatc
TRAM 8F	gatagtatgctgacctgtct
TRAM 8R	tggcaatgttaggcactgac
TRAM 9F	gattacaggcgtctgccac
TRAM 9R	atgattcaatgtagagaaactg
TRAM 10F	tgatagaatgtattcagtggc
TRAM 10R	tgtggaatgcagtaagattac
TRAM 11F	ttctgaaggtatctttacatat
TRAM 11R	atcaaagagcacagactgtat

APPENDIX 3

Details of SPG5A candidate genes

Candidate genes from within the SPG5A locus were selected based on known or predicted gene products with pathways involved in intracellular transport processes or mitochondrial function which had been previously implicated in genes responsible for different types of HSP. Details of each gene are shown below.

AP3M2

This gene encodes a subunit of the heterotetrameric adaptor-related protein comlex 3 (AP-3), which belongs to the adaptor complexes medium subunits family. The AP-3 complex plays a role in protein trafficking to lysosomes and specialized organelles.

LOC138051

LOC138051 was initially thought to code for a paraplegin-like protein with over 80% homology to paraplegin. This has since been recognised as a pseudogene.

ATP6VH1

This gene encodes the vacuolar ATpase H+ transporting V1 subunit. The vacuolar ATPase is a multisubunit enzyme that facilitates the acidification of intracellular compartments and plays a role in receptor-mediated endocytosis, intracellular trafficking, and protein degradation. ATP6V1H is a subunit of the 570-kD V1 peripheral complex responsible for hydrolysis of ATP.

SDCPB

Syndecan binding protein (syntenin) is part of the syndecan group of proteins. These are transmembrane proteoglycans that place structurally heterogeneous heparan sulfate chains at the cell surface and a highly conserved polypeptide in the cytoplasm. Versatile heparan sulfate moieties support various processes of molecular recognition, signaling, and intracellular trafficking.

TRAM

Translocation associated membrane protein is involved in the recognition and translocation of secretory proteins in the endoplasmic reticulum.